Interpretation of maximum absorbance data obtained from turbidimetry in plasma samples with varying fibrinogen concentration

CM Nunes

orcid.org/ 0000-0003-1933-7036

Mini-dissertation submitted in fulfilment of the requirements for the degree *Masters of Science in Dietetics* at the North-West University

Supervisor: Dr Z de Lange

Co-supervisor: Prof. M Pieters

Graduation: May 2019

Student number: 23554355

I, Claudia Maria Nunes declare herewith that this mini-dissertation is my own work, has been text-edited in accordance with the requirements and has not already been submitted to any other university.

Signature of student: CNunes Date: 08/11/2018

Signature of supervisor/promoter: Date: 08/11/2018

ACKNOWLEDGMENTS

First and foremost, I would like to thank our Heavenly Father, for His guidance and strength during the past two years. **All glory and honour to Him!**

"I will sing to the Lord because He is good to me" - Psalm 13:6

I would also like to thank the following people:

Dr Zelda de Lange, my supervisor, for her valuable input, advice and encouragement throughout the study.

Prof. Marlien Pieters, my co-supervisor, for her valuable input, advice and encouragement throughout the study.

Dr Anine Jordaan and Dr Innocent Shuro, for their assistance with the use of the scanning electron microscope.

Gerda Beukman, for her assistance in obtaining required research articles.

The National Research Foundation for providing financial support regarding living expenses.

Lastly, a huge thank you to my people - my family, boyfriend, friends and officemates. Their continuous support helped me cross the finish line.

ABSTRACT

INTRODUCTION AND AIM

Cardiovascular disease (CVD) has become South Africa's second largest cause of death. CVD is often associated with vascular injury, which initiates the coagulation cascade and formation of an occlusive or non-occlusive thrombus. Clots can be characterised by various properties, which determine their behaviour in the vasculature. Structural clot properties can be determined directly by microscopy and indirectly by turbidimetry. In purified fibrinogen systems, with a fixed fibrinogen concentration, increase in absorbance measurement, obtained from turbidity curves, is used as a proxy marker for fibrin fibre diameter. However, in plasma samples with varying fibrinogen concentrations disagreement exists regarding the interpretation of maximum absorbance, as it also increases with an increase in fibrinogen concentration and may thus not be a true reflection of fibre diameter, but rather of increased clot density. In this study the main aim was to characterise structural clot properties from plasma samples with varying fibrinogen concentrations, using both direct (scanning electron microscopy) and indirect methods (turbidimetry, permeability) to provide clarity on the interpretation of maximum absorbance values from plasma samples.

PARICIPANTS AND METHODS

Data was collected in the South African Prospective Urban and Rural Epidemiology (PURE) study, in North West, Potchefstroom during 2015 from apparently healthy black women and men (n=900) residing in urban or rural settlements. A sub-sample of 30 participants was systematically selected based on maximum absorbance values and fibrinogen concentrations. The methods pertaining to this study include the following fibrin network determinations: total fibrinogen and fibrinogen γ' concentration, turbidimetry, permeability, scanning electron microscopy, fibrin content and rheometry.

RESULTS

In the 30 investigated plasma samples, maximum absorbance showed strong, positive significant correlations with lag time, slope, clot lysis time (CLT), porosity, elastic modulus (G'),

viscous modulus (G''), total fibrinogen concentration and fibre diameter. The correlation between maximum absorbance and total fibrinogen was stronger than between maximum absorbance and fibre diameter. Aside from its significant correlation with maximum absorbance, fibre diameter correlated with slope only. After controlling for total fibrinogen concentration in our samples, we found no significant correlations between fibre diameter and other clot properties, whereas maximum absorbance still significantly correlated with lag time, slope, CLT, porosity, elastic and viscous moduli. Maximum absorbance however no longer correlated significantly with fibre diameter. Three covariates identified for possible contribution to clot property variance, after plasma samples were divided into two groups (low and high maximum absorbance) matched for fibrinogen concentration, were body mass index (BMI), C-reactive protein (CRP) and low-density lipoprotein cholesterol (LDL-C). BMI correlated significantly with CLT, CRP with total fibrinogen concentration, slope, maximum absorbance and porosity and LDL-C with lag time, maximum absorbance and CLT.

CONCLUSION

From our data obtained from plasma samples with varying fibrinogen concentration, we found both increased maximum absorbance and increased total fibrinogen concentration to be associated with the formation of thicker fibrin fibres. Our results show that although maximum absorbance is related to fibre diameter, in plasma samples with varying fibrinogen concentration, it is not equivalent to fibre diameter. We suggest that maximum absorbance is more likely indicative of clot (protein) density. In addition, other environmental and biological factors including BMI, CRP and LDL-C may influence fibrin clot properties, including maximum absorbance in plasma samples.

KEY TERMS:

Maximum absorbance; turbidimetry; SEM; rheometry; permeability; fibrinogen; platelet poor plasma; PURE; black South African population

TABLE OF CONTENTS

LIST OF TABLES

LIST OF FIGURES

LIST OF ABBREVIATIONS AND SYMBOLS

A	Cross-sectional area of clot container
A	Alpha
AFM	Atomic force microscopy
Am	Ante meridiem
ANCOVA	Analysis of covariance
au/s	Absorbance unit per second
β	Beta
BMI	Body mass index
BSA	Bovine serum albumin
^{o}C	Degrees Celsius
$CaCl_2$	Calcium chloride
CAD	Coronary artery disease
CLT	Clot lysis time
Cm	Centimetre
cm^2	Square centimetre
CRP	C-reactive protein
CVD	Cardiovascular disease
D	Fractal dimension
EDTA	Ethylenediaminetetraacetic

EtOH	Ethanol
F	Factor
FPA	Fibrinopeptide A
FPB	Fibrinopeptide B
γ’	Gamma prime
G	G-force / relative centrifugal force
G’	Elastic / storage modulus
G’’	Viscous / loss modulus
g/L	Gram per litre
H_2O	Water
H_2SO_4	Sulphuric acid
HCl	Hydrochloric acid
HDL-C	High-density lipoprotein cholesterol
HMDS	Hexamethyldisilazane
HMK	High molecular weight kininogen
HRP	Horseradish peroxidase
KCl	Potassium chloride
kDa	Kilodaltons
kg/m^2	Kilogram per square metre
Ks	Permeability coefficient
L	Clot length
LDL-C	Low-density lipoprotein cholesterol

LSCM	Laser scanning confocal microscopy
µl	Microlitre
M	Mole
mA	Milliamps
mg/ml	Milligram per millilitre
mg/L	Milligram per litre
MI	Myocardial infarction
Min	Minute
Ml	Millilitre
MLR	Mass-length ratio
mM	Millimole
mmol/L	Millimoles per litre
mPa-s	Millipascal per second
N	Population size
NaCl	Sodium chloride
Na_2CO_3	Sodium carbonate
$NaHCO_3$	Sodium bicarbonate
NaOH	Sodium hydroxide
NCD	Non-communicable disease
ng/ml	Nanogram per millilitre
Nm	Nanometre
NWU	North-West University

p-value	Statistical significance test
%	Percentage
ΔP	Pressure drop
Pa	Pascal
PAD	Peripheral arterial disease
PAI-1	Plasminogen activator inhibitor
PE	Pulmonary embolism
PK	Pre-kallikrein
PL	Platelets
PPP	Platelet poor plasma
PURE	Prospective Urban and Rural Epidemiology
R	Correlation coefficient
rad/s	Radian per second
Rpm	Revolutions per minute
SA	South Africa
SEM	Scanning electron microscopy
SMC	Smooth muscle cells
T	Time
TC	Total cholesterol
TEA	Trimethylamine
TEG	Thromboelastography
TEM	Transmission electron microscopy

TF	Tissue factor
TG	Triglycerides
TIRFM	Total internal reflection fluorescence microscopy
Torr	Unit of pressure
tPA	Tissue plasminogen activator
U/ml	Units per millilitre
USA	United States of America
UV	Ultraviolet
vs.	Versus
VTE	Venous thromboembolic
η	Viscosity
Q	Volume of liquid
Λ	Wavelength
WHO	World Health Organization
Yrs	Years

CHAPTER 1: INTRODUCTION

1.1 BACKGROUND

The prevalence of cardiovascular disease (CVD) is increasing at an alarming rate, with a prediction to increase by 4.7 million from 2012 to 2030 worldwide (WHO, 2014). Currently in South Africa, CVD is the second largest cause of death (Stats SA, 2015). CVDs are progressive diseases resulting in the formation, development and ultimate rupture of plaque formed in the arterial wall (Raymond & Couch, 2012). Plaque formation occurs over time starting out as a lesion known as a fatty streak; thereafter, a fibrous plaque forms, ultimately resulting in the formation of an advanced plaque (Raymond & Couch, 2012).

This plaque rupture leads to the onset of the activation of the coagulation cascade, where soluble fibrinogen is converted to fibrin, forming a clot (Bridge *et al*., 2014; Liu *et al*., 2010). The behaviour and lysis of the clot in the vasculature are greatly influenced by structural and mechanical properties of the fibrin network comprising the clot; thereby influencing the severity of the ensuing thrombotic event. Multiple factors influence clot properties, one of the most important being fibrinogen concentration (Bridge *et al*., 2014; Mills *et al*., 2002; Pieters & Vorster, 2008).

Various direct and indirect methods are used to determine clot properties. Scanning electron microscopy (SEM), transmission electron microscopy (TEM) and thromboelastography (TEG), amongst others, are direct methods used to determine structural properties, whereas direct measures of mechanical (viscoelastic) properties include techniques such as rheometry (Chernysh & Weisel, 2008; Hategan *et al*., 2013; Litvinov & Weisel, 2016a; Sjøland, 2007). Clot turbidimetry, nephelometry and permeability measurements are indirect methods used to determine structural clot properties (Morais *et al*., 2006; Undas & Zeglin, 2006a).

Structural clot properties provide information on the fibrin fibre length, fibre diameter, pore size and density of fibrin network (Chernysh & Weisel, 2008; Mills *et al*., 2002). Being direct measurements, imaging techniques such as SEM and TEM provide good visuals of the studied clot. However, these techniques are limited by the occurrence of artefacts due to the drying process therefore solely allowing the visualisation of dried rather than native fibrin fibres (Chernysh & Weisel, 2008; Hategan *et al*., 2013; Sjøland, 2007). SEM and TEM are

also time consuming and can therefore not be used in large-scale clinical and epidemiological studies.

In comparison to direct methods, turbidimetry is a fast and highly sensitive technique used to determine structural clot properties indirectly (Carter *et al.*, 2007; Morais *et al.*, 2006). This high-throughput method can be used in large-scale clinical and epidemiological studies with good reproducibility (Carter *et al.*, 2007; Morais *et al.*, 2006). A turbidity curve is recorded by plotting light absorbency against time (Sjøland, 2007). Three main variables can be obtained from this curve, namely the lag time, slope and maximum absorbance. The lag time indicates the time needed for fibrin fibres to grow sufficiently so that lateral aggregation can commence (Mills *et al*., 2002; Pieters *et al*., 2008; Weisel & Nagaswami, 1992). The rate of lateral aggregation is indicated by the slope of the turbidity curve (Mills *et al*., 2002; Weisel & Nagaswami, 1992; Pieters *et al*., 2008), while maximum absorbance is an indication of the fibrin fibre diameter at a fixed fibrinogen concentration (Chernysh & Weisel, 2008; Mills *et al.,* 2002; Pieters *et al*., 2008; Sjøland, 2007). This method has been successfully used in studies using purified fibrinogen solutions where all samples have a fixed fibrinogen concentration (Carr & Hermans, 1978; Weisel & Nagaswami, 1992). However, in plasma samples, with varying fibrinogen concentrations, the interpretation of maximum absorbance becomes challenging as it is also known to increase with increased fibrinogen concentration, where a higher fibrinogen concentration is associated with the formation of denser clots (Chernysh & Weisel, 2008; Mills *et al.,* 2002; Sjøland, 2007). The increased maximum absorbance associated with increased plasma fibrinogen concentration may therefore not solely be a reflection of fibre thickness but also that of increased protein density. In the literature, maximum absorbance is however still interpreted as an indication of fibre diameter, even when plasma samples are used.

Since the interpretation of maximum absorbance in plasma samples is complicated by varying fibrinogen concentrations and it is not entirely clear which fibrin property (or combination) it is indicative of, the present study made use of additional techniques to characterise the clot properties of samples with known maximum absorbance and fibrinogen concentrations to investigate the true interpretation of maximum absorbance obtained from plasma samples. The current interpretation of maximum absorbance as either an indication of fibre thickness or protein density can be ambiguous in terms of CVD risk. Thicker fibres seem to lyse easier, however, more dense clots lyse slower. The first is linked to lower CVD risk whilst the latter to increased risk (Bridge *et al*., 2014; Collet *et al.,* 1996; Dunn & Ariëns, 2004; Fatah *et al*., 1992). In the literature, CVD is indeed linked to both decreased (Bouman *et al*., 2016; Undas *et al*., 2006b) and increased (Undas *et al*., 2009a; Undas *et al*., 2010c;

Undas *et al*., 2011b) maximum absorbance compared to healthy control individuals. Refining the interpretation of maximum absorbance obtained from plasma samples and whether it is in fact an indication of fibre thickness, protein density or both, may demonstrate to be very valuable for improved identification of individuals at risk of CVD through turbidimetry. Since the structural properties significantly influence the mechanical clot properties, complementary measurements of mechanical clot properties (using rheometry) were also carried out in this study, to support data obtained from the structural methods.

In this study, black South Africans participating in the Prospective Urban and Rural Epidemiology (PURE) study with varying maximum absorbance values, stratified for fibrinogen concentration, were investigated. In addition to fibrinogen concentration (total and γ' fibrinogen) and turbidimetry analyses, fibrin-clot properties were characterised using SEM (fibrin fibre diameter), rheometry (mechanical / viscoelastic properties) and clot permeability (pore size). In addition, fibrin content was also investigated to determine whether differences in maximum absorbance are due to differences in the amount of fibrin present in the sample. Maximum absorbance was then related to the different clot properties, taking the fibrinogen concentration into consideration so as to gain a better understanding of the interpretation of turbidity data obtained from plasma samples with different fibrinogen concentrations.

1.2 AIM AND OBJECTIVES

The aim of this study was to clarify the interpretation of maximum absorbance data obtained from turbidimetry in plasma samples, with varying fibrinogen concentration, collected from black South Africans who participated in the Prospective Urban and Rural Epidemiological study in the North-West Province, South Africa (PURE-SA), using the PURE-2015 data set.

The specific objectives of this study were to select individuals with varying maximum absorbance values, stratified for fibrinogen concentration across the fibrinogen concentration range and carry out the following:

- Measure plasma clot structural properties (fibre diameter, clot pore size) using a direct scanning electron microscopy (SEM) and an indirect technique (permeability).
- Perform complementary measurements to determine mechanical clot properties (rheometry) as well as clot fibrin content.
- Relate the maximum absorbance value to measures of clot formation (lag time and slope obtained from turbidimetry), clot lysis (turbidimetry), structural

properties (fibre diameter - SEM and pore size - Ks), mechanical properties (clot stiffness and plasticity - rheometry) as well as fibrin content while taking plasma fibrinogen concentration into consideration.

- Compare the association between maximum absorbance and the other measured clot properties with the association between fibre diameter and the other clot properties; to determine whether they are equivalent.
- Compare samples matched for fibrinogen concentration with low and high maximum absorbance values to characterise the fibrin clot properties of the two groups and to identify other biological factors that contribute to potential variance in clot properties in the two groups.

1.3 RESEARCH TEAM

Table 1-1: Research team

Partner name	Team member	Qualification	Professional registration	Role in study
Centre of Excellence of Nutrition, Potchefstroom campus, North-West University	Ms Claudia Nunes	B.Sc. Dietetics	HPCSA – dietitian	M.Sc. student: Protocol development, writing of literature review, performing fibrin network analyses (permeability, SEM, fibrin content and rheometry), data capturing, statistical analysis, interpretation of results and writing up of mini-dissertation.
	Dr Zelda de Lange	Ph.D. Nutrition	N/A	Supervisor of M.Sc. student: guidance regarding writing of protocol, literature review and mini-dissertation; training student in methodology of turbidimetry, SEM and rheometry; guidance in data capturing, statistical analysis and interpretation of results.

Table 1-1 continued

Partner name	Team member	Qualification	Professional registration	Role in study
Centre of Excellence of Nutrition, Potchefstroom campus, North-West University	Prof. Marlien Pieters	Ph.D. Dietetics	HPCSA - dietitian	Co-supervisor of M.Sc. student: guidance regarding writing of protocol and mini-dissertation, training student in methodology of fibrin content and permeability and guidance regarding interpretation of results.

SEM = scanning electron microscopy

1.4 STRUCTURE OF MINI-DISSERTATION

This mini-dissertation is written in chapter format, enclosing five chapters. All chapters were edited by a qualified language editor and technical requirements were met in accordance with the North-West University (NWU), with referencing adhering to the Harvard style as stipulated by the NWU. This introductory chapter is followed by Chapter 2, a literature review. In the literature review, the coagulation cascade, biochemical structure of fibrinogen and the role of clot formation and its fibrin properties in thrombotic diseases are discussed. An overview of fibrin network determinations is also provided including both direct and indirect methods that measure kinetics of clot formation, structural properties and mechanical (viscoelastic) properties. In addition, the interpretation of fibrin structure properties in thrombotic disease patients compared to healthy controls in plasma samples is reviewed.

Chapter 3 describes the study design and characteristics of the PURE study population, as well as the sub-sample used for this study. A detailed description of the methods used for the fibrin network determinations included in this study is also discussed, including total fibrinogen and fibrinogen γ' concentration, turbidimetry, permeability assay, scanning electron microscopy (SEM), fibrin content and rheometry. The statistical analyses performed in the study are also included in Chapter 3.

Chapter 4 presents the results obtained in this study. The chapter provides the demographic, anthropometric, biochemical and haemostatic characteristics of the sub-sample, as well as the characteristics of the sub-sample divided into two categories (low and high maximum absorbance) based on the stratification of the participants according to fibrinogen concentration (PURE fibrinogen concentration range: 1.5 – 7.5 g/L), where each 0.5 g/L fibrinogen concentration increment contains two individuals with the lowest and highest maximum absorbance value. The relationship between maximum absorbance, fibrinogen concentration and the measured clot property variables (lag time, rate of lateral aggregation, clot lysis time, fibre diameter and mechanical clot properties), as well as the influence of fibrinogen concentration and sample characteristics on the interpretation of maximum absorbance, are depicted in Chapter 4.

Chapter 5 discusses all the findings of this study with motivation, as well as the limitations of the study and recommendations for future research. This is followed by a conclusion in combination with the standing literature. A reference list, containing sources cited throughout all fives chapters and addenda, concludes this mini-dissertation.

CHAPTER 2: LITERATURE REVIEW

2.1 INTRODUCTION

Worldwide, the mortality rate of non-communicable diseases (NCDs) is estimated to increase by 14 million from 2012 to 2030 (WHO, 2014). In 2012, the leading cause of NCD deaths were cardiovascular diseases (CVDs), causing 17.5 million deaths globally (WHO, 2014). CVDs include coronary heart disease, cerebrovascular disease, peripheral arterial disease, rheumatic heart disease, congenital heart disease and deep vein thrombosis (WHO, 2016). Eighty-two percent of CVD deaths have been reported to occur in middle- to low socio-economic countries (WHO, 2016). Currently, CVD is largely responsible for the high mortality rate in South Africa, being the second largest cause of death (Stats SA, 2015; WHO, 2015). Studies conducted regarding this high CVD mortality rate have shown one of the main precursors to be urbanisation of South African population groups, specifically black ethnic groups (Vorster, 2002). Urbanisation has been shown to play an important role in the increased prevalence of CVD risk factors, namely obesity, hypercholesterolemia, hypertension, diabetes, and increased alcohol and tobacco use (Vorster, 2002).

CVDs are progressive, chronic inflammatory diseases encompassing the formation, development and ultimate rupture of plaque build-up in the arterial wall (Raymond & Couch, 2012). This rupture leads to the onset of the coagulation cascade, where soluble fibrinogen is converted to fibrin, forming a clot (Bridge *et al*., 2014; Liu *et al*., 2010).

The structural and mechanical properties of the fibrin network comprising the clot are vital to the behaviour and lysis of the clot in the vasculature and influence the severity of the ensuing thrombotic event. Denser blood clots with more branch points, smaller intrinsic pores and closely packed fibres are less permeable and therefore more resistant to fibrinolysis (clot breakdown), thereby associated with an increased CVD risk (Bridge, *et al*., 2014; Collet, *et al*., 2000). Clots with loosely packed, thicker fibrin fibres and larger pores are more permeable and therefore have an increased lysis rate, thus associated with a decreased CVD risk (Bridge, *et al*., 2014, Collet, *et al*., 2000).

Clot properties can be determined by various direct and indirect methods. The direct methods used to determine structural properties include scanning electron microscopy (SEM), transmission electron microscopy (TEM), total internal reflection fluorescence microscopy (TIRFM) and light microscopy techniques (deconvolution and confocal

microscopy), and thromboelastography (TEG) (Chernysh & Weisel, 2008; Hategan *et al*., 2013; Litvinov & Weisel, 2016a; Sjøland, 2007). The indirect methods used to determine structural properties include clot turbidimetry, nephelometry and permeability measurements (Morais *et al*., 2006; Undas & Zeglin, 2006a). Mechanical (viscoelastic) clot properties, however, are largely determined by direct measures such as rheometry and combined atomic force microscopy (AFM) / optical microscopy (Chernysh & Weisel, 2008; Hategan *et al*., 2013; Litvinov & Weisel, 2016a; Sjøland, 2007).

Although direct measures allow for better visualisation of the fibrin clot properties, the drying process that forms part of some of these techniques may cause artefacts to occur and only allows for the visualisation of dried rather than native fibrin fibres (Chernysh & Weisel, 2008; Hategan *et al*., 2013; Sjøland, 2007). In addition, it requires highly specialised equipment not available in all research laboratories and is extremely time consuming making it impractical to use in studies employing large participant numbers. For this reason, indirect measures such as turbidimetry has been developed, which can be performed in studies with large sample sizes such as epidemiological studies using a standard spectrophotometer. Turbidity is a fast and highly sensitive technique, which records clot formation and structure onto a sigmoidal curve, where light absorbency is plotted against time (Sjøland, 2007). From this turbidity curve three main variables can be obtained, namely the lag time and slope (indicators of clot formation) and maximum absorbance (indicator of clot structure).

In purified fibrinogen systems, with a fixed fibrinogen concentration, the increase in absorbance, obtained from turbidity curves, is used as a proxy marker for fibrin fibre diameter (Carr & Hermans, 1978; Weisel & Nagaswami, 1992). However, in plasma samples, where fibrinogen concentrations vary, uncertainty exists regarding the interpretation of maximum absorbance as it is also known to increase with increased fibrinogen concentration, which in turn is associated with the formation of denser clots (Mills *et al.,* 2002; Sjøland, 2007; Undas *et al.,* 2006c). The increased maximum absorbance associated with increased plasma fibrinogen concentration may thus not simply be a reflection of fibre diameter, but also of increased plasma protein density. In the literature, maximum absorbance is however still interpreted as an indication of fibre diameter, even when plasma samples are used. Therefore, the question arises: what is the true interpretation of maximum absorbance values obtained from plasma samples with varying fibrinogen concentrations?

The outline and focus of this literature review include: an overview of the coagulation cascade; a description of the fibrinogen molecule and the clot formation process, as well as clot properties and CVD. A discussion is also provided on the different clot properties and

the various methods used to measure these, with a detailed explanation of turbidimetry being the focal method of this mini-dissertation. In addition, the current ambiguity in the literature regarding the interpretation of the maximum absorbance variable from turbidimetry is highlighted.

2.2 CLOT FORMATION

In general, prior to clot formation, the process of plaque build-up occurs. The initial changes that take place prior to plaque formation cause endothelial dysfunction of the artery, where endothelial permeability increases allowing lipoproteins to migrate into the tunica intima (innermost layer of blood vessel) (Libby *et al.*, 2002; Ross, 1999). This movement of lipids into the blood vessel activates leukocyte migration into the tunica intima (Figure 2-1 A), resulting in the uptake of lipoprotein particles by the macrophages forming foam cells. The build-up of low-density lipoprotein cholesterol (LDL-C) in the tunica intima induces the formation of a lesion known as a fatty streak, made up of foam cells (lipid-laden macrophages) and T-lymphocytes (Raymond & Couch, 2012; Ross, 1999) (Figure 2-1 B). Fatty streaks can occur from a young age existing throughout an individual's lifetime (Ross, 1999). The fatty streak progresses to an intermediate lesion as smooth muscle cells (SMC) migrate into the tunica intima forming a fibrous cap between the fibrous formed plaque and arterial lumen (Libby *et al.*, 2002; Ross, 1999) (Figure 2-1 B). With excessive and unabated inflammation, the advanced plaque expands further into the lumen disturbing blood flow. Ultimately over time, the fibrous cap formed becomes weaker and more susceptible to rupture (Libby *et al.*, 2002) (Figure 2-1 C). This following section describes the process of clot formation and its role in thrombotic disease.

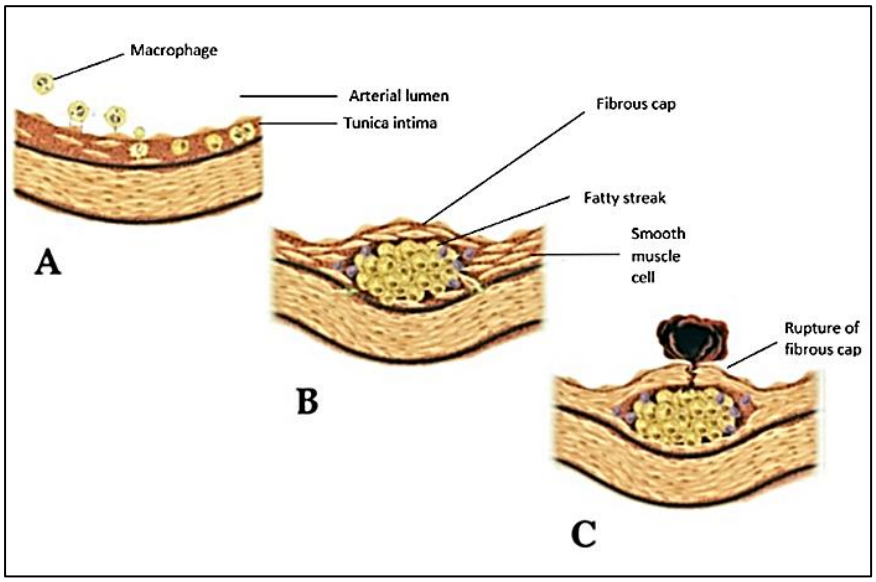

Figure 2-1: Stages of atherosclerosis (Adapted from Libby *et al.* (2002) and Ross (1999))

2.2.1 Overview: Coagulation cascade and fibrinogen

Vascular injury initiates the activation of platelets and the coagulation cascade. Both the coagulation pathway and platelet aggregation are required for adequate stability of the ensuing clot (Kamath & Lip, 2003). The coagulation cascade (Figure 2-2) consists of two pathways, the intrinsic and extrinsic pathway, during which plasma proteins are activated and converted to serine proteases through proteolysis (Davie *et al.*, 1991; Kamath & Lip, 2003; Lefevre *et al*., 2004; Pulanić & Rudan, 2005). Multiple reactions involved in these pathways require phospholipids and calcium ions for activation (Davie *et al.*, 1991). The intrinsic pathway begins with the activation of Factor (F)XII (Davie *et al.*, 1991; Kamath & Lip, 2003). The active form, FXIIa, becomes a catalyst for the conversion of FXI to its active form, FXIa, which subsequently is then a catalyst for the conversion of FIX to its active form FIXa, resulting in the activation of FX (Figure 2-2) (Davie *et al.*, 1991; Kamath & Lip, 2003). Tissue factor (TF), a glycoprotein released from the arterial endothelium in response to vascular injury, triggers the extrinsic pathway (Davie *et al.*, 1991; Kamath & Lip, 2003; Lefevre *et al*., 2004). TF has a strong association with phospholipids and a high affinity for the plasma protein, FVII, circulating in the vasculature (Davie *et al.*, 1991). Triggered within the lumen of the blood vessel in response to vascular injury, TF activates FVII, in the presence of calcium ions, into its active form, FVIIa (Davie *et al.*, 1991; Kamath & Lip, 2003; Lefevre *et al*., 2004; Smith *et al*., 2015). The two pathways converge at FX, where FVIIa activates FX as well as FIX (Hoffman & Monroe, 2001; Pulanić & Rudan, 2005). FXa and FVa combine to form a complex known as prothrombinase (Davie *et al*., 1991; Rosing *et al*.,

1980). This complex subsequently activates prothrombin (FII) forming thrombin (FIIa) through hydrolysis (Pulanić & Rudan, 2005; Rosing *et al*., 1980). Thrombin then activates fibrinogen (FI), forming fibrin (FIa) (Kamath & Lip, 2003; Lefevre *et al*., 2004; Pulanić & Rudan, 2005). Thrombin also plays a role in the activation of other procoagulant enzymes, namely FV, FVII, FVIII, FXI and FXIII. The activation of FXIII is dependent on the presence of calcium ions and plays a vital role in fibrin cross-linking (Ariëns *et al.*, 2002; Standeven *et al*., 2005) which is discussed further in Section 2.2. The intrinsic pathway is vital for the growth and maintenance of fibrin clot formation, while the extrinsic pathway is the initiator of fibrin formation (Davie *et al.*, 1991). The ensuing fibrin clot, formed from the conversion of fibrinogen to fibrin and stabilised by FXIII, is the final product of the coagulation cascade (Standeven *et al*., 2005).

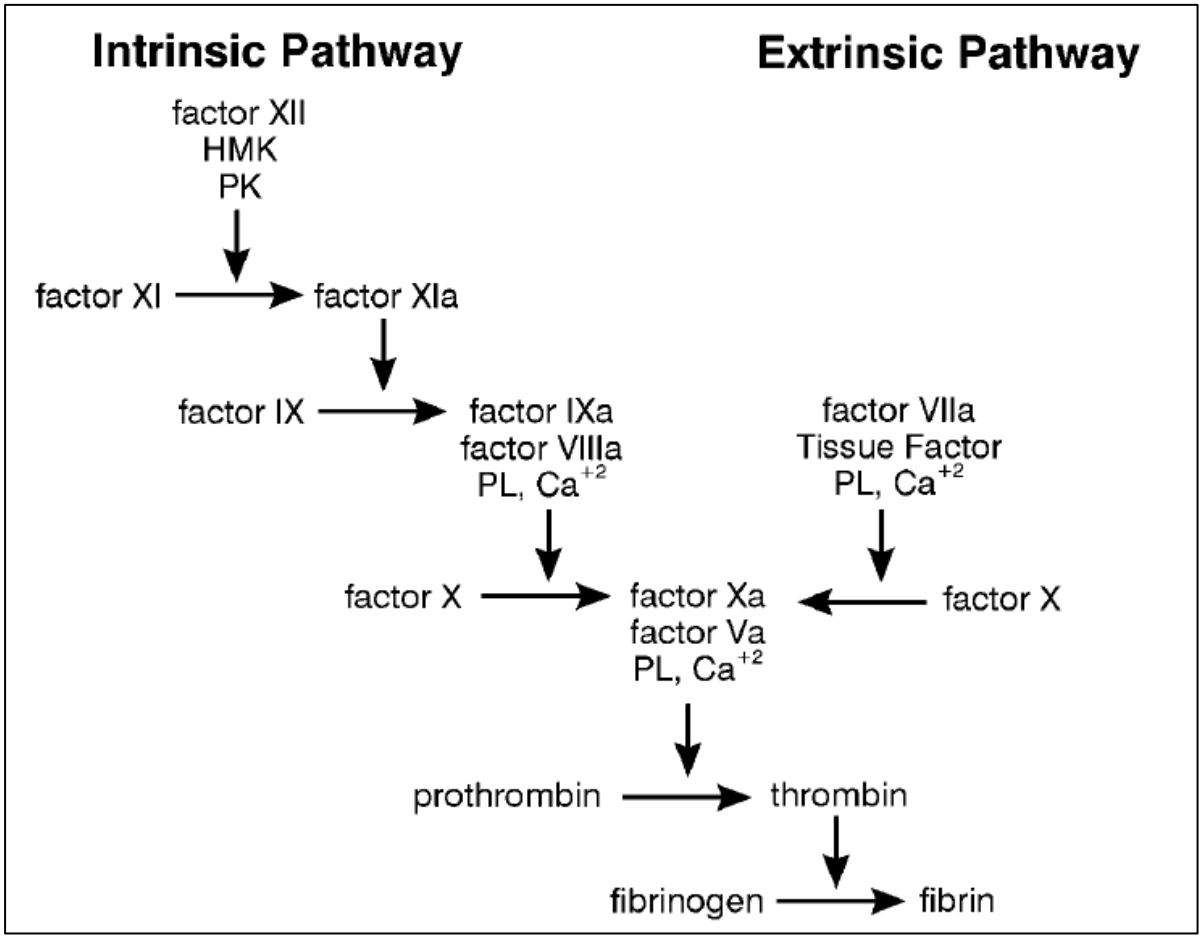

Figure 2-2: Coagulation cascade (Hoffman & Monroe, 2001)

HMK = high molecular weight kininogen; PK = pre-kallikrein; PL = platelets

Fibrinogen is a large, soluble, plasma glycoprotein, synthesised predominately in hepatocytes. The fibrinogen molecule is 45 nm in length, with a molecular weight of 340 kDa

and is found in plasma at a concentration ranging between 1.5-4.5 g/l (De Moerloose *et al*., 2010; Kamath & Lip, 2003; Mosesson *et al*., 2001; Pulanić & Rudan, 2005; Weisel & Litvinov, 2013). During acute inflammation, fibrinogen can potentially increase beyond 7 g/l in the plasma (Kattula *et al*., 2017).

The trinodular fibrinogen molecule is made up of a central E-region connected by two identical subunits, a three-stranded coiled-coil segment, to two distal D-regions where binding pockets vital for fibrinogen polymerisation are found (Kamath & Lip, 2003; Kattula *et al*., 2017; De Moerloose *et al*., 2010; Mosesson, 2005; Mosesson *et al*., 2001; Standeven, 2005; Tsurupa *et al.*, 2009). The E-region is made up of the amino-termini of the two identical subunits which consist of two identical pairs of three non-identical polypeptide chains (Aα, Bβ and γ) interconnected by twenty-nine disulfide bonds (Mosesson *et al*., 2001; Standeven, 2005; Sjøland, 2007; Tsurupa *et al.*, 2009; Weisel, 2004; Weisel & Litvinov, 2013). The amino-termini of the α and β polypeptide chains in the E-region are known as fibrinopeptide A (FPA) and B (FPB) respectively (Pulanić & Rudan, 2005). FPA, consisting of 16 residues, and FPB, consisting of 14 residues, are the two sites in the E-region for thrombin cleavage (Riedel *et* al., 2011; Yang *et al*., 2000). Each D-region is made up of the carboxyl-termini of the β- and γ-polypeptide chains, whereas the carboxyl-termini of the α-chains are extended into αC-domains as a protuberance beyond the D-regions (Tsurupa *et al.*, 2009). The αC-domain connects the three polypeptides in each D-region, forming a "fourth strand" in the coiled coil, with globular-like end structures located near the E-region (Ariëns *et al.*, 2002). Both αC-domains make up about 25 % of the mass of fibrinogen and play a vital role in the cross-linking of the fibrin clot (Ariëns *et al.*, 2002). This is discussed further in Section 2.2.2. In summary, the region composition of a fibrinogen molecule can be simplified as "D-coil-E-coil-D". A depiction of fibrinogen is shown in Figure 2-3.

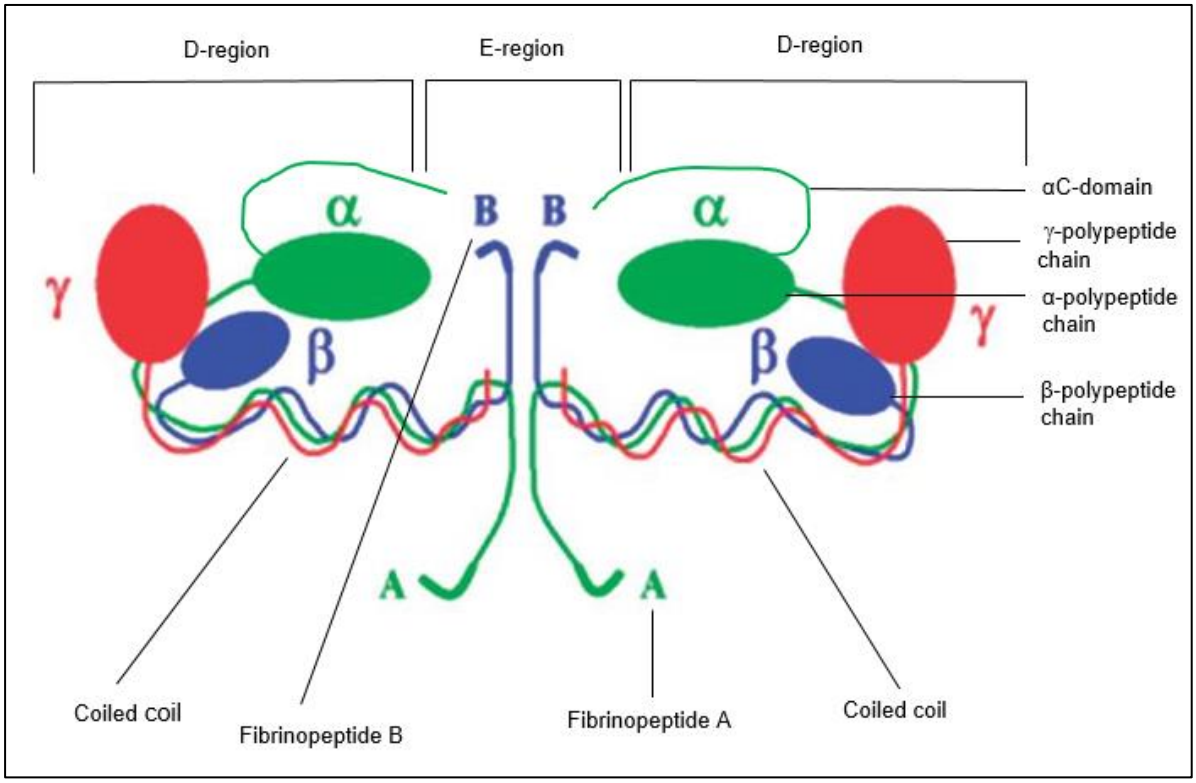

Figure 2-3: Structure of fibrinogen (Adapted from Berg *et al.* (2002), Standeven *et al.* (2005))

Upon activation of the coagulation cascade, the soluble fibrinogen molecule is converted to fibrin, forming a gel-like network (Bridge *et al*., 2014, Liu *et al*., 2010). The process of this fibrin clot formation is discussed in Section 2.2.2.

2.2.2 Process of clot formation

Thrombin converts fibrinogen to fibrin monomers by inducing the cleavage of firstly FPA at a rapid rate and subsequently FPB at a slower rate, from the α and β chains respectively, initiating the spontaneous aggregation and polymerisation of fibrin monomers as depicted in Figure 2-4 (Bridge *et al*., 2014; De Moerloose *et al*., 2010; Mills, 2002; Pulanić & Rudan, 2005; Riedel *et al*., 2011; Weisel, 2007). Four polymerisation sites (knobs) in the E region are exposed consequent to the release of FPA (E_A) and FPB (E_B) during thrombin-mediated cleavage (Mosesson, 1998; Mosesson *et al*., 2002; Riedel *et al*., 2011; Yang *et al*., 2000). Each binding site (hole) then binds to a complementary site (D_a or D_b) in the D-region of a different fibrin molecule (Mosesson *et al*., 2002; Riedel *et al.*, 2011; Yang *et al*., 2000). E_A fits into D_a located on the distal carboxyl-termini of the γ-polypeptide chains and E_B fits into D_b located on the distal carboxyl-termini of the β-polypeptide chains (Mosseson *et al*., 2001;

Weisel, 2005; Yang *et al*., 2000). The half-staggered fibrin monomers link to each other forming two-stranded protofibrils that have a cross-striation periodicity of 22.5 nm (Riedel *et* al., 2011; Weisel, 2007; Weisel & Litvinov, 2013). These protofibrils aggregate laterally in a specific way to form thicker fibrils, by twisting around each other forming fibrin fibres (Mosseson *et al*., 2001; Weisel, 2007; Weisel & Dempfle, 2013). As fibrin fibre growth continues with the addition of new protofibrils, the periodicity is maintained, and therefore the protofibrils must be stretched to a certain degree (Standeven *et al*., 2005; Weisel, 2007). Fibre growth stops when the energy of protofibril bonding is less than the energy needed for stretching (Standeven *et al*., 2005; Weisel, 2007).

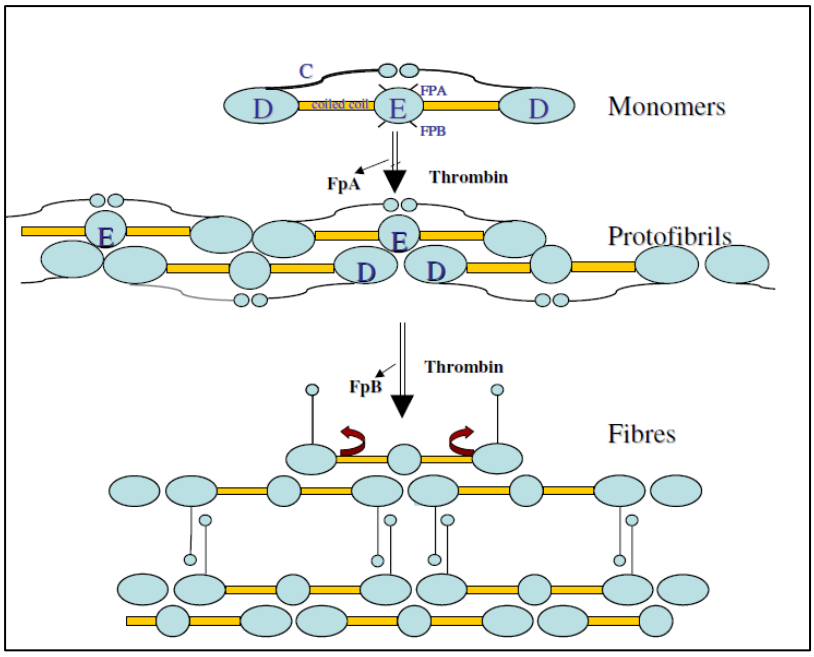

Figure 2-4: Fibrin polymerisation (Standeven *et al*., 2005)

After polymerisation, branching takes place forming the three-dimensional fibrin clot network (Weisel, 2007; Weisel & Litvinov, 2013). Branching plays a vital role in fibrin network structure, with the existence of two types of branching (Mosesson, 2005; Mosesson *et al*., 2001). The first type of branching, called a tetramolecular or bilateral branch junction, forms when two double-stranded fibrils joined side-to-side are cleaved (Mosesson, 2005; Mosesson *et al*., 2001) (Figure 2-5). This type of branching provides rigidity and strength to the fibrin network structure (Mosesson *et al*., 2001). The second type of branching, known as a trimolecular or equilateral branch junction, is formed by the cleavage of one double-stranded fibril, equal in thickness (Mosesson, 2005; Mosesson *et al*., 2001) (Figure 2-5). When the cleavage of fibrinopeptides is slow, equilateral branches will form at a greater frequency; this allows for a more branched fibrin network with fewer pores (Mosesson, 2005; Mosesson *et al*., 2001). There is a general indirect association between the quantity of

branch points in a clot structure and the fibrin fibre diameter, i.e. as the amount of branch points increase, the fibres become thinner (Weisel & Dempfle, 2013).

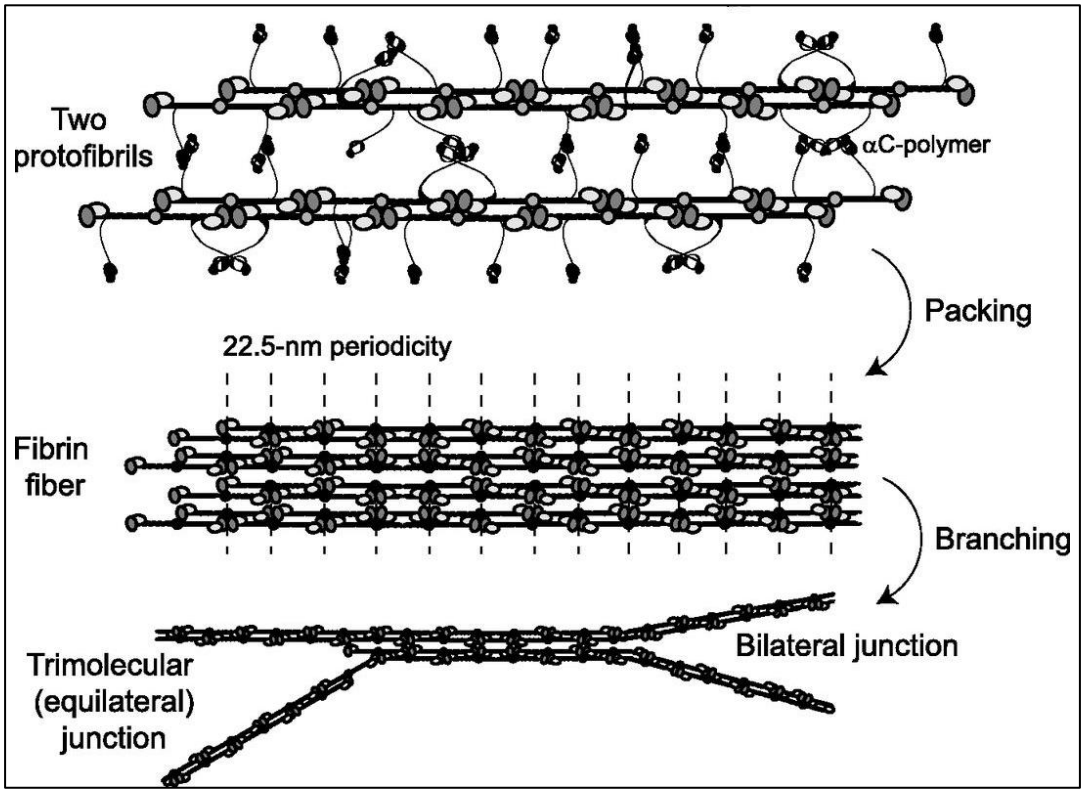

Figure 2-5: Branching types – bilateral junction and trimolecular (equilateral) junction (Weisel *et al*., 2013)

During the final events of the coagulation cascade, in the presence of fibrin, FXIII is converted to its active form (FXIIIa) by thrombin to ensure a stable fibrin clot by inducing the covalent cross-linkage of fibrin polymers (Kamath & Lip, 2003; Pulanić & Rudan, 2005; Standeven *et al*., 2005). A depiction of cross-linking is shown in Figure 2-6. Cross-links are formed initially between the γ-polypeptide chains, subsequently followed by the cross-linkage of the α-polypeptide chains at the αC-domains in the D-regions (Ariëns *et al.*, 2002; Davie *et al.*, 1991). The γ-chain cross-linking takes approximately 5 to 10 minutes, joining the D-regions of two fibrin polymers with two isopeptide bonds (Ariëns *et al.*, 2002). The cross-linkage of the α-chains occur at a slower rate than that of the γ-polypeptide chains (Ariëns *et al.*, 2002; Weisel & Dempfle, 2013). Cross-linking stabilises the three-dimensional fibrin network by forming an elastic and rigid structure with the ability to stop any bleeding in the vasculature (Pulanić & Rudan, 2005; Standeven *et al*., 2005). A cross-linked fibrin clot is a strong clot, less susceptible to any mechanical disturbances or proteolytic reactions (Davie *et al.*, 1991; Standeven *et al*., 2005). By critically affecting the stability of a fibrin clot, the degree to which cross-linking occurs is a determinant of thrombosis and haemostasis,

influencing viscoelastic properties of the formed fibrin clot as well as fibrinolysis regulation (Ariëns *et al.*, 2002; Kattula *et al*., 2017).

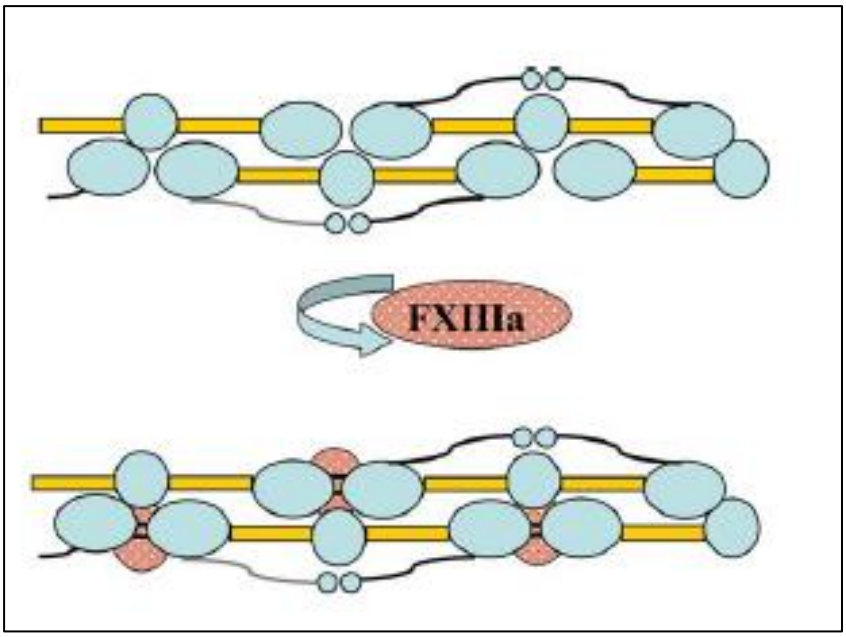

Figure 2-6: Cross-linking (Standeven *et al*., 2005)

2.2.3 Clot properties and thrombotic disease

Generally, clots that have thinner fibres which are densely packed, with smaller pores and a larger quantity of branch points, have an increased resistance to fibrinolysis (Dunn & Ariëns, 2004). A clot's resistance to fibrinolysis may increase an individual's risk of CVD, as observed in both arterial and venous thrombotic disease patients (Bridge *et al*., 2014; Collet *et al.,* 1996; Dunn & Ariëns, 2004; Fatah *et al*., 1992). The following section describes the role of fibrin clot properties in different types of thrombotic diseases.

2.2.3.1 Arterial thrombotic disease

The formation of a clot within an artery is known as an arterial thrombus, generally triggered when an atherosclerotic plaque ruptures (Mackman, 2008). This type of clot can lead to myocardial infarction (MI), ischemic stroke, coronary artery disease (CAD) or peripheral arterial disease (PAD) (Bridge *et al*., 2014; Mackman, 2008). Arterial thrombi are often referred to as white clots, as they are generally rich in platelets and are not largely reliant on fibrin for clot formation (Casa *et al*., 2015; Litvinov & Weisel, 2016b; Tracy, 2003). These clots are formed in conditions where blood flow has a high shear rate, resulting in rapid platelet aggregation where all bleeding is ceased through a process reliant on platelets

(Casa *et al*., 2015, Sakariassen *et al*., 2015). This process contributes to the rate and extent of arterial clot formation and is crucial for the prevention of large bleeding in the arterial system (Casa *et al*., 2015; Sakariassen *et al*., 2015). However, fibrin has been found to be a major component of arterial clots related to CAD and acute middle cerebral artery ischemic stroke with fibrin constituting 60% of those ischemic stroke clots (Liebeskind *et al*., 2011; Silvain *et al*., 2011). The prevalence of fibrin in these clots has been shown to increase with post-occlusion age, where older clots contain a larger percentage of fibrin due to an existing positive correlation between thrombus fibrin content and ischemic time (Silvain *et al*., 2011). The structure of *ex vivo* plasma clots related to a variety of arterial thrombotic diseases have been shown to be altered with an increase in mechanical rigidity and an increased resistance to fibrinolysis (Collet *et al*., 2006; Litvinov & Weisel, 2016b) as detailed below.

Ex vivo plasma clots from patients with CAD have been found to be less permeable, with an increased fibrin polymerisation rate and an increased resistance to fibrinolysis compared to clots from healthy individuals (Pretorius *et al*., 2011; Undas *et al*., 2009c; Undas *et al*., 2010b). An association has also been found between premature CAD and fibrin clot structure. Clots formed from these patients were less permeable (smaller pore sizes) with an enhanced resistance to fibrinolysis (Collet *et al*., 1996; Fatah *et al*., 1992; Mills *et al*., 2002; Scrutton *et al*., 1994). Compared with acute CAD, *ex vivo* plasma fibrin clots from patients with stable CAD had a higher permeability and lower resistance to fibrinolysis (Litvinov & Weisel, 2016b; Undas *et al*., 2008a). Abnormal tightness and stiffness of *ex vivo* plasma clots, with an enhanced resistance to fibrinolysis, have also been associated with the prevalence of advanced CAD in elderly patients (mean age of 62 years) (Bridge *et al*., 2014; Undas *et al*., 2007) compared to healthy individuals of the same age group.

Young patients with a previous MI, formed *ex vivo* plasma fibrin clots that are tighter and stiffer, with a higher resistance to fibrinolysis, compared to healthy individuals (Blomback *et al*., 1992; Bridge *et al*., 2014; Collet *et al*., 2006; Fatah *et al*., 1996). Plasma fibrin clots from acute MI patients were found to have an increased fibrin fibre diameter and higher fibrin polymerisation rate compared to patients with stable angina (Undas *et al*., 2008b; Undas, 2014). Figure 2-7b depicts a scanning electron microscopy (SEM) image of a plasma clot from a MI patient.

Ischemic stroke patients also show altered fibrin clot structure with *ex vivo* plasma clots presenting with increased fibrin polymerisation, lower permeability, increased density and increased resistance to fibrinolysis (Bridge *et al*., 2014). A study conducted by Undas *et al.* (2009c) showed that plasma clots from ischemic stroke patients are denser and have a larger fibrin fibre diameter with enhanced resistance to fibrinolysis. The reduced permeability

and increase in resistance to fibrinolysis suggests hypo-fibrinolysis as a persistent characteristic of ischemic stroke clots (Rooth *et al*., 2011). Figure 2-7c depicts a SEM image of a plasma clot from an ischemic stroke patient.

2.2.3.2 Venous thrombosis

Venous thrombi, formed within a vein, are often referred to as red clots, as they are generally rich in erythrocytes (red blood cells) and fibrin (Casa *et al*., 2015; Litvinov & Weisel, 2016b). Venous thrombi generally manifest as pulmonary embolism (PE) and deep-vein thrombosis (DVT) (Mackman, 2008). In some venous clots, the concentration of fibrin is more than erythrocytes, with fibrin constituting 80% of clots obtained from acute PE patients (Mazur *et al*., 2013; Undas *et al.,* 2010a). Venous clots differ from arterial thrombi as they occur in conditions where blood flow has a low shear rate or in the presence of stagnant blood flow which consequently contributes to the rate and extent of venous clot formation (Casa *et al*., 2015). As in arterial disease, fibrin clot structure is altered in venous thrombotic disease patients (Bridge *et al*., 2014).

Ex vivo plasma clots of patients with venous thromboembolic (VTE) disease demonstrated reduced permeability, consisted of fibres that were densely packed, with an increased resistance to fibrinolysis in comparison to healthy individuals (Bridge *et al*., 2014; Undas *et al.*, 2009a). Hypo-fibrinolysis is also thought to be a persistent characteristic of the clots of DVT patients with a higher polymerisation rate than PE fibrin clots (Lisman *et al*., 2005; Undas *et al*., 2009a). DVT patients, with residual vein thrombosis (RVT) as a complication, presented with even denser plasma clots with lower permeability and a higher polymerisation rate (Undas *et al*., 2012; Zolcinski *et al*., 2012). Figure 2-7a depicts a SEM image of a plasma clot from a DVT patient.

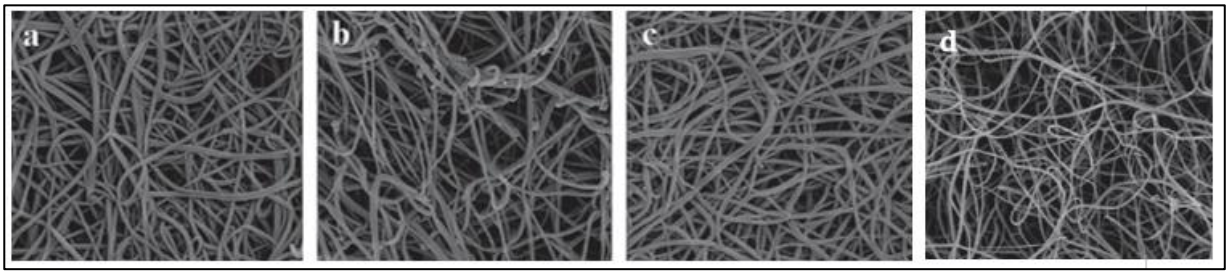

Figure 2-7: Scanning electron microscope (SEM) images of plasma clots from (a) deep-vein thrombosis patients, (b) myocardial infarction patients, (c) ischemic stroke patients and (d) healthy controls (Undas, 2014)

Regardless of the known characteristics of arterial thrombi (platelet rich) and venous thrombi (erythrocyte and fibrin rich), the structural properties of *in vitro* fibrin clots in both arterial and venous thrombotic diseases are similar (Litvinov & Weisel, 2016b). This suggests that fibrin is a major component of not only venous thrombi but also arterial thrombi and must therefore be considered when managing both types of thrombotic diseases (Litvinov & Weisel, 2016b).

2.3 MEASURING CLOT PROPERTIES

2.3.1 Overview: Fibrin network determinations

The gel network of a formed fibrin clot is characterised and determined by clot formation kinetics as well as its structural and mechanical properties (Collet *et al*., 1996; Weisel & Nagaswami, 1992). Clot properties can be determined by various direct and indirect methods. A summary of these methods is provided in this section.

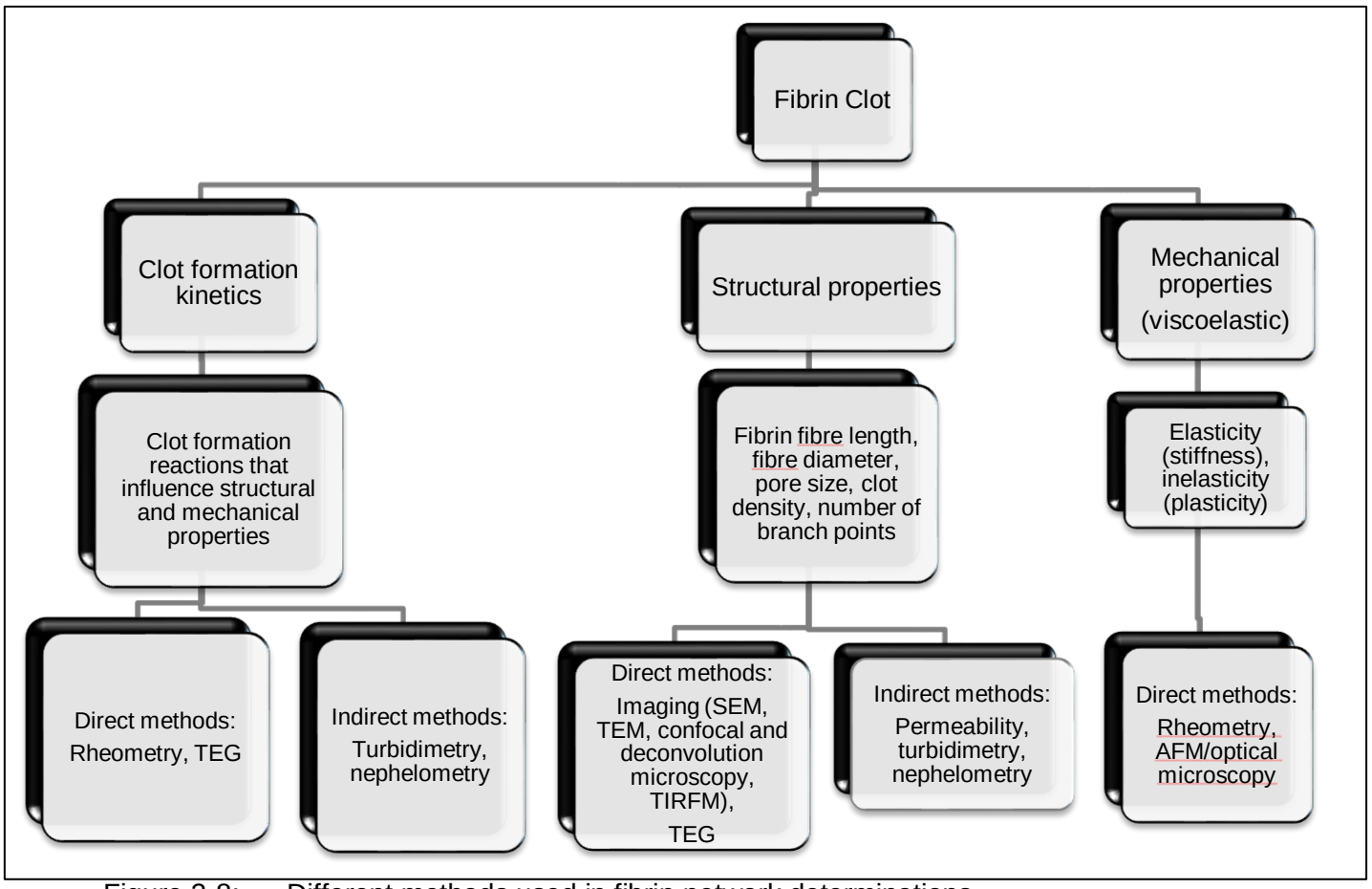

Figure 2-8: Different methods used in fibrin network determinations

SEM = scanning electron microscopy; TEM = transmission electron microscopy; TIRFM = total internal reflection fluorescence microscopy; TEG = thromboelastography; AFM = atomic force microscopy

2.3.1.1 Kinetics of clot formation

The kinetics of clot formation is greatly involved in determining the final clot structure (Sjøland, 2007). Blood coagulation results in the formation of a three-dimensional fibrin network, as described in Section 2.2. The direct methods used to determine clot formation kinetics include rheometry and TEG (Evans *et al*., 2008a; Evans *et al*., 2008b; Litvinov & Weisel, 2016a); the indirect methods include nephelometry (Morais *et al*., 2006) and turbidimetry (Carter *et al*., 2007; Morais *et al*., 2006; Sjøland, 2007; Weisel & Nagaswami, 1992). Turbidimetry is discussed in more detail in Section 2.3.2, as this technique forms the focal point of this mini-dissertation.

2.3.1.2 Structural properties

Structural clot properties include fibrin fibre length, diameter, pore size, branch points, as well as the density of the clot (Weisel & Dempfle, 2013). The direct methods used to

determine these properties include imaging techniques namely scanning electron microscopy (SEM), transmission electron microscopy (TEM), total internal reflection fluorescence microscopy (TIRFM) and light microscopy techniques (confocal and deconvolution microscopy) (Chernysh & Weisel, 2008; Hategan *et al*., 2013; Sjøland, 2007).

Investigating structural clot properties using SEM requires fibrin clots to be rinsed, dehydrated, dried and mounted on SEM stubs. Subsequently the clots are sputter coated with a layer of gold or palladium forming conductive materials, to generate electromagnetic radiation (CFAMM, 2016). Electrons are focused into the conductive clots, where atoms are charged and secondary electrons are released (Sjøland, 2007). The clot's surface is then scanned, computing a SEM image as depicted in Figure 2-9 (Sjøland, 2007). This microscope is made up of six main components namely, an electron column, vacuum and scanning system, detector, display screen and controls as illustrated in Figure 2-10. Images can be magnified extensively and provide information on the density, fibre diameter and branching points of the visualised clot (Sjøland, 2007).

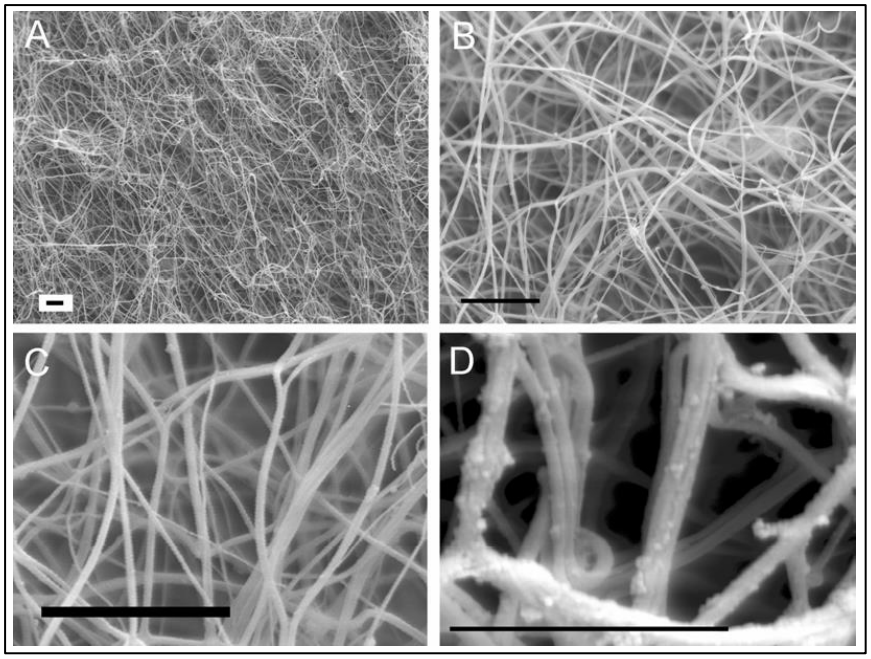

Figure 2-9: Fibrin clot scanning electron microscope (SEM) images at a magnification of (A) x1 700, (B) x5 000, (C) x12 000 and (D) x80 000 (Sjøland, 2007)

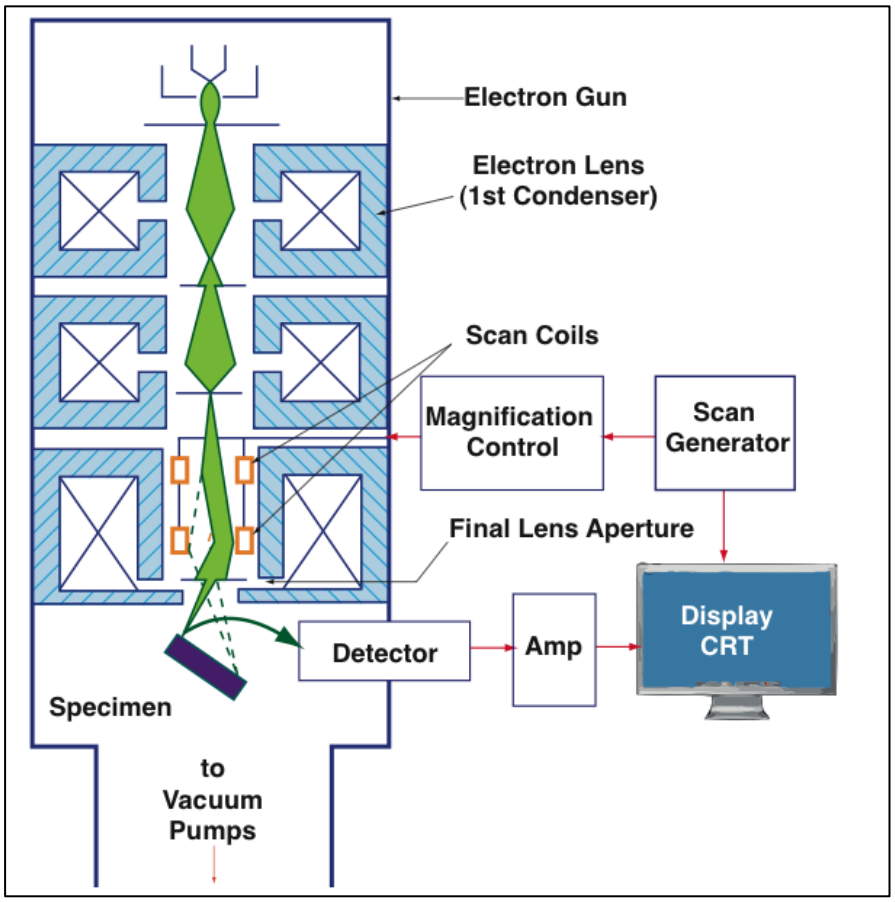

Figure 2-10: Main components constituting a scanning electron microscope (SEM) (CFAMM, 2016)

Light microscopy techniques are highly effective in investigating hydrated samples and assessing time-dependent changes in a sample (Chernysh & Weisel, 2008). The basic principle in confocal microscopy is based on the blockage of all unfocused fluorescent light so as to collect light solely from the focal plane, increasing the signal to noise ratio (Chernysh & Weisel, 2008). Deconvolution microscopy is based on the principle of excluding light from below and above the focal plane and is effective in forming quality images of light-sensitive samples at extremely low lighting over an extended time period (Chernysh & Weisel, 2008). The wave propagation technique, thromboelastography (TEG), is also used to directly determine structural clot properties (Evans *et al*., 2008a; Evans *et al*., 2008b; Litvinov & Weisel, 2016a). This technique involves immersing a small cylindrical pin into a plasma sample within a round cuvette, slowly rotating the cuvette, progressing in circular amplitude as clot stiffness increases (Litvinov & Weisel, 2016a).

The indirect methods used to determine structural properties include clot turbidimetry, nephelometry and permeability measurements (Morais *et al*., 2006; Undas & Zeglin, 2006c). Turbidimetry and nephelometry are similar techniques used to measure turbidity based on the concept of scattering light by a solution with dispersed particles (Lawler, 2005; Morais *et al*., 2006). A detailed description of turbidimetry is provided Section 2.3.2. The difference between turbidimetry and nephelometry is that in nephelometry the detector is situated at set angle, 37°, 70° or 90°, from the incident light beam, whereas in turbidimetry a specific angle is not used (Morais *et al*., 2006). Nephelometry is preferred over turbidimetry when measuring solutions with smaller particles and lower turbidity (Lawler, 2005; Morais *et al*., 2006).

In fibrin clots, the permeability coefficient (Ks) represents the shape and size of the pores in the fibrin gel and is an important determinant of the transport of fibrinolytic agents, thereby the fibrinolysis rate (Blomback & Okada, 1982; Van Gelder *et al*., 1995). A major advantage of this method is that the fibrin gel structure is not disturbed (Carr *et al*., 1977). The permeability assay is conducted using permeation stands (Figure 2-11), specifically built for this method, where clots are placed in a container attached to the permeation stand. The clot is then permeated with a buffer at a specific pressure for a specific time period and the volume of permeate collected used to calculate the average pore size in cm^2. A detailed description of the method is given in Chapter 3.

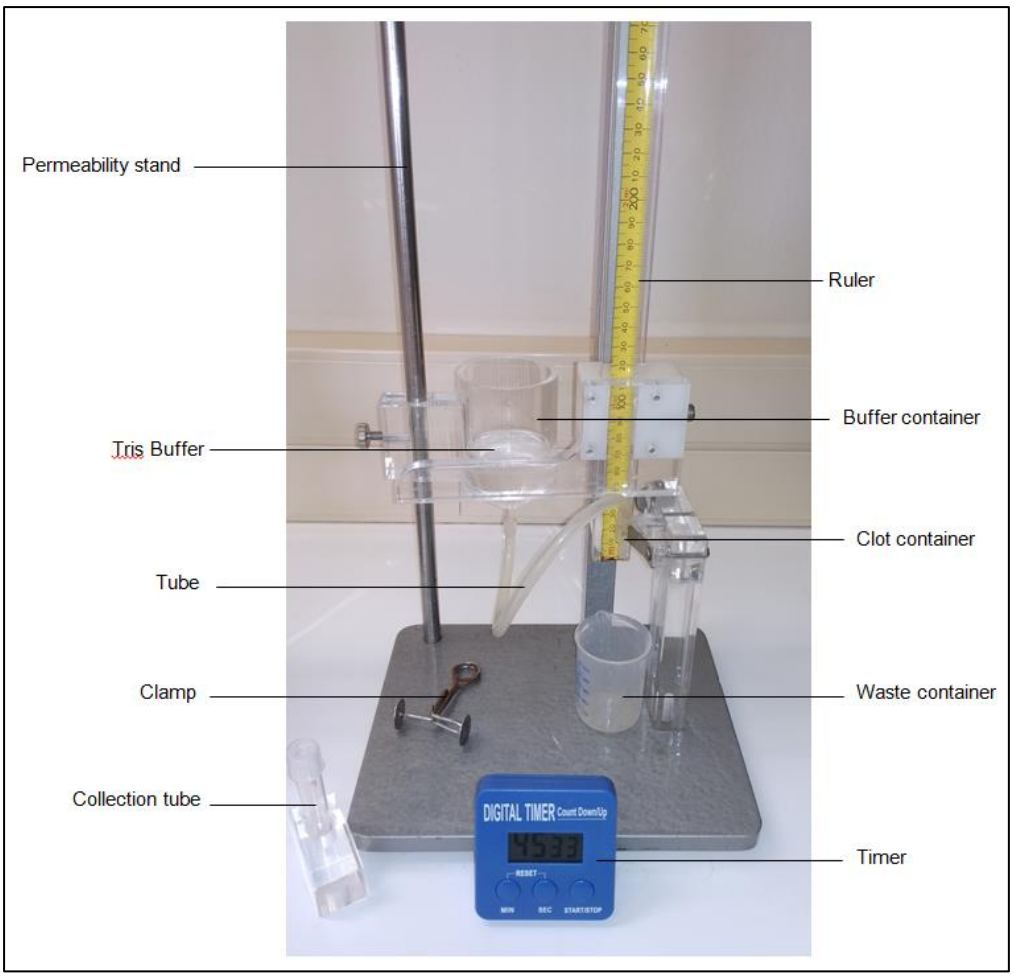

Figure 2-11: Permeability assay apparatus

2.3.1.3 Mechanical (viscoelastic) properties

The structural properties of the fibrin network significantly influence the mechanical (viscoelastic) clot properties, therefore influencing clot behaviour in the vasculature (Evans *et al*., 2008a; Evans *et al*., 2008b). The mechanical properties include the elasticity / storage modulus (G') and inelasticity / loss modulus (G'') of the clot, where the storage modulus describes clot stiffness and the loss modulus describes the inelastic part of the clot (plasticity) (Martinez *et* al., 2014; Weisel, 2004). During the conversion of fibrinogen into a fibrin gel network, an elastic-viscous fluid (pre-gel) is converted into a viscoelastic solid (post-gel) (Evans *et al*., 2008b). The clot's ability to simultaneously form a stable, rigid plug and withstand blood flow pressure, as well as allowing the perfusion of lysis agents, is influenced by these properties (Weisel, 2004; Weisel & Dempfle, 2013). Mechanical clot properties can be determined by using direct measures including techniques such as rheometry with the use of rheometers and combined AFM / optical microscopy (Litvinov & Weisel, 2016a; Liu *et al*., 2010; Ryan *et al*., 1999).

AFM, a type of scanning probe microscopy (SPM), makes use of a silicon or silicon nitride cantilever that touches the analysed sample with its sharp tip, measuring the sample's oscillation or deflection amplitude (Geisse, 2009). Combining AFM with an optical microscope allows for characterisation of a variety of samples, integrating the capability to image live processes to the AFM's higher resolution (Geisse, 2009).

Rheometry is performed with the use of a rheometer generally consisting of two plates set at a specific temperature; where the clot is formed on the base plate and a stainless-steel flat plate or cone set at a certain geometric gap perform the measurements. Various types of rheometers include concentric-cylinder, capillary-tube, cone-and-plate and rotational rheometers (Guthold *et al*., 2004; Kim, 2002). Several procedures (tests) can be conducted by a rotational rheometer including flow, step transient, oscillation and axial tests (TA Instruments, 2017). Figure 2-12 illustrates a rotational rheometer, the ARES-G2 (TA Instruments, New Castle, Delaware, USA).

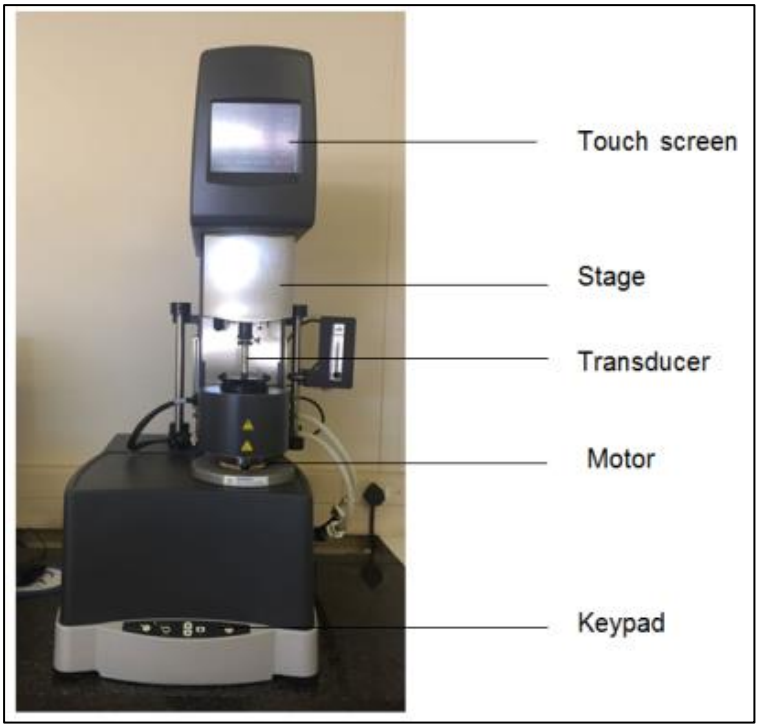

Figure 2-12: ARES-G2 rheometer

2.3.2 Turbidimetry

Turbidimetry is a concept based on the timely changes of light absorbance of a solution, with the use of a spectrophotometer (Lawler, 2005). In a cuvette where solid particles are dispersed, light will pass through the clear medium and be either absorbed, transmitted or

scattered in many directions (Lawler, 2005). This turbidimetric method measures the concentration of the observed substance, the quantity of light absorbed and the quantity of light transmitted (Carr & Hermans, 1978; Sjøland, 2007). Fibrin polymerization can be observed over time by measuring the quantity of light transmitted through the solution after a clotting agent such as thrombin or tissue factor has been added to the fibrinogen solution (Sjøland, 2007). The developing fibrin fibres cause scattering of light, which leads to an increase in the turbid appearance of the clotting solution as light absorbency increases (Carr & Hermans, 1978; Sjøland, 2007).

Turbidity is recorded onto a curve, where light absorbency is plotted against time (Sjøland, 2007), as depicted in Figure 2-13. From this turbidimetric curve three main variables can be obtained, namely the lag time, slope and maximum absorbance. The lag time indicates the time required for the adequate growth of fibrin fibres for lateral aggregation to commence (Weisel & Nagaswami, 1992). This variable is sensitive to, amongst others, fibrinogen levels and the fibrinopeptide A cleavage rate (Dunn *et al*., 2004). The slope indicates the rate of lateral aggregation (Mills *et al*., 2002; Pieters *et al*., 2008; Weisel & Nagaswami, 1992), while maximum absorbance is an indication of the fibrin fibre diameter at a fixed fibrinogen concentration (Chernysh & Weisel, 2008; Mills *et al.,* 2002; Pieters *et al*., 2008; Sjøland, 2007).

In comparison to direct methods, turbidimetry is a fast technique used to determine structural clot properties indirectly (Carter *et al.*, 2007; Morais *et al.*, 2006). A major advantage of turbidimetry is that the fibrin gel structure is not disturbed, as mechanical stresses that could possibly cause changes to the clot structure are avoided (Carr *et al*., 1977). This high-throughput method can be used in large-scaled clinical and epidemiological studies with good reproducibility (Carter *et al.*, 2007; Morais *et al.*, 2006).

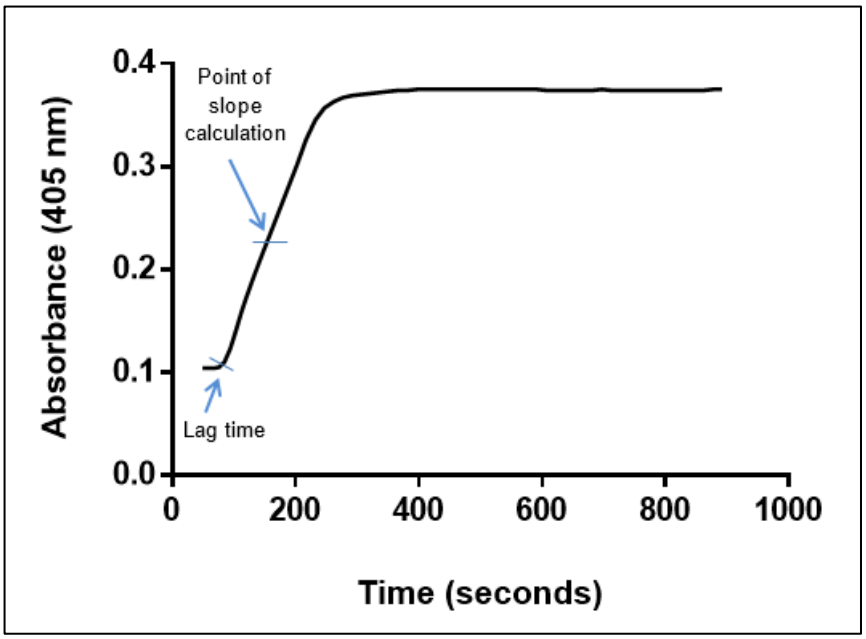

Figure 2-13: Illustration of turbidimetric curve (Pieters *et al.,* 2018)

Turbidimetry has been successfully used in studies using purified fibrinogen solutions where each sample had a similar fibrinogen concentration. Under these conditions, maximum absorbance is directly related to fibrin fibre diameter (thicker fibres) (Carr & Hermans, 1978; Mills *et al.,* 2002; Pieters *et al*., 2008; Weisel & Nagaswami, 1992). However, in plasma samples, where fibrinogen concentrations vary, it is difficult to interpret maximum absorbance, as it is also known to increase with increased fibrinogen concentration, which in turn is associated with the formation of denser clots consisting of thinner fibres (Mills *et al.,* 2002; Sjøland, 2007; Undas *et al*., 2006c). The increased maximum absorbance associated with increased plasma fibrinogen concentration may thus be a reflection of increased protein density rather than fibre diameter. Using maximum absorbance to identify an individual's CVD risk can be ambiguous as the interpretation can either be an indication of fibre thickness (thicker fibres lyse faster subsequently lowering the risk of CVD) or protein density (denser clots lyse slower subsequently increasing the risk of CVD) (Bridge *et al*., 2014; Collet *et al.,* 1996; Dunn & Ariëns, 2004; Fatah *et al*., 1992). Table 2-1 clearly depicts the ambiguous interpretation of maximum absorbance in plasma samples. The numerous studies described in Table 2-1, interpret maximum absorbance solely as an indication of fibrin fibre thickness, leading to contradictory results among turbidimetry plasma studies.

Table 2-1: Fibrin structure properties in thrombotic disease patients compared to healthy controls in plasma samples

Study reference	**Study design; number of subjects**	**Thrombotic disease**	**Fibrinogen concentration (disease *vs*. control)**	**Maximum absorbance interpreted from turbidimetry (disease *vs*. control)**	**Fibre thickness measured / interpreted from turbidimetry (disease *vs*. control)**	**Porosity measured from permeability assay (Ks) (disease *vs*. control)**	**Clot density (disease *vs*. control)**
Mills *et al*., 2002	Case control; 100 (males only)	Premature coronary artery disease	↑	↑	↓ (thinner fibres) *SEM*	↓	↑ *Interpretation from SEM images*
Undas *et al*., 2006b (At baseline)	Case-control; 48 (males only)	Advanced coronary artery disease	↔	↓	↓ * (thinner fibres)	↓	Not stated
Undas *et al*., 2006c	Case-control; 40 (males only)	Acute myocardial infarction	↑	↓	↓ * (thinner fibres)	↓	Not stated
Undas *et al*., 2009c	Case-control; 147	Ischemic stroke	↔	↑	↑ (thicker fibres) *SEM*	↓	↑ *Interpretation from SEM images*
Undas *et al*., 2009a	Case-control; 100	Venous thromboembolism	↔	↑	↑ * (thicker fibres)	↓	↑ *Interpretation from Ks and ↑ CLT*

Table 2-1 continued

Study reference	Study design; number of subjects	Thrombotic disease	Fibrinogen concentration (disease *vs*. control)	Maximum absorbance interpreted from turbidimetry (disease *vs*. control)	Fibre thickness measured / interpreted from turbidimetry (disease *vs*. control)	Porosity measured from permeability assay (Ks) (disease *vs*. control)	Clot density (disease *vs*. control)
Palka *et al*., 2010	Case-control; 36	Chronic heart failure	↑	↔	↔	↓	Not stated
Undas *et al*., 2010b	Case-control; 45	Acute ischemic stroke	↑	↑	↑ * (thicker fibres)	↓	Not stated
Undas *et al*., 2010c	Case-control; 47	In-stent thrombosis	↔	↑	↑ * (thicker fibres)	↓	↑ *Interpretation from Ks and ↑ CLT*
Undas *et al*., 2011b	Case-control; 106	Peripheral arterial disease	↔	↑	↑ * (thicker fibres)	↓	↑ *Interpretation from Ks*
Undas *et al*., 2011b	Case-control; 20	Thromboangiitis obliterans (Buerger disease),	↑	↑	↑ * (thicker fibres)	↓	↑ *Interpretation from Ks*
Okraska-Bylica *et al*., 2012	Case-control; 31	Peripheral arterial disease (< 55 yrs)	↔	↔	Not stated	↓	Not stated

Table 2-1 continued

Study reference	Study design; number of subjects	Thrombotic disease	Fibrinogen concentration (disease *vs*. control)	Maximum absorbance interpreted from turbidimetry (disease *vs*. control)	Fibre thickness measured / interpreted from turbidimetry (disease *vs*. control)	Porosity measured from permeability assay (Ks) (disease *vs*. control)	Clot density (disease *vs*. control)
Pera *et al*., 2012	Case-control; 52	Ischaemic stroke	↔	↓	Not stated	↓	Not stated
Pera *et al*., 2012	Case-control; 49	Hemorrhagic stroke	↔	↓	Not stated	↓	Not stated
Zolcinski *et al*., 2012 (At baseline)	Case-control; 28	First occurrence of venous thromboembolism	↔	↑	Not stated	↓	Not stated
Bouman *et al*., 2016	Case-control; 60	Long-term history of venous thromboembolism	↔	↓	↓ * (thinner fibres)	↔	↑ *Interpretation from turbidimetry*
Siudut *et al*., 2015	Case-control; 50	Cerebral venous sinus thrombosis	↔	↑	Not stated	↓	↑ *Interpretation from Ks*

SEM = scanning electron microscopy; LSCM = laser scanning confocal microscopy; CLT = clot lysis time; ↑ = higher than healthy controls; ↓ = lower than healthy controls; ↔ = equivalent / similar to healthy controls

*Interpretation by authors based on maximum absorbance data

As presented in Table 2-1, Undas *et al*. (2009c) showed an increased maximum absorbance in ischemic stroke patients associated with thicker fibres from the SEM results. Mills *et al.* (2002) also found an increased maximum absorbance in premature CAD patients; however, the SEM results showed the fibrin fibres to be thinner. This controversy could potentially be explained by the influence of varying fibrinogen concentration on maximum absorbance. In Undas *et al*. (2009c) there was no difference in fibrinogen concentration between the healthy controls and stroke patients, and therefore the higher maximum absorbance may indeed reflect thicker fibres. However, in Mills *et al*. (2002) fibrinogen concentration does vary with the CAD patients having a higher concentration than the healthy controls. This higher fibrinogen concentration could potentially explain why a higher maximum absorbance was associated with thinner fibres.

With regard to maximum absorbance's relation to CVD, studies conducted by Bouman *et al*. (2016) and Undas *et al.* (2006b) showed a decreased maximum absorbance in advanced CAD and VTE patients, respectively. On the other hand, Undas *et al.* (2009a), Undas *et al.* (2010c) and Undas *et al*. (2011b) showed an increased maximum absorbance in VTE, in-stent thrombosis and PAD patients, respectively. All five studies deduced fibre thickness based solely on maximum absorbance data without any conducted direct measurements.

Some studies (Mills *et al*., 2012; Undas *et al*., 2010b; Undas *et al*., 2011b) found an increased maximum absorbance associated with a higher fibrinogen concentration; whereas Undas *et al*. (2006c) contradicts those findings showing that a decreased maximum absorbance in acute MI patients is associated with a higher fibrinogen concentration. There are also studies where an increased maximum absorbance (Undas *et al*., 2009c; Undas *et al*., 2009a; Undas *et al*., 2010c; Undas *et al*., 2011b;Zolcinski *et al*., 2012) and a decreased maximum absorbance (Undas *et al*., 2006b; Pera *et al*., 2012; Bouman *et al*., 2016) were shown in the absence of varying fibrinogen concentrations between cases and controls.

Conflicting results are also shown with regard to the association between maximum absorbance and permeability. In some studies (Mills *et al*., 2002; Siudut *et al*., 2015; Undas *et al*., 2009c; Undas *et al*., 2009a; Undas *et al*., 2010c; Undas *et al*., 2011b) an increased maximum absorbance is associated with lower permeability and denser clots, whereas in other studies (Pera *et al*., 2012; Undas *et al*., 2006b; Undas *et al*., 2006c) it is associated with higher permeability.

The ambiguity presented in Table 2-1 clearly demonstrates the necessity for investigating the correct interpretation of the maximum absorbance variable obtained from turbidimetry when analysing plasma samples.

2.4 CONCLUSION

The structural and mechanical properties of the fibrin network comprising a thrombotic clot are vital to the behaviour and lysis of the clot in the vasculature. Various direct and indirect methods are used to determine fibrin clot properties. The indirect method, turbidimetry, provides the variable maximum absorbance, used as an indicator of fibre thickness in purified fibrinogen systems. However, from this review it is evident that the interpretation of maximum absorbance in plasma samples with varying fibrinogen concentration is less clear. We aim to elucidate this ambiguous interpretation of maximum absorbance in plasma samples. In addition to total fibrinogen concentration and turbidimetry, the present study characterises plasma fibrin clot properties in detail using SEM (fibrin fibre diameter), rheometry (mechanical / viscoelastic properties) and clot permeability to provide an in-depth characterisation of clots with different maximum absorbance values in order to determine whether differences in maximum absorbance are reflective of structural properties only, differences in the amount of fibrin present in the sample or a combination of both. The methodology used to determine fibrin network characteristics in this study, as shortly described in Section 2.3.1, is presented in detail in Chapter 3.

CHAPTER 3: METHODS

3.1 INTRODUCTION

Ambiguity exists regarding the interpretation of maximum absorbance obtained from plasma samples as it is complicated by varying fibrinogen concentrations, and it is not entirely clear which fibrin property (or combination) it is indicative of. The aim of the study is to clarify the interpretation of maximum absorbance data obtained from turbidimetry in plasma samples, with varying fibrinogen concentrations, collected from black South Africans who participated in the Prospective Urban and Rural Epidemiological study in the North West Province, South Africa (PURE-SA). Specific objectives were to select individuals with varying maximum absorbance values, stratified for fibrinogen concentration across the fibrinogen concentration range and carry out the following:

- Measure plasma clot structural properties (fibre diameter, clot pore size) using a direct (SEM) and an indirect technique (permeability).
- Perform complementary measurements to determine mechanical clot properties (rheometry) as well as clot fibrin content.
- Relate the maximum absorbance value to measures of clot formation (lag time and slope obtained from turbidimetry), clot lysis (turbidimetry), structural properties (fibre diameter - SEM and pore size - Ks), mechanical properties (clot stiffness and plasticity - rheometry) as well as fibrin content while taking plasma fibrinogen concentration into consideration.
- Compare the association between maximum absorbance and the other measured clot properties with the association between fibre diameter and the other clot properties; to determine whether they are equivalent.
- Compare samples matched for fibrinogen concentration with low and high maximum absorbance values to characterise the fibrin clot properties of the two groups and to identify other biological factors that contribute to potential variance in clot properties in the two groups.

3.2 ETHICS APPROVAL

This sub-study is nested within one of the South African arms of the international Prospective Urban and Rural Epidemiological study (PURE) (Teo *et al*., 2009). Ethical approval for this sub-study was obtained from the Health Research Ethics Committee of the North-West University (NWU-HREC) (NWU-00034-17-A1-01) in June 2017 (refer to Addendum A for ethics certificate of sub-study). All members of the research team have completed NWU-HREC ethics training and carried out all aspects of the study in an ethically sound manner.

3.3 STUDY DESIGN

The large PURE study is an international study, with 27 countries taking part including South Africa. Two study sites exist in South Africa, one in the Western Cape and the other in the North West province, Potchefstroom. PURE-South Africa (SA, North West) is a prospective, epidemiological study, where the baseline data was collected in 2005 and follow-up data collected in 2010 and 2015. This sub-study is a cross-sectional study that made use of plasma samples obtained in 2015 from 900 participants who partook in the PURE study conducted in the North West province of South Africa.

For this sub-study, a sub-sample was selected based on maximum absorbance values and fibrinogen concentrations. The selection of these participants was done systematically, based on the already determined fibrinogen concentration and maximum absorbance values. Participants were stratified according to fibrinogen concentration (PURE fibrinogen concentration range: 1.5 – 7.5 g/L). Two individuals with the lowest and highest maximum absorbance value, respectively, in each 0.5 g/L fibrinogen concentration increment were selected for inclusion. Samples were selected across the physiological range of fibrinogen concentration, to include lower, normal and high fibrinogen levels.

3.3.1 Study population

In the North West PURE-SA study, Tswana speaking individuals from Ikageng, Zonderwater, Extension 7 or Extension 11 (urban settlements); Ganyesa (urban-rural town); or Tlakgameng (rural area) were recruited. The South African Department of Health, Potchefstroom and Ganyesa city mayors, tribal chiefs, community leaders and household heads, granted permission to access and recruit the participants. Individuals were eligible to

participate in the PURE study if they were older than 30 years, apparently healthy (no known diseases or conditions including tuberculosis, HIV positivity and lifestyle diseases) and were not using any acute or chronic medication. Participants were excluded if the household head refused permission for their participation in the study.

After being well informed regarding all aspects of the study, participants gave written voluntary informed consent prior to the baseline data collection in 2005. Participants were informed that they could withdraw from the study at any time, regardless of prior consent. Data collected included, demographic information, dietary, physical activity, psychosocial and anthropometric data and biological samples. All tests, measurements and sample collection were performed by well trained staff. Medical assistance was available in case of an emergency. All procedures were carried out in accordance to the revised version (2000) of the Helsinki Declaration of 1975. Participants received individual, confidential feedback on the day of data collection. All data was stored safely and kept confidential. Ethical approval was also obtained for the subsequent data collection in 2010 and 2015. Participants completed informed consent forms for each of the follow-up collections and all aspects of data collection, sample analyses and data management were ethically sound. Methods used to analyse the PURE 2015 data and pertaining to this MSc study specifically are presented in detail below.

3.4 MEASURING CLOT PROPERTIES

Blood samples were collected from each participant. Participants were required to fast for 10 hours prior to blood sample collection. Blood samples were collected between 7:00 am and 11:00 am. A quantity of 30 ml of fasting blood sample was collected into 3.2 % citrate tubes from the antecubital vein by a registered nurse with the use of sterile winged infusion sets and syringes with disposable needles. Samples were centrifuged at 2 000 g for 15 minutes within 30 minutes of collection to prepare platelet poor plasma (PPP), which was stored at -80 °C until analysis. This citrated plasma was then used to perform the fibrin network analyses, as discussed in sections 3.4.1 to 3.4.6. All safety procedures were followed in relation to handling of samples, reagents and bio-hazardous products. The haemostasis and fibrin network analyses performed for this sub-study consist of the following methods:

3.4.1 Total fibrinogen and fibrinogen γ' concentration

3.4.1.1 Total fibrinogen

Total fibrinogen concentrations were quantified using a modified Clauss method (Clauss, 1957) on the Automated Coagulation Laboratory (ACL) 200 (Instrumentation Laboratory, Milan, Italy). This analysis focuses on the prothrombin time, where rapid thrombin production and formation of fibrin fibres occur (Mackie *et al*., 2003).

A fibrinogen-C kit (HemosIL, Instrumentation Laboratory, Bedford, USA) was used where a high concentration of bovine thrombin (35 U/ml) was added to the plasma samples. A calibration plasma (HemosIL, Instrumentation Laboratory, Milan, Italy) containing 3.24 g/L fibrinogen, control pool plasma, factor diluent (HemosIL, Instrumentation Laboratory, Milan, Italy) acting as a buffer and a maximum of 14 samples per run were placed in the assigned positions of the ACL's rotor. The clotting time was then measured.

A standard curve was prepared, using a series of diluted calibration plasma at 25%, 50% and 100% to calculate the quantity of fibrinogen concentration in the sample plasma, expressed as g/L.

3.4.1.2 Fibrinogen γ'

Fibrinogen γ' concentrations were determined using an enzyme-linked immunosorbent assay (ELISA) that includes the use of a Santa Cruz Biotechnology (Santa Cruz, USA) 2.G2.H9 mouse monoclonal coating antibody against human γ' fibrinogen, and an Abcam (Cambridge, USA) goat polyclonal horseradish peroxidase (HRP)-conjugated antibody against human fibrinogen (Uitte de Willige *et al*., 2005).

A 96-well microtiter plate (Merck, Darmstadt, Germany) was first coated with the mouse monoclonal coating antibody against γ' fibrinogen, where after it was incubated overnight at 4℃. The following day, a blocking buffer consisting of bovine serum albumin (BSA) (Merck, Darmstadt, Germany) mixed in washing buffer (2 M trimethylamine (TEA); 5 M sodium chloride (NaCl); 0.5 M ethylenediaminetetraacetic acid (EDTA); pH of 7.5) (Merck, Darmstadt, Germany) was added to the plate and incubated for one hour at room temperature. Plasma sample diluted with a dilution buffer (2 M TEA; 5 M NaCl; 0.5 EDTA; 1 M Benzamidine; pH 7.5 (Merck, Darmstadt, Germany) was then added to the wells and the plate was incubated for another hour at room temperature. Thereafter, the goat polyclonal HRP-conjugated antibody against human fibrinogen was added to detect the quantity of bound γ' fibrinogen and incubated for a further hour at room temperature. A substrate buffer

(TMB and UP; bioMérieux**,** Boxtel, Netherlands) was then added to the plate and left to incubate for 15 minutes at room temperature, followed by the addition of 1 M sulphuric acid (H_2SO_4) (Merck, Darmstadt, Germany) to stop the reaction. After each incubation period the wells of the plate were washed three times with a washing buffer. A Multiskan FC spectrophotometer (Thermo Fisher Scientific, Waltham, USA) was used to read the absorbance of each sample at 450 nm.

Three repeats of 1:25, 1:50, 1:100, 1:200 and 1:400 dilutions of pool plasma (with a known γ' fibrinogen concentration) were used to set up the standard curve according to which the quantity of γ' fibrinogen present in the plasma samples was calculated. In addition, three repeats of the pooled plasma, with a similar dilution as that of the participant plasma samples, were included in each run to serve as controls and to determine within- and between run coefficients of variation. Both the absolute γ' fibrinogen concentration (g/L) and γ' ratio, (γ' fibrinogen expressed as the percentage of total fibrinogen concentration), were calculated.

3.4.2 Turbidimetry

The analyses of clot formation, structure and lysis were completed using the global fibrinolytic assay (refer to Addendum B for plasma fibrinolytic potential protocol). A modified method of Lisman *et al*. (2005) was used where a mixture of tissue factor (TF) (Dade Innovin, Siemens Healthcare Diagnostics Inc. Marburg, Germany) and calcium chloride ($CaCl_2$) (Merck, Darmstadt, Germany) was added to PPP to initiate the coagulation process while tissue plasminogen activator (tPA) (Actilyse, Boehringer Ingelheim, Ingelheim, Germany) was used for clot lysis.

Frozen plasma samples were thawed at 37 °C in a water bath. Citrate plasma samples were then pipetted to wells of a separate, untreated, microtiter plate (Merck, Darmstadt, Germany) (eighty samples per plate) followed by dilution (50%) with the addition of assay buffer, using a multi-channel pipette, and shook on a plate-shaker for 10 seconds at 1 100 revolutions per minute (rpm). An assay mixture of 1 400 µl was prepared at room temperature consisting of 18.75 x diluted TF, 113 mM $CaCl_2$, 167 ng/ml tPA, 67 µM phospholipids (Rossix, Mölndal, Sweden) and assay buffer (25 mM HEPES; 137 mM sodium chloride (NaCl); 3.5 mM potassium chloride (KCl); 1% BSA; pH 7.4) (Merck, Darmstadt, Germany). Thereafter, the assay mixture was added to each well of a Nunc® MaxiSorp™ microtiter plate (Merck, Darmstadt, Germany). The diluted plasma samples were pipetted over to the plate

containing the assay mixture using a multi-channel and shook on a plate-shaker for 10 seconds at 1 400 rpm. Each well was then covered with liquid paraffin oil and placed into a Multiskan Ascent spectrophotometer plate reader (Labsystems, Virginia, USA). The plasma clots were made up of a final concentration of 1 750 x diluted TF, 17 mmol/l $CaCl_2$, 80 ng/ml tPA and 10 mmol/l phospholipid vesicles.

The spectrophotometer was used to follow turbidimetric curves, at an absorbance of 405 nm every 9 seconds for the first two minutes, every 15 seconds up to 30 minutes and every minute until clot lysis or up to 270 minutes.

The data obtained from the curves were analysed using Origin® software version 8.5 (Origin lab®, 2010). The lag time, slope, maximum absorbance and clot lysis time (CLT) were calculated for each participant. The time needed for the initiation of coagulation and adequate growth of fibrin fibres for lateral aggregation to commence is indicated by the calculated lag time (minutes). The slope of the turbidity curve indicated the rate of lateral aggregation. The maximum absorbance, currently viewed as a representation of fibrin diameter, was calculated by obtaining the difference between the absorbance at the starting point of the curve and highest point (peak). The CLT, in minutes, was calculated by obtaining the difference between the midpoint in turbidity of clot formation and midpoint of the turbidity of clot lysis.

3.4.3 Permeability (Ks) assay

3.4.3.1 Preparation

A permeation buffer containing 0.05 M Tris (Merck, Darmstadt, Germany) and 0.10 M NaCl (Merck, Darmstadt, Germany) with a pH of 7.5 (brought to pH with 5M hydrochloric acid (HCl)) was prepared and filtered through a 0.22-micron filter, thereafter stored at 2-8 °C. Before initiating the experiment, the buffer was left to reach room temperature to avoid any air bubble generation caused by difference in temperature. The apparatus required for this assay is depicted in Figure 3-1. This includes a permeability stand with a ruler, buffer container and tube; a clamp to hinder buffer flow, waste container, clot container, collection tube and a timer. This assay was performed in triplicate for each sample (refer to Addendum C for standardised permeability assay protocol).

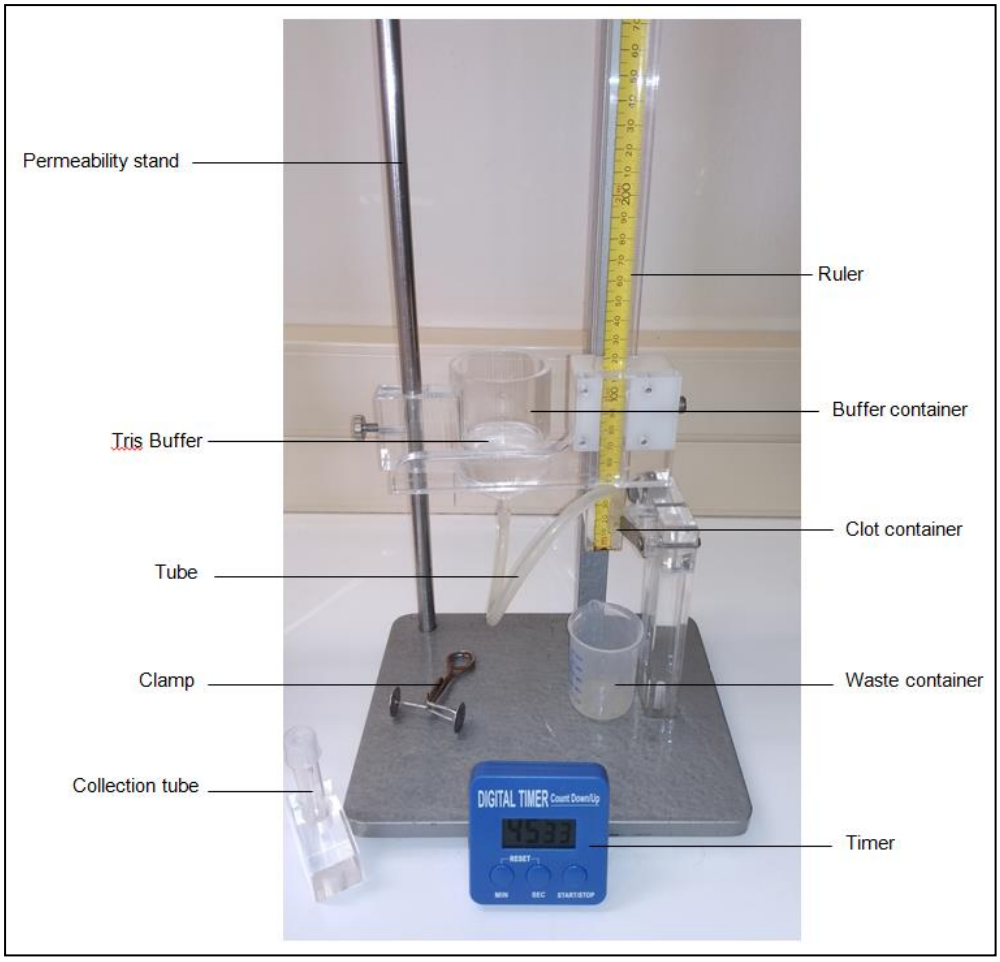

Figure 3-1: Apparatus for permeability assay

The buffer container was filled with the permeation buffer to the required level, allowing the tubing connected to the clot container to be filled and clamped until permeation.

Cut-off tips of 1 ml plastic, serological pipettes were used as clot containers with the inside of the container, total length that will be filled with 100 µl plasma sample, mechanically scratched to improve sample adherence to the container. The bottom edge of the clot containers was covered with parafilm M (Bemis NA, Neenah, USA). Three collection tubes, required for each sample repeat, were weighed prior to the experiment and recorded.

Lastly, an activation mixture of 100 µl volume was prepared containing 11 U/ml human α-thrombin (Merck, Darmstadt, Germany) and 0.22 M $CaCl_2$ (Merck, Darmstadt, Germany). Both the thrombin stock and activation mixture were kept on ice (not longer than one hour) to prevent thrombin deactivation.

3.4.3.2 Fibrin clot formation

Frozen citrate plasma samples were thawed at 37 °C in a water bath. A volume of 12 µl of activation mix was added to 120 µl of plasma, thereafter quickly pipetting 100 µl of the sample into a clot container. This step was performed as accurately as possible to ensure no air bubbles were inserted into the clot. The clot container was then completely covered with parafilm M, placed upright in a humid chamber and left for two hours to polymerise and stabilise the fibrin gel structure through crosslinking.

3.4.3.3 Permeation measurement

After two hours, the top parafilm M seal was removed from the clot container and the container filled to the top with buffer solution, ensuring no air bubbles were inserted. Thereafter the clamp was removed from the bottom end of the tubing on the permeability stand and the clot container was connected to the tubing, ensuring no air bubbles were present in the permeation system. The clot container was then clipped in place in a designated clip in the permeation stand with the difference between the surface level of the bottom end of the clot container and the top of the buffer container being 4 cm water (H_2O). The parafilm M seal was removed from the bottom end of the clot container, where the first few drops of buffer were collected in a waste container placed beneath the clot container, washing the clot. Once the clot had been washed, the waste container was replaced with the pre-weighed collection tube. The timer started when the first drop fell after the plasma colour cleared out and was stopped when similar volumes for each sample were collected. The collection tube was then weighed again, determining the weight of permeate collected.

3.4.3.4 Permeability coefficient (Ks) calculation

The permeability of the clots was calculated using the following formula, where the density of the 1.0 Tris-buffer and weight of permeate is used to determine the volume (Q) collected (Pieters *et al*., 2012):

$$Ks = \frac{\mathrm{Q \times L \times \eta}}{\mathrm{T \times A \times \Delta P}}$$

Where:

Q = volume of liquid (ml = cm^3)

L = clot length (cm)

η = viscosity (10^{-2} poise = 10^{-7} N s cm^{-2})

T = time (s)

A = cross-sectional area of clot container (cm^2)
ΔP = pressure drop (density x g x height = 1 x 980 x 4 = 3 920 dyne cm^{-2} = 0.0392 N cm^{-2}).

3.4.4 Scanning electron microscopy (SEM)

3.4.4.1 Preparation

The same PPP clots made for the permeability assay were used for the scanning electron microscopy (SEM) analysis (refer to Addendum D for SEM protocol). For SEM preparation, a buffer containing 50 mM cacodylate (Merck, Darmstadt, Germany) and 100 mM NaCl (Merck, Darmstadt, Germany) with a pH of 7.4 (brought to pH with HCl) was prepared. After completion of permeation, each clot container was placed in a glass container with cacodylate buffer and rinsed twice for 10 minutes. When rinsing was completed the samples were fixed in 2% glutaraldehyde (Merck, Darmstadt, Germany) and left covered with parafilm M in the fridge overnight.

The next day, the clots were removed from the clot containers using slight pressure. Thereafter, the clots were rinsed twice in cacodylate buffer for 10 minutes. Dehydration of the samples then took place, with the use of ethanol (EtOH) (Merck, Darmstadt, Germany) in successive dose increases, starting with 30% EtOH for 10 minutes, 50% EtOH for 10 minutes, 70% EtOH for 10 minutes, 80% EtOH for 10 minutes, 90% EtOH for 10 minutes and finally two rinses of 100% pure EtOH, 15 minutes each. Thereafter, under a fume hood, the clots were left in a 50% Hexamethyldisilazane (HMDS) (Merck, Darmstadt, Germany) solution (500 µl EtOH and 500 µl HMDS added) for 10 minutes and then a 100% HMDS solution for the next 10 minutes. Finally, after the second addition of HMDS, the clots were left in 100% HMDS solution overnight, uncovered in the fume hood for the HMDS to evaporate.

3.4.4.2 Sputter coating

The following day, the dried clots were mounted on SEM stubs using carbon tape and sputter coated using an Eiko engineering ion coater IB-2 (Eiko Engineering, Ibaraki, Japan). Sputter coating took place in two phases, namely carbon coating followed by gold / palladium coating.

3.4.4.3 SEM viewing and analysis

Once sputter coated, the clots were imaged and photographed using a FEI Corporation Quanta 200ESEM (Hillsboro, Oregon, USA). Eight randomly selected areas were photographed per clot at a machine magnification of x12 000. ImageJ (v 1.48, NIH, Bethesda, Maryland, USA) was used to measure the fibre diameter of individual clot fibres, by first selecting the clearest five images per clot, and then in a systematically and standardised manner, measuring 100 fibres in each image.

3.4.5 Fibrin content

A modified method (Pieters, 2002) based on the method of Ratnoff and Menzie (1951) was used to determine fibrin content (refer to Addendum E for fibrin content protocol).

3.4.5.1 Fibrin clot formation

Firstly, frozen citrate plasma samples were thawed at 37 °C in a water bath. Thereafter, 132 µl citrated PPP were pipetted into 5 ml glass tubes. A thrombin dilution was then prepared by adding Tris buffer (0.05 M Tris, 0.10 M NaCl, 7.5 pH) (Merck, Darmstadt, Germany) to human α-thrombin (Merck, Darmstadt, Germany). Subsequently the diluted thrombin was added to $CaCl_2$ (Merck, Darmstadt, Germany), resulting in a thrombin mix with a final concentration of 1 U/ml thrombin and 25 mM $CaCl_2$. The thrombin mix was then added to the plasma. Thereafter, the clots were left overnight at room temperature for maximum polymerisation.

3.4.5.2 Sample preparation

The following day, the glass tubes with the clots were centrifuged at 2 000 g for 15 minutes at a temperature of 15 °C and washed with Tris buffer (0.05 M Tris, 0.10 M NaCl, 7.5 pH) alternately three times. Excess fluid was removed with the use of a dropper between washes. After completion of centrifugation and washing, 143 µl of 2.5 M sodium hydroxide (NaOH) (Merck, Darmstadt, Germany) was then added to the glass tubes to hydrolyse the formed fibrin network, where they were covered and left overnight in an incubator at 30 °C.

On day three, 1 ml double distilled deionised H_2O and 429 µl of 1.9 M sodium carbonate (Na_2CO_3) (Merck, Darmstadt, Germany) were added followed by the tubes being vortexed and the contents mixed with 93 µl Folin & Ciocalteu's (Merck, Darmstadt, Germany) reagent, where the solution became blue in colour. The colour intensity formed by Folin & Ciocalteu's

reagent is dependent on the fibrin concentration. The glass tubes were then left for 20 minutes at room temperature, where after absorbance of the formed blue chromogen was measured at 650 nm with a Multiskan Ascent spectrophotometer (Labsystems, Virginia, USA).

3.4.5.3 Standard curve

A standard curve, prepared by using a purified fibrinogen solution, was used to calculate the fibrin content (g/L) of the plasma samples.

For fibrinogen preparation, a buffer containing 0.02 M sodium bicarbonate ($NaHCO_3$) (Merck, Darmstadt, Germany) and 0.13 M NaCl with a pH of 9.1 (brought to pH with 0.02 M Na_2CO_3 and 0.13 M NaCl) was prepared. Purified human fibrinogen (MP Biomedicals, Santa Ana, USA) was diluted with buffer forming five dilutions with estimate concentrations of 8 g/L, 6 g/L, 4 g/L, 2 g/L and 0.5 g/L. The absorbance of the five dilutions was measured, with the use of 1% fibrinogen solutions, at 280 nm using a UV-1601 spectrophotometer (Shimadzu, Kyoto, Japan). From these results, the actual fibrinogen concentration of each dilution was calculated using 13.6 absorbance units (0.136 in a 1% solution) as the known absorbance of 10 g/L fibrinogen.

Thereafter, the five dilutions went through the same preparation process as the samples, excluding the centrifugation and washing step and only 857.3 µl double distilled deionised H_2O was added to the glass tubes (refer to Section 3.4.5.2). A lower volume of H_2O is added to compensate for the excluded washing step, so as to reach the same total volume as with the plasma samples. These absorbance values of the five dilutions, obtained from the Multiskan Ascent spectrophotometer, with the calculated fibrinogen concentrations were used in the formation of the standard curve.

3.4.5.4 Fibrinogen concentration

Before performing this analysis on our plasma samples, it was first performed on control plasma for method development purposes. During this period, we noted that the fibrin content was similar to the fibrinogen concentration of the samples and therefore it was decided to use the fibrinogen concentration of our study samples as a proxy marker of the fibrin content thereof.

3.4.6 Rheometry

3.4.6.1 Method set-up

An ARES-G2 Rheometer (TA Instruments, New Castle, Delaware, USA) with the use of TRIOS software (v4.3.1, New Castle, DE) was used to determine viscoelastic properties during plasma clot formation, by performing oscillatory shear measurements at 37 ºC (refer to Addendum F for rheometry protocol) The time-sweep test was performed using a 40 mm stainless steel cone, under an oscillation procedure of 3 % strain, at an angular frequency of 5 radians per second (rad/s) (10 half sampling cycles) with a sampling interval of 3 points per second. The geometry (truncation) gap and loading gap were set at 0.045 mm and 15.0 mm, respectively.

3.4.6.2 Sample preparation

Frozen citrate PPP samples were thawed at 37 °C in a water bath. The plasma was activated at room temperature with a final concentration of 20 mM $CaCl_2$ (Merck, Darmstadt, Germany) and 1 U/ml human α-thrombin (Merck, Darmstadt, Germany). The activated plasma was placed on the base plate of the rheometer set to 37 ºC. After lowering the stainless-steel cone to the indicated geometric gap, immersion oil (100 – 120 mPa·s*)* (Merck, Darmstadt, Germany*)* was placed around the plates, using a dropper, to prevent the clot from drying out. The test was performed for 40 minutes, measuring the elastic / storage modulus (G') and inelastic / loss modulus (G'') for each plasma sample at 3 second intervals.

3.5 STATISTICAL ANALYSES

Statistical analyses were performed using Statistica® software version 13. A p-value of ≤ 0.05 was used to indicate statistical significance. The normality of the data was determined using histograms (visual inspection) and Shapiro-Wilks test. Data that was normally distributed is reported as mean and standard deviation. Data that was not normally distributed, namely age, body mass index (BMI), C-reactive protein (CRP), plasminogen activator inhibitor (PAI-1), fibrinogen γ' ratio, storage modulus (G'), loss modulus (G'') and tan (delta), was log transformed to improve the normality thereof for further statistical analyses but are reported as median and percentiles (25th and 75th percentiles) in descriptive tables. To investigate the association between maximum absorbance and fibrinogen concentration and other fibrin clot properties, Pearson's correlation test and scatterplots were used. To account for the contribution of varying total fibrinogen

concentrations in the plasma samples, partial correlation tests were performed to determine the association of maximum absorbance with the other clot properties in samples adjusted for fibrinogen concentration. Thereafter, the plasma samples that were selected based on low and high maximum absorbance values and matched for fibrinogen concentration were compared using t-tests. This was done to characterise the other clot properties of the two groups and to identify other demographic, anthropometric and biochemical variables that differed between the two groups. These co-variates were then adjusted for using analysis of co-variance (ANCOVA) to determine their potential contribution to the differences in clot properties between the two groups.

CHAPTER 4: RESULTS

4.1 INTRODUCTION

The main aim of this study was to clarify the interpretation of maximum absorbance data obtained using turbidimetry in plasma samples with varying fibrinogen concentrations. Because of variation in fibrinogen concentration, the interpretation of maximum absorbance is unclear. Maximum absorbance is a direct indicator of fibre diameter in purified fibrinogen solutions with fixed fibrinogen concentrations (Carr & Hermans, 1978; Mills *et al.,* 2002; Weisel & Nagaswami, 1992). However, in plasma samples, the different fibrinogen concentrations can additionally influence maximum absorbance through the formation of denser clots since more fibrin is incorporated into the clot (Mills *et al.,* 2002; Sjøland, 2007; Undas *et al.,* 2006c). The interpretation of maximum absorbance in plasma samples may thus be a reflection of plasma clot density, rather than fibre diameter, or some combination of both.

To achieve the aim of the study, descriptive and comparative statistical analyses were performed, presenting the characteristics of the study sub-sample and investigating the association of maximum absorbance with fibrinogen concentration and other fibrin clot properties. The influence of total fibrinogen concentration on the interpretation of maximum absorbance in plasma samples is presented with the aid of partial correlations between maximum absorbance and the other clot properties measured, as well as fibre diameter and clot properties, controlling for fibrinogen concentration. Next, clot properties of samples matched for fibrinogen concentration but with a low and high maximum absorbance are compared, to determine the clot characteristics of the two groups and to identify potential covariates contributing to these differences in clot properties.

4.2 DESCRIPTIVE CHARACTERISTICS OF STUDY SUB-SAMPLE

The descriptive characteristics of the study sample are presented in Table 4-1. Of the 30 participants with total fibrinogen concentration ranging from 2.4 to 6.39 g/L, selected from the PURE (Prospective Urban and Rural Epidemiological) study, 76.7 % were women. The median age was 58.6 (53.5-66.7) years with a median body mass index (BMI) of 26.2 (21.8-33.8) kg/m^2, falling within the overweight range. The median C-reactive protein (CRP) of

5.09 (2.64-10.5) mg/L is higher than the healthy range of 0 to 3 mg/L (Heart and Stroke Foundation South Africa, 2017) and the mean low-density lipoprotein cholesterol (LDL-C) of 2.87 ± 1.38 mmol/L falls within the normal range (< 3 mmol/L) (Bansal *et* al., 2014). The mean total fibrinogen concentration of 4.16 ± 0.85 g/L falls within the normal ranges for healthy individuals (1.5 – 4.5 g/L) (De Moerloose *et al*., 2010; Kamath & Lip, 2003). The median fibrinogen γ' ratio was 9.18 (8.36-12.9) %, falling within the normal range of 8-15 % (Chung & Davie, 1984; Fornace *et al*., 1984). Mean lag time, slope, maximum absorbance, clot lysis time (CLT), fibre diameter, permeability, median stiffness/elasticity, reported as storage modulus (G'), median plasticity/viscosity, reported as loss modulus (G'') and median tan (delta) (ratio between stiffness and plasticity) were 4.18 ± 0.66 min, 10.8 ± 5.00 au/s, 0.71 ± 0.24 nm, 64 ± 9.47 min, 191 ± 18.5 nm, 9.50 x 10-9 ± 3.20 x 10^{-9} cm^2, 56.2 (35.1-102) Pa, 2.55 (1.69-3.94) Pa and 0.05 (0.04-0.06) respectively. Normal, healthy ranges of the last nine mentioned variables do not exist yet and therefore, a comparison of the obtained variables with healthy ranges is not possible.

Table 4-1: Descriptive characteristics of study sample

Variable	**Study sample**
Total group n	30
Sex (men / women) n (%)	7 (23.3 %) / 23 (76.7 %)
Age (years)	58.6 (53.5-66.7)
Tobacco users (current and former) n (%)	11 (36.3 %)
Alcohol users n (%)	8 (26.7 %)
Oral contraceptive users n (%)	5 (21.7 %)
Systolic blood pressure (mmHg)	131 [29.4]
Diastolic blood pressure (mmHg)	85.3 [17.5]
Hypertensive n (%)	17 (56.7 %)
BMI (kg/m^2)	26.2 (21.8-33.8)
Glucose (mmol/L)	5.63 [1.97]
PAI-1 (U/ml)	1.91 (0.05-8.45)
CRP (mg/L)	5.09 (2.64-10.5)
TC (mmol/L)	4.59 [1.43]
HDL-C (mmol/L)	1.36 [0.42]
LDL-C (mmol/L)	2.87 [1.38]

Table 4-1 continued

Variable	Study sample
TG (mmol/L)	1.18 [0.56]
Total fibrinogen (g/L)	4.16 [0.85]
Fibrinogen γ' ratio (%)	9.18 (8.36-12.9)
Lag time (min)	4.18 [0.66]
Slope (au/s)	10.8 [5.00]
Maximum absorbance (nm)	0.71 [0.24]
CLT (min)	64.0 [9.47]
Fibre diameter (nm)	191 [18.5]
Porosity (Ks) (cm^2)	9.50×10^{-9} [3.20×10^{-9}]
Storage modulus (G')	56.2 (35.1-102)
Loss modulus (G'')	2.55 (1.69-3.94)
Tan (delta) (G'/G'')	0.05 (0.04-0.06)

BMI = body mass index; PAI-1 = plasminogen activator inhibitor-1; CRP = C-reactive protein; TC = total cholesterol; HDL-C = high-density lipoprotein cholesterol; LDL-C = low-density lipoprotein cholesterol; TG = triglycerides; γ' = gamma prime; au/s = absorbance units per second; CLT = clot lysis time; Ks = permeability coefficient

Data with a normal distribution is reported as mean [standard deviation] and data not normally distributed is reported as median (25th – 75th percentile).

4.3 RELATIONSHIP BETWEEN CLOT PROPERTIES IN STUDY SAMPLE

In order to investigate the relationship of maximum absorbance with the other measured clot properties, Pearson's correlations were performed as presented in Table 4-2. One of the aims was to have a direct measure of the fibrin content of the clots, in order to relate maximum absorbance to the absolute amount of fibrin present in the clots. Fibrin content analyses, according to the method of Ratnoff and Menzie (1951), were consequently performed. Based on initial experiments, we determined that the measured fibrin content, of plasma samples was similar to their respective fibrinogen concentrations, determined using the Clauss method (Clauss, 1957). Hence, it was decided to use the fibrinogen concentration as a proxy marker of fibrin content in further analyses. Figure 4-1 depicts scanning electron images of clots prepared from plasma samples with varying fibrinogen concentrations. Based on visual comparison, clots prepared from plasma with higher

fibrinogen concentrations contained more fibrin and were denser than clots prepared from plasma samples with a lower fibrinogen concentration.

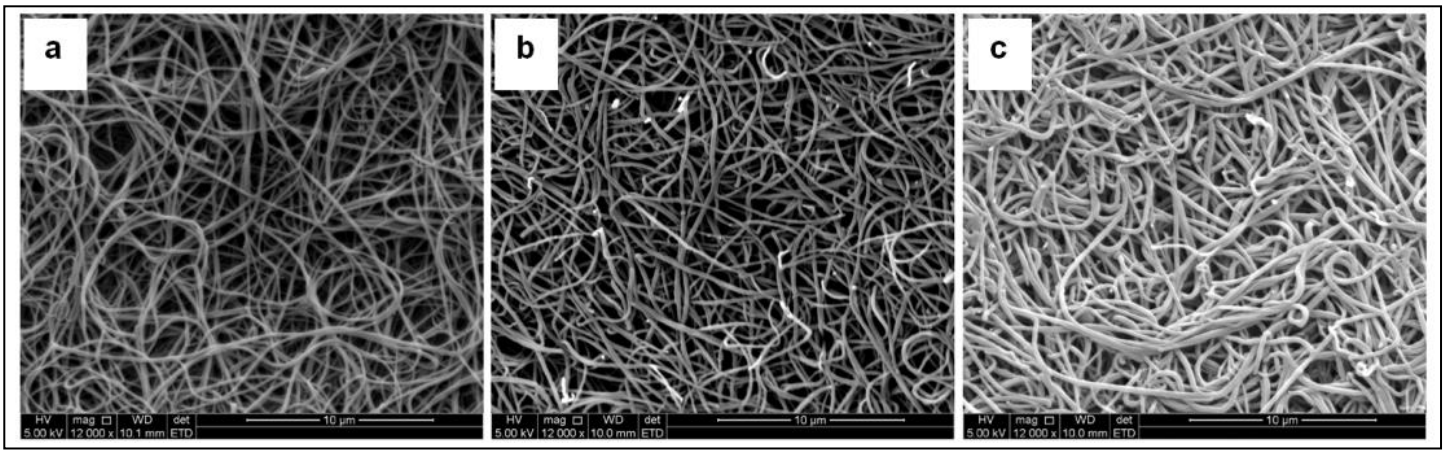

Figure 4-1: Scanning electron microscope (SEM) images, at a machine magnification of x12 000, of plasma clots with varying total fibrinogen concentration and increasing fibre diameters as follows: (a) 2.4 g/L, 162 nm; (b) 4.17 g/L, 196 nm and (c) 6.34 g/L, 218 nm)

Table 4-2 presents the correlations between all measured clot properties. Maximum absorbance demonstrated significant positive correlations with both fibrinogen concentration and fibre diameter, with the correlation with fibrinogen being the stronger association ($r = 0.65$, $p < 0.001$ compared to $r = 0.47$, $p = 0.01$). This suggests that maximum absorbance has a stronger association with the protein density of the clot than fibre diameter. The association of fibre diameter with maximum absorbance and of fibre diameter with fibrinogen concentration was however similar ($r = 0.47$, $p = 0.01$ and $r = 0.45$, $p = 0.01$). The positive significant correlation between total fibrinogen and fibre diameter indicates that in the investigated platelet poor plasma (PPP) clots, a higher fibrinogen concentration was associated with thicker fibres (also depicted in Figure 4-1 and Table 4-4). There was no association between maximum absorbance and γ' fibrinogen.

In addition, the associations between maximum absorbance and fibre diameter with other clot properties were compared, investigating possible similarities. Maximum absorbance had strong significant correlations with lag time ($r = 0.39$, $p = 0.03$), slope ($r = 0.69$, $p < 0.001$), CLT ($r = 0.63$, $= p < 0.001$), permeability ($r = - 0.67$, $p < 0.001$), stiffness (storage modulus, G') ($r = 0.67$, $p = < 0.001$) and plasticity (loss modulus, G'') ($r = 0.68$, $p < 0.001$). In contrast, aside from its significant correlation with maximum absorbance, fibre diameter correlated significantly with slope ($r = 0.38$, $p < 0.001$) only. This demonstrates that although maximum absorbance correlates well with fibre diameter, it is not equivalent to this clot property.

Next, partial correlations were conducted where the varying total fibrinogen concentration in these investigated plasma samples were controlled for. The results from the partial correlations are presented in Table 4-3. There were no significant correlations between fibre diameter and other clot properties after controlling for total fibrinogen concentration. Maximum absorbance still significantly correlated with lag time ($r = 0.43$, $p = 0.02$), slope ($r = 0.47$, $p = 0.01$), CLT ($r = 0.61$, $p < 0.001$), permeability ($r = - 0.49$, $p = 0.07$), stiffness (storage modulus, G') ($r = 0.62$, $p = < 0.001$) and plasticity (loss modulus, G'') ($r = 0.60$, $p = 0.001$), although the strength of the associations were reduced for slope and permeability, suggesting that fibrinogen concentration partly mediates these relationships. However, maximum absorbance no longer correlated significantly with fibre diameter ($r = 0.26$, $p = 0.18$) indicating that the association between maximum absorbance and fibre diameter is largely dependent on the fibrinogen concentration. In a separate analysis, when adjusting for fibre diameter, the association between maximum absorbance and fibrinogen concentration was only moderately reduced ($r = 0.56$, $p = 0.002$ *vs*. $r = 0.65$, $p < 0.0001$). This suggests that the relationship between maximum absorbance and fibrinogen is only partly attributable to fibre size with the remaining relationship likely reflecting the protein density of the network. When interpreting the above results, it should be kept in mind that maximum absorbance, lag time, slope and CLT were all obtained from one assay (turbidimetry) and therefore were determined under the same assay conditions. Fibre diameter was obtained from clots prepared for permeability for which the assay conditions differed from that of the turbidimetry. In addition, while the permeability data was obtained using native plasma clots, the fibre diameter was obtained from dried fibrin fibres. These issues were taken into consideration when discussing the results in Chapter 5.

Table 4-2: Correlations between investigated clot properties in study sample

	Maximum absorbance (nm)	Fibre diameter (nm)	Fibrinogen (g/L)	Fibrinogen γ' ratio (%)	Lag time (min)	Slope (au/s)	CLT (min)	Permeability (Ks) (cm^2)	Storage modulus (G') (Pa)	Loss modulus (G'') (Pa)	Tan (delta) (G'/G'')
Maximum absorbance (nm)		r = 0.47 p = 0.01	r = 0.65 p = < 0.001	r = - 0.12 p = 0.54	r = 0.39 p = 0.03	r = 0.69 p < 0.001	r = 0.63 p < 0.001	r = - 0.67 p < 0.001	r = 0.67 p < 0.001	r = 0.68 p < 0.001	r = - 0.19 p = 0.30
Fibre diameter (nm)	r = 0.47 p = 0.01		r = 0.45 p = 0.01	r = - 0.21 p = 0.28	r = 0.04 p = 0.84	r = 0.38 p < 0.001	r = 0.30 p = 0.12	r = - 0.05 p = 0.779	r = 0.24 p = 0.20	r = 0.26 p = 0.16	r = - 0.09 p = 0.63
Fibrinogen (g/L)	r = 0.65 p = < 0.001	r = 0.45 p = 0.01		r = - 0.13 p = 0.51	r = 0.11 p = 0.57	r = 0.64 p < 0.001	r = 0.29 p = 0.13	r = - 0.54 p = 0.002	r = 0.37 p = 0.046	r = 0.41 p = 0.02	r = 0.04 p = 0.82
Fibrinogen γ' ratio (%)	r = -0.12 p = 0.54	r = - 0.21 p = 0.28	r = - 0.13 p = 0.51		r = - 0.19 p = 0.32	r = 0.17 p = 0.37	r = 0.03 p = 0.87	r = - 0.04 p = 0.83	r = - 0.15 p = 0.43	r = - 0.10 p = 0.59	r = 0.26 p = 0.16
Lag time (min)	r = 0.39 p = 0.03	r = 0.04 p = 0.84	r = 0.11 p = 0.57	r = - 0.19 p = 0.32		r = - 0.02 p = 0.91	r = 0.006 p = 0.98	r = - 0.12 p = 0.53	r = 0.30 p = 0.12	r = 0.27 p = 0.15	r = - 0.12 p = 0.54
Slope (au/s)	r = 0.69 p < 0.001	r = 0.38 p < 0.001	r = 0.64 p < 0.001	r = 0.17 p = 0.37	r = - 0.02 p = 0.91		r = 0.56 p = 0.001	r = - 0.63 p < 0.001	r = 0.27 p = 0.15	r = 0.31 p = 0.09	r = 0.05 p = 0.79
CLT (min)	r = 0.63 p < 0.001	r = 0.30 p = 0.12	r = 0.29 p = 0.13	r = 0.03 p = 0.87	r = 0.006 p = 0.98	r = 0.56 p = 0.001		r = - 0.36 p = 0.048	r = 0.49 p = 0.006	r = 0.51 p = 0.004	r = - 0.14 p = 0.45
Permeability (Ks) (cm^2)	r = - 0.67 p < 0.001	r = - 0.05 p = 0.78	r = - 0.54 p = 0.002	r = - 0.04 p = 0.83	r = - 0.12 p = 0.53	r = - 0.63 p < 0.001	r = - 0.36 p = 0.048		r = - 0.41 p = 0.02	r = - 0.46 p = 0.01	r = - 0.18 p = 0.35

Table 4-2 continued

	Maximum absorbance (nm)	Fibre diameter (nm)	Fibrinogen (g/L)	Fibrinogen γ' ratio (%)	Lag time (min)	Slope (au/s)	CLT (min)	Permeability (Ks) (cm^2)	Storage modulus (G') (Pa)	Loss modulus (G'') (Pa)	Tan (delta) (G'/G'')
Storage modulus (G') (Pa)	r = 0.67 p < 0.001	r = 0.24 p = 0.20	r = 0.37 p = 0.046	r = - 0.15 p = 0.43	r = 0.30 p = 0.12	r = 0.27 p = 0.15	r = 0.49 p = 0.006	r = - 0.41 p = 0.02		r = 0.98 p < 0.001	r = -0.49 p = 0.006
Loss modulus (G'') (Pa)	r = 0.68 p < 0.001	r = 0.26 p = 0.16	r = 0.41 p = 0.02	r = - 0.10 p = 0.59	r = 0.27 p = 0.15	r = 0.31 p = 0.09	r = 0.51 p = 0.004	r = - 0.46 p = 0.01	r = 0.98 p < 0.001		r = - 0.33 p = 0.08
Tan (delta) (G'/G'')	r = - 0.19 p = 0.31	r = - 0.09 p = 0.64	r = 0.04 p = 0.82	r = 0.26 p = 0.16	r = - 0.12 p = 0.54	r = 0.05 p = 0.78	r = - 0.14 p = 0.46	r = - 0.18 p = 0.35	r = - 0.49 p = 0.006	r = - 0.33 p = 0.08	

γ' = gamma prime; au/s = absorbance unit per second; CLT = clot lysis time; Ks = permeability coefficient

Significant values where p < 0.05

Table 4-3: Partial correlations between maximum absorbance, fibre diameter and investigated clot properties, adjusted for fibrinogen concentration

	Unadjusted maximum absorbance (nm)	*Adjusted maximum absorbance (nm)	Unadjusted fibre diameter (nm)	*Adjusted fibre diameter (nm)
Maximum absorbance (nm)			r = 0.47 p = 0.01	r = 0.26 p = 0.18
Fibre diameter (nm)	r = 0.47 p = 0.01	r = 0.26 p = 0.18		
Fibrinogen γ' ratio (%)	r = -0.12 p = 0.54	r = - 0.05 p = 0.82	r = - 0.21 p = 0.28	r = - 0.17 p = 0.38
Lag time (min)	r = 0.39 p = 0.03	r = 0.43 p = 0.02	r = 0.04 p = 0.84	r = - 0.01 p = 0.96
Slope (au/s)	r = 0.69 p < 0.001	r = 0.47 p = 0.01	r = 0.38 p < 0.001	r = 0.13 p = 0.49
CLT (min)	r = 0.63 p < 0.001	r = 0.61 p < 0.001	r = 0.30 p = 0.12	r = 0.20 p = 0.30
Permeability (Ks) (cm^2)	r = - 0.67 p < 0.001	r = - 0.49 p = 0.07	r = - 0.05 p = 0.779	r = 0.25 p = 0.19

Table 4-3 continued

	Unadjusted maximum absorbance (nm)	*Adjusted maximum absorbance (nm)	Unadjusted fibre diameter (nm)	*Adjusted fibre diameter (nm)
Storage modulus (G' (Pa)	r = 0.67 p < 0.001	r = 0.62 p = < 0.001	r = 0.24 p = 0.20	r = 0.09 p = 0.63
Loss modulus (G'') (Pa)	r = 0.68 p < 0.001	r = 0.60 p = 0.001	r = 0.26 p = 0.16	r = 0.10 p = 0.60
Tan (delta) (G'/G'')	r = - 0.19 p = 0.31	r = - 0.29 p = 0.12	r = - 0.09 p = 0.63	r = - 0.12 p = 0.52

γ' = gamma prime; au/s = absorbance unit per second; CLT = clot lysis time; Ks = permeability coefficient

*Adjusted for total fibrinogen concentration

Significant values where p < 0.05

4.4 COMPARISON OF SAMPLES WITH LOW AND HIGH MAXIMUM ABSORBANCE, MATCHED FOR FIBRINOGEN CONCENTRATION

Despite the strong relationship between maximum absorbance and fibrinogen concentration, samples with similar fibrinogen concentrations, had maximum absorbance values that differed up to 2-fold (Table 4-4). Of the 15 pairs, 10 (66.6 %) of the samples with the higher maximum absorbance values also had thicker fibre diameters, 12 (80 %) had a longer lag time, 14 (93.3 %) had an increased slope, 14 (93.3 %) had a longer CLT, 12 (80 %) had decreased permeability, all 15 (100%) had an increased stiffness (G'), 13 (86.7 %) had an increased plasticity (G") and 10 (66.7%) had a lower ratio of stiffness to plasticity (tan (delta)) compared to their fibrinogen-matched counterparts with the lower maximum absorbance.

Table 4-4: Clot properties of plasma samples with low and high maximum absorbance values, matched for fibrinogen concentration

Sample pairs	Total fibrinogen concentration (g/L)	Maximum absorbance (nm)	Fibre diameter (nm)	Lag time (min)	Slope (au/s)	Clot lysis time (min)	Permeability (Ks) (cm^2)	Storage modulus (G') (Pa)	Loss modulus (G") (Pa)	Tan (delta) (G'/G'')
1	2.40	0.28	162	4.00	2.17	49.3	13.2×10^{-9}	14.2	0.68	0.05
	2.40	0.56	186	4.41	5.43	64.1	12.6×10^{-9}	133	5.25	0.04
2	3.08	0.38	161	3.50	3.78	65.9	13.0×10^{-9}	31.8	1.27	0.04
	3.09	0.83	203	4.05	10.3	68.3	11.8×10^{9}	52.8	2.16	0.04
3	3.67	0.39	200	3.91	6.34	68.1	11.9×10^{-9}	23.4	1.28	0.07
	3.65	0.68	188	3.79	9.52	60.9	9.73×10^{-9}	84.2	3.11	0.04
4	3.83	0.46	189	2.92	12.0	70.9	9.51×10^{-9}	45.2	1.82	0.04
	3.78	0.84	185	5.37	12.4	75.7	9.01×10^{-9}	102	3.94	0.06
5	4.00	0.58	167	4.41	6.88	60.4	12.6×10^{-9}	91.5	3.32	0.04
	3.99	0.81	188	3.88	10.0	75.3	8.69×10^{-9}	142	5.12	0.04
6	4.05	0.58	162	3.89	9.55	54.9	5.20×10^{-9}	35.1	1.74	0.07
	4.02	0.82	171	4.3	11.1	59.0	7.6×10^{-9}	40.5	2.07	0.07
7	4.07	0.47	195	3.10	21.5	57.7	11.3×10^{-9}	15.4	0.81	0.06
	4.07	0.83	214	3.98	9.07	64.0	7.22×10^{-9}	180	6.89	0.05
8	4.15	0.50	195	3.71	6.13	55.4	11.8×10^{-9}	42.0	2.92	0.08
	4.17	0.82	196	4.68	12.9	62.0	10.2×10^{-9}	146	5.00	0.04

Table 4-4 continued

Sample pairs	Total fibrinogen concentration (g/L)	Maximum absorbance (nm)	Fibre diameter (nm)	Lag time (min)	Slope (au/s)	Clot lysis time (min)	Permeability (Ks) (cm^2)	Storage modulus (G') (Pa)	Loss modulus (G") (Pa)	Tan (delta) (G'/G")
9	4.21	0.54	182	3.98	8.38	45.0	5.79×10^{-9}	80.0	3.35	0.05
	4.25	0.88	172	4.88	14.8	66.2	7.36×10^{-9}	88.9	3.18	0.04
10	4.24	0.48	165	3.55	12.5	62.4	7.99×10^{-9}	14.7	0.85	0.07
	4.25	0.93	196	5.04	10.4	67.1	9.06×10^{-9}	97.6	3.65	0.04
11	4.39	0.60	206	4.87	10.6	60.7	11.3×10^{-9}	16.8	1.07	0.07
	4.38	0.93	225	5.37	14.4	62.9	9.71×10^{-9}	40.9	1.69	0.05
12	4.4	0.50	214	3.50	5.48	62.4	18.1×10^{-9}	59.6	2.19	0.04
	4.43	1.03	206	3.97	15.9	78.1	6.04×10^{-9}	42.7	1.80	0.06
13	4.51	0.57	194	4.75	5.48	53.8	12.0×10^{-9}	52.9	1.98	0.04
	4.51	0.93	167	5.15	12.7	76.0	6.11×10^{-8}	171	6.34	0.05
14	5.02	0.70	188	4.02	8.13	50.1	11.3×10^{-9}	26.4	1.02	0.04
	5.03	0.95	220	4.13	13.4	65.5	5.39×10^{-9}	78.3	3.08	0.05
15	6.39	1.07	203	5.02	16.3	65.2	5.87×10^{-9}	209	8.31	0.05
	6.34	1.32	218	3.27	25.5	91.4	3.06×10^{-9}	273	12.4	0.05

au/s = absorbance unit per second; Ks = permeability coefficient

When comparing the means of the two groups, the group with the higher maximum absorbance values had significantly longer mean CLT's ($p = 0.001$), lag times ($p = 0.04$) and increased slopes ($p = 0.05$), significantly decreased permeability (p 0.03) and significantly increased stiffness (G') ($p < 0.001$) and plasticity (G'') ($p < 0.001$) compared to the lower maximum absorbance group (Table 4-5). The mean fibre diameter was also larger, although not significantly so (186 ± 17.9 *vs.* 195 ± 18.8, $p = 0.14$). However, when comparing the distribution range of fibre diameters in the two groups, it is clear that there were proportionally a larger number of thicker fibres in the samples in the higher maximum absorbance group compared to the lower maximum absorbance group (Figure 4.2). The fibre diameter range with the highest frequency of plasma clots in the high maximum absorbance group was 185 – 190 nm, whereas the highest frequency in the low maximum absorbance group was 160 – 165 nm.

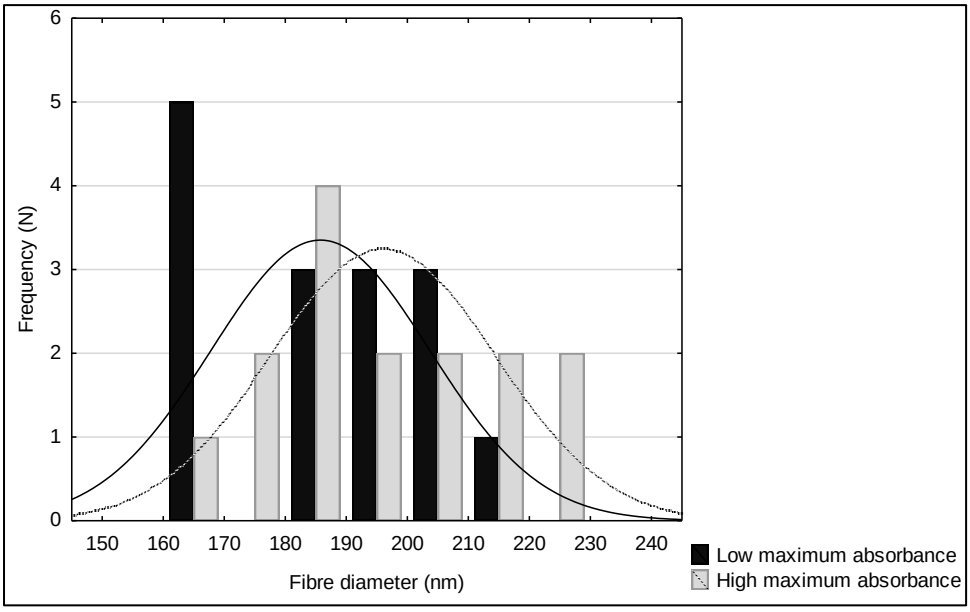

Figure 4-2: Frequency histogram of measured fibre diameters (nm) in low and high maximum absorbance groups

In an attempt to identify factors contributing to the different clot properties observed in the two groups, despite similar fibrinogen concentrations, covariates that differed significantly between the two groups were identified and their association with clot properties investigated. BMI (22.8 (20.5-33.6) *vs.* 29.3 (24.5-34.3) kg/m^2), CRP (7.82 (2.41-11.1) *vs.* 3.35 (2.64-10.5) mg/L) and LDL-C (2.34 ± 1.01 *vs.* 3.41 ± 1.53 mmol/L) differed significantly between the two groups. Adjusting for these covariates using analysis of co-variance (ANCOVA), altered the differences in lag time, CLT and permeability between the two groups, as obtained with t-tests (unadjusted model), demonstrating their mediating effect on the clot properties. These associations were furthermore supported by the identification of significant correlations between BMI, CRP and LDL-C and the measured clot properties. BMI correlated significantly with CLT ($r = 0.40$, $p = 0.037$), CRP with total fibrinogen

concentration (r = 0.65, p <0.001), slope (r = 0.62, p < 0.001), maximum absorbance (r = 0.48, p = 0.010) and permeability (r = - 0.52, p = 0.005) and LDL-C with lag time (r = 0.49, p = 0.008), maximum absorbance (r = 0.48, p = 0.011) and CLT (r = 0.60, p = 0.001).

Table 4-5: Investigated clot properties with similar fibrinogen concentration

Variable	Low maximum absorbance	High maximum absorbance	p-value	ANCOVA p-value
Total fibrinogen (g/L)	4.16 [0.87]	4.16 [0.86]	0.99	1.0
Fibrinogen γ' ratio (%)	9.17 (7.73-16.2)	10.3 (8.42-12.9)	0.92	0.62
Lag time (min)	3.94 [0.61]	4.42 [0.64]	0.04	0.36
Slope (au/s)	9.02 [5.03]	12.5 [4.47]	0.05	0.03
Maximum absorbance (nm)	0.54 [0.18]	0.88 [0.17]	<0.001	<0.001
Clot lysis time (min)	58.8 [7.41]	69.1 [8.63]	0.001	0.02
Fibre diameter (nm)	186 [17.9]	195 [18.8]	0.14	0.14
Permeability (Ks) (cm^2)	11.07×10^{-9} [3.41×10^{-9}]	8.26×10^{-9} [2.51×10^{-9}]	0.03	0.004
Storage modulus (G') (Pa)	35.11 (16.8-59.6)	97.6 (52.8-146)	< 0.001	< 0.001
Loss modulus (G'') (Pa)	1.74 (1.02-2.92)	3.65 (2.16-5.25)	< 0.001	< 0.001
Tan (delta) (G'/G'')	0.06 (0.04-0.07)	0.05 (0.04-0.05)	0.11	0.06

ANCOVA = analysis of covariance; γ' = gamma prime; au/s = absorbance unit per second; Ks = permeability coefficient

Data with a normal distribution is reported as mean [standard deviation] data not normally distributed is reported as median (25th – 75th percentile).

T-test used to determine significant difference between the two independent maximum absorbance groups.

ANCOVA p-values used to determine significant difference between the two independent maximum absorbance groups, after adjustment for covariates (BMI, CRP and LDL-C).

Significant values where p < 0.05

The results presented in this chapter are interpreted and discussed in Chapter 5, in combination with the standing literature.

CHAPTER 5: DISCUSSION AND CONCLUSION

5.1 INTRODUCTION

The main focus of this study was to elucidate the interpretation of maximum absorbance data obtained from turbidimetry in plasma samples, with varying fibrinogen concentrations. Currently, it is unclear which fibrin clot property (or combination of properties) maximum absorbance is indicative of in plasma clots. Specific objectives were to select individuals with varying maximum absorbance values, stratified for fibrinogen concentration across the fibrinogen concentration range of the PURE 2015 population and carry out the following:

- Measure plasma clot structural properties (fibre diameter, clot pore size) using a direct (SEM) and an indirect technique (permeability).
- Perform complementary measurements to determine mechanical clot properties (rheometry) as well as clot fibrin content.
- Relate the maximum absorbance value to measures of clot formation (lag time and slope obtained from turbidimetry), clot lysis (turbidimetry), structural properties (fibre diameter - SEM and pore size - Ks), mechanical properties (clot stiffness and plasticity - rheometry) as well as fibrin content while taking plasma fibrinogen concentration into consideration.
- Compare the association between maximum absorbance and the other measured clot properties with the association between fibre diameter and the other clot properties; to determine whether they are equivalent.
- Compare samples matched for fibrinogen concentration with low and high maximum absorbance values to characterise the fibrin clot properties of the two groups and to identify other biological factors that contribute to potential variance in clot properties in the two groups.

In this chapter, the results obtained from this study are discussed in alignment with the aim and objectives of the study. Firstly the relationship between maximum absorbance and other clot properties is described. This is followed by the influence of environmental factors on fibrin clot network, the limitations of this study and recommendations for future studies.

5.2 RELATIONSHIP BETWEEN FIBRIN CLOT PROPERTIES

In purified fibrinogen solutions, where total fibrinogen concentration is constant, maximum absorbance is used as an indication of fibrin fibre diameter (higher maximum absorbance, thicker fibres) (Carr & Hermans, 1978; Weisel & Nagaswami, 1992). This concept is based on the observation by Ferry and Morrison (Ferry, 1948; Ferry & Morrison, 1947) that fibrin gels with varying turbidity (maximum absorbance) contain fibres with varying fibre diameters. Carr & Hermans (1978) confirmed these observations and demonstrated how fibrin gel turbidity can be used to calculate an average fibre mass-length ratio (MLR) (average fibre size), based on the concept that the light scattering pattern of rod-like shaped fibrin fibres would be equivalent to that of theoretically predicted rod-like shapes. MLR is calculated by means of the intercept (A) of a plot where $c/T\lambda^3$ is plotted as a function of $1/\lambda^2$. The variable c represents the fibrinogen concentration (mg/ml), T represents the turbidity (2.303 x optical density) and λ represents the wavelength. MLR is then determined from the following equation (Carr & Hermans, 1978):

$$\text{MLR (Dalton/cm)} = \frac{10}{1.48\text{A}} \times 10^{12}$$

With this method, Carr & Hermans (1978) confirmed that clot turbidity is directly related to the average cross-sectional area of fibrin fibres.

This concept may also be applicable to plasma samples; however, fibrinogen concentration needs to be constant for maximum absorbance to accurately indicate fibre diameter. In plasma samples where fibrinogen concentration varies, the interpretation of maximum absorbance therefore becomes complex. When fibrinogen concentration varies between samples, maximum absorbance is not only influenced by fibre size but also by fibrin (protein) content, as the amount of light absorbed is dependent both on the size of the fibres as well as the amount of protein present. In addition, fibrinogen concentration also influences fibre diameter; however, this relationship is somewhat less clear, with contradicting evidence in the available literature.

During the process of clot formation, thrombin converts fibrinogen (45 nm in length) to fibrin monomers through the cleavage of fibrinopeptides A and B; subsequently two-stranded protofibrils are formed from the linkage of the half-staggered fibrin monomers (Bridge *et al*., 2014; De Moerloose *et al*., 2010; Pulanić & Rudan, 2005; Riedel *et al*., 2011; Weisel, 2007; Weisel *et al*., 1985). Upon reaching a sufficient length (generally 600-800 nm), protofibrils aggregate laterally and twist around each other forming fibrin fibres (clot network begins to form) (Chernysh & Weisel, 2008; Mosseson *et al*., 2001; Weisel, 2007; Weisel & Dempfle, 2013). As fibrin fibre growth continues with the accumulation of new protofibrils, the periodicity of 22.5 nm (corresponding to half the length of a fibrinogen molecule) is maintained, resulting in protofibrils stretching to a certain extent (Standeven

et al., 2005; Weisel, 2007; Weisel & Medved, 2001). Fibre growth ceases once the energy required for stretching exceeds the energy of protofibril bonding (Chernysh & Weisel, 2008; Standeven *et al*., 2005; Weisel, 2007). During clot formation, it has been suggested that, once a stable gel network is formed (at the gel point), the structure is further extended by additional longitudinal growth and branching of fibrin fibres (Chernysh & Weisel, 2008). After completion of longitudinal fibre growth and branching, lateral aggregation of fibres however continues with the remaining fibrin monomers being added laterally to increase fibre diameter (Chernysh & Weisel, 2008). The thickness of fibres is therefore dependent on the degree of lateral aggregation as well as the fibrinogen concentration (Houser *et al.,* 2010). Furthermore, under conditions where fibrinopeptide cleavage occurs at a slower rate, such as a low thrombin concentration, fibrin monomers are formed more slowly (Weisel & Nagaswami, 1992). This results in the formation of a smaller number of individual fibres with more protofibrils being available for lateral aggregation of existing protofibrils, forming thicker fibres that also grow longer (Weisel & Nagaswami, 1992). Increasing fibrinogen concentrations will consequently have an impact on the relative thrombin concentration by decreasing the thrombin-to-fibrinogen ratio (Weisel & Nagaswami, 1992) theoretically leading to the formation of thicker fibres. A number of purified fibrinogen studies have indeed demonstrated higher fibrinogen concentrations to result in increased fibre diameter (thicker fibres) (Blombäck & Okada, 1982; Blombäck *et al.,* 1989; Shah *et al.,* 1985; Weisel & Nagaswami, 1992). In addition, reduced clot permeability and fibrinolytic resistance have also been associated with higher fibrinogen concentrations (Blombäck *et al.,* 1989; Fatah *et al.,* 1996). On the other hand, a number of other purified fibrinogen studies have also reported an inverse association between fibrinogen concentration and fibre diameter (using calculated fibre mass-to-length ratio), which they attributed to accelerated fibrin monomer production from the higher quantity of substrate present, forming denser, stiffer fibrin networks with thinner fibres (Carr & Alvin, 1995; Herbert *et al.,* 1998; Ryan *et al*., 1999). The latter is supported by a case-control study by Mills *et al* (2002), using plasma samples, demonstrating higher fibrinogen concentration to associate with the formation of thinner fibrin fibres (measured by scanning electron microscopy (SEM)) in premature coronary artery disease (CAD) patients. In light of the limited number of studies available linking fibre diameter measured with a direct measure such as SEM, to fibrinogen concentration in plasma samples, this relationship remains unclear and complex as it is likely also influenced by the varying concentrations of other plasma components, such as thrombin, in the samples of individuals.

Plasma clot networks are generally defined as either fine or coarse networks (Mosesson *et al.,* 1993; Siebenlist & Mosesson, 1994). Fine fibrin networks are defined as tight networks with a high quantity of fibres per clot volume composed of thin fibrin fibres, whereas coarse fibrin networks are defined as those containing thicker fibres with a looser network arrangement (Blombäck, 1996; Weisel, 2007; Wolberg, 2010). Clots composed of thinner fibres typically form denser, more rigid clots, with a stiffer network arrangement, reduced permeability (smaller pore sizes) and enhanced resistance to

fibrinolysis (thrombogenic); whereas clots consisting of thicker fibres generally contain looser and less rigid networks that are more susceptible to fibrinolysis (non-thrombogenic) (Campbell *et al.,* 2009; Carr & Alving, 1995; Collet *et al*., 1996; Fatah *et al.,* 1996; Machlus *et* al., 2011). In plasma (case-control) studies, the above-mentioned relationships are however less clear, with inconsistencies existing regarding the association between maximum absorbance, which is used as a proxy marker / indirect measurement of fibre diameter and other clot properties. For example, some studies show increased maximum absorbance to be associated with higher permeability (Ks) (Pera *et al*., 2012; Undas *et al*., 2006b; Undas *et al*., 2006c), whereas in other studies a higher maximum absorbance was associated with denser clots and decreased permeability (Ks) (Mills *et al*., 2002; Siudut *et al*., 2015; Undas *et al*., 2009c; Undas *et al*., 2009a; Undas *et al*., 2010c; Undas *et al*., 2011b). Although limited, conflicting results are also present regarding the association between maximum absorbance and fibre diameter. Two plasma, case-control studies, where fibre diameter was directly measured from SEM images, both found increased maximum absorbance in thrombotic patients (Mills *et al*., 2002; Undas *et al*., 2009c). However, Undas *et al* (2009c) reported these fibres to be thicker whereas Mills *et al* (2002) reported thinner fibres. In addition, contradictory results regarding the association between fibre diameter and permeability was also demonstrated in these two studies. All other plasma, case-control studies, deduced fibre diameter based solely on maximum absorbance data without performing any direct measures of fibre diameter. In studies where plasma fibrinogen concentration is similar between healthy individuals and patients (Pera *et al*., 2012; Siudut *et al*., 2015; Undas *et al*., 2006b; Undas *et al*., 2009a; Undas *et al*., 2010c; Undas *et al*., 2011b), the assumed fibrin thickness is likely to be accurate based on the known concepts identified in purified fibrinogen solutions with similar fibrinogen concentrations. However, in studies where the fibrinogen concentration differs between cases and controls, the assumed thickness of the fibrin fibres, based on maximum absorbance measures, may be less accurate as maximum absorbance may also reflect the difference in protein density/content between the samples. Additionally, the fact that samples from healthy individuals are compared to cardiovascular disease (CVD) patients further complicates the interpretation as altered clot properties in CVD patients may also be the result of factors associated with the disease rather than fibrinogen concentration. This is evident from studies reporting altered clot properties in CVD patients despite having similar fibrinogen concentration than the healthy controls (Pera *et al*., 2012; Siudut *et al*., 2015; Undas *et al*., 2006b; Undas *et al*., 2009a; Undas *et al*., 2010c; Undas *et al*., 2011b).

This study, using plasma clots from apparently healthy individuals (therefore not CVD patients) with varying total fibrinogen concentration, demonstrated that maximum absorbance associated positively with both fibre thickness (SEM) and total fibrinogen concentration, with the latter being the stronger association. In addition, after adjusting for fibrinogen concentration, maximum absorbance no longer associated with fibre diameter indicating that fibrinogen concentration plays a significant role in the relationship between maximum absorbance and fibre diameter.

In an attempt to elucidate the interpretation of maximum absorbance in plasma samples with varying fibrinogen concentrations, possible similarities between maximum absorbance and fibre diameter were investigated by comparing the association between maximum absorbance and other clot properties and the association between fibre diameter and other clot properties. Increased maximum absorbance was found to be associated with thicker fibres (SEM), increased total fibrinogen concentration, longer lag times and higher fibrin polymerisation rates (slope); formation of stiffer clots (G') with lower permeability (Ks) and higher resistance to fibrinolysis (clot lysis time (CLT)). Fibre diameter however associated with total fibrinogen concentration and fibrin polymerization rate only. The respective associations between maximum absorbance and fibre diameter with other clot properties were therefore not similar, suggesting that maximum absorbance is not equivalent to fibre diameter and can therefore not solely be indicative of fibre diameter. Based on the visual inspection of the SEM images, it was clear that the clots prepared from samples with higher fibrinogen concentrations also had a higher protein density as it contained more fibrin, which would consequently absorb more light in the chromatographic-based turbidimetry assay, contributing to the increased maximum absorbance observed in these samples. Also, when adjusting for fibre diameter, the association between maximum absorbance and fibrinogen concentration was only moderately reduced, indicating that this relationship is only partly attributable to fibre size with the remaining association likely reflecting protein density. This data suggests that although a significant association exists between maximum absorbance and fibre diameter, maximum absorbance should not merely be used as a proxy marker of fibre diameter, but rather of clot/protein density. This interpretation would also fit better with the pro-thrombotic clot phenotype of CVD patients reported in case-control studies also having increased maximum absorbance. The increased protein density of these clots, stemming from the increased fibrinogen concentration often seen in CVD, renders these clots less porous, increases fibre stiffness and decreases lysis rates.

5.3 THE INFLUENCE OF PLASMA AND ENVIRONMENTAL FACTORS ON CLOT NETWORK

As alluded to above, when working in the plasma-based rather than the purified setting, other components present in plasma (apart from fibrinogen concentration) can additionally influence fibrin clot properties. For instance, a number of plasma-based, case-control studies reported increased maximum absorbance and lower permeability (Siudut *et al*., 2015; Undas *et al*., 2009c; Undas *et al*., 2009a; Undas *et al*., 2010c; Undas *et al*., 2011b; Zolcinski *et al*., 2012) in CVD patients compared to healthy controls, while others demonstrated decreased maximum absorbance and lower permeability (Pera *et al*., 2012; Undas *et al*., 2006b) despite there being no significant difference in mean fibrinogen concentration between the patients and the controls.

Also in this study, clots prepared from samples with similar fibrinogen concentrations, demonstrated an up to two-fold difference in maximum absorbance values. Consequently, samples matched for fibrinogen concentration were divided into two groups; those with high maximum absorbance and those with low maximum absorbance at each given fibrinogen concentration. This was done in order to characterise the clot properties of the two groups and to identify potential covariates contributing to differences in clot properties. The group with the higher maximum absorbance values also had significantly longer mean CLT, lag time and increased slope, significantly decreased permeability (Ks) and significantly increased stiffness (G') and plasticity (G'') compared to the lower maximum absorbance group. There was also a proportionally larger number of thicker fibres in the samples in the higher maximum absorbance group compared to the lower maximum absorbance group. These differences were not only observed when comparing the means of the groups, but also when comparing each fibrinogen concentration-matched set of samples.

In this study, CRP, BMI and LDL-C were identified as potential contributors to variance in fibrin clot properties as they were found to differ significantly between the two groups. From the three covariates, CRP was the only variable that had an association with total fibrinogen concentration in our study. In addition, increased CRP associated with other fibrin clot properties including increased fibrin polymerisation rate (slope), higher maximum absorbance and lower clot permeability. Increased BMI associated with higher resistance to fibrinolysis, while increased LDL-C associated with a longer lag time, higher maximum absorbance and enhanced resistance to fibrinolysis.

There is also evidence from the literature for an association between these factors and fibrinogen concentration and/or fibrin clot structure (Dunn *et al*., 2005; Undas & Ariëns, 2011a). Well-known associations exist between fibrinogen and CRP (Black, 2003; Kritchevsky *et al.,* 2005; Redman & Xia, 2000) both being acute-phase proteins, fibrinogen and BMI (Danesh *et al.,* 2005; Friedlander *et al.,* 1995; Kamath & Lip, 2003) as well as fibrinogen and LDL-C (Danesh *et al.,* 2005; James *et al.,* 2000; Pearson *et al.,* 1997). The inflammatory response to a disease, infection or tissue damage, is the possible linking factor between the association of increased CRP, BMI and LDL-C and higher fibrinogen concentration (Fransson *et al.,* 2010; Kamath & Lip, 2003; Kannel, 2005; Nguyen *et al.,* 2009; Rudež *et al.,* 2009). As described below, associations between these three factors and fibrin clot properties have also been demonstrated, although to a very limited extent only.

Elevated CRP was found to be associated with clots that are less permeable with an enhanced resistance to fibrinolysis (Sjøland, 2007; Undas *et al.,* 2007; Undas *et al.,* 2009b). It is suggested that CRP initiates prothrombogenic activity in vascular endothelial cells by increasing local tissue factor (TF) expression, enhancing coagulation as well as fibrinolytic resistance, thereby triggering processes involved in alteration of fibrin clot properties (Cermak *et al.,* 1993; Devaraj *et al.,* 2003). CRP occurs natively in the vasculature as pentameric CRP (pCRP) but can be modified due to a variety of factors (high temperature, low pH, low calcium ion levels) and form monomeric CRP

(mCRP) (Taylor & Van den Berg, 2007). Li *et al* (2012) found modified clot properties associated with mCRP and demonstrated increased clot density with a higher fibrin polymerisation rate. Furthermore, CRP has the ability to bind to fibrinogen, thereby modifying the ensuing fibrin network structure (Salonen *et al.,* 1984). In a study by Kotzé *et al* (2014), where total fibrinogen concentration was controlled for, elevated CRP also associated with increased fibrin polymerisation rate (slope) and higher maximum absorbance. In addition, Kotzé *et al* (2014) investigated the association between BMI and clot properties but found no existing associations after controlling for fibrinogen concentration. In contrast, Malan (1999) demonstrated an association between obese individuals (BMI > 29.9 kg/m^2) and tighter, stiffer clot networks with an enhanced resistance to fibrinolysis, despite fibrinogen concentration being similar between obese and healthy individuals.

Adipose tissue is known to be an active organ carrying out metabolic and endocrine functions, subsequently associated with prothrombotic activity (Brzezinska-Kolarz *et al*., 2014). It is suggested that adipose tissue may modify the coagulation process through the synthesis of TF and plasminogen activator inhibitor 1 (PAI-1) (Anfossi *et al.,* 2010; Hajer *et al*., 2008), as well as affecting hepatic function, thereby enhancing the synthesis of clotting factors including fibrinogen (Faber *et al.,* 2009). In support of the above, Carter *et al (*2007) demonstrated an association between denser clots with a longer CLT and an increase in the number of metabolic syndrome components, including BMI. Furthermore, a reduction in BMI was found to be associated with a shorter CLT, thereby decreasing fibrinolytic resistance (Brzezinska-Kolarz *et al*., 2014).

Increased LDL-C has been reported to be associated with stiffer clots (Skrzydlewski, 1976), slower lag time (Kim *et al.,* 2015), lower clot permeability (Bhasin *et al*., 2008; Fatah *et al.,* 1992) and enhanced resistance to fibrinolysis (Puccetti *et al.,* 2001; Skrzydlewski, 1976). The oxidation of lipids may furthermore influence the effect of lipids on clot structure. It is suggested that fibrin may be directly affected by highly oxidised LDL, subsequently altering the ensuing clot network by enhancing hypercoagulation and fibrinolytic resistance in comparison to non-oxidised LDL (Azizova *et al.,* 2000). This inhibited fibrinolysis is suggested to be the result of LDL binding to fibrin clots with hydrogen and ion bonds, hindering permeation of lytic enzymes (Kunz *et al*., 1992; Skrzydlewski, 1976). In addition, surface-bound LDL has been found to bind to tissue plasminogen activator (tPA), thus preventing the formation of plasmin (Simon *et al.,* 1991).

5.4 LIMITATIONS AND FUTURE RECOMMENDATIONS

A limitation of this study was the difference in assay conditions used for turbidimetry from that of permeability and rheometry because standardised protocols, with pre-specified assay conditions, were followed. Furthermore, while native plasma clots were used to obtain permeability data,

dehydrated fibrin clots were prepared for SEM to obtain fibre diameter measurements. However, these assays were used with the intention of being complementary to one another, supporting data obtained from dissimilar methods. Furthermore, maximum absorbance demonstrated strong significant associations not only with other clot properties obtained from the turbidity assay, but also from the other assays, supporting internal consistency of the data. Another limitation was the absence of a direct measurement of clot/protein density. This was due to two reasons. Firstly, there is limited evidence in the literature regarding the availability of such a direct method. Confocal microscopy has been suggested (Gersh *et al*., 2009; Bouman *et al*., 2016) as a potential method but it has not been validated. Furthermore, we could not investigate its potential use in our study due to a lack of sample. We therefore recommend that future studies investigate the development and or validation of direct measurements of clot protein density, to further assess the association between maximum absorbance and protein density. In addition, it is recommended to assess genetic influences on clot properties of plasma samples with varying fibrinogen concentration as it is known that genetic factors contribute to variance in fibrin clot structure (Undas *et al.,* 2011b; De Vries *et al*., 2016). Although we identified environmental and plasma components that contributed to altered clot properties in this well-phenotyped study population, the possibility of residual confounding cannot be excluded. Being a cross-sectional study, we could furthermore not determine causality which limits the conclusions that can be drawn from the data.

5.5 CONCLUSION

Despite the limitations mentioned above, this study significantly contributes to our understanding of the interpretation of maximum absorbance data obtained from turbidimetry. Despite being an indirect measure of clot properties, turbidity is widely used as it is an inexpensive method that can be employed in studies with large sample numbers and which can be performed with frozen plasma samples, which is the type of sample most often collected and used when working with population or patient samples. Being an indirect method, the correct interpretation of the data obtained is therefore crucial.

Our data, obtained from plasma samples with varying fibrinogen concentration, suggest the following:

- Increased maximum absorbance is associated with the formation of thicker fibrin fibres.
- Increased plasma fibrinogen concentration is also associated with the formation of thicker fibrin fibres in apparently healthy individuals.

- Although maximum absorbance is related to fibre diameter, in plasma samples with varying fibrinogen concentrations, it is not equivalent to fibre diameter.
- Maximum absorbance is not solely indicative of fibre diameter, but rather of a combination of both fibre diameter and clot protein density, with the latter likely being the stronger contributor.
- Aside from fibrinogen concentration, environmental and other plasma factors including BMI, CRP and LDL-C can also influence plasma clot properties.

REFERENCE LIST

Anfossi, G., Russo, I., Doronzo, G., Pomero, A. & Trovati, M. 2010. Adipocytokines in atherothrombosis: focus on platelets and vascular smooth muscle cells. *Mediators of inflammation,* 2010:1-26.

Ariëns, R.A.S., lai, T.S., Weisel, J.W., Greenberg, C.S. & Grant, P.J. 2002. Role of factor XIII in fibrin clot formation and effects of genetic polymorphisms. *Blood,* 100(3):743-754.

Bansal, T., Pandey, A., Deepa, D. & Asthana, A.K. 2014. C-reactive protein (CRP) and its association with periodontal disease: a brief review. *Journal of clinical and diagnostic research,* 8(7):ZE21-ZE24.

Berg, J.M., Tymoczko, J.L. & Stryer, L. 2002. Biochemistry. New York, NY: W.H. Freeman and Company.

Bhasin, N., Ariëns, R.A.S., West, R.M., Parry, D.J., Grant, P.J. & Scott, J.A. 2008. Altered fibrin clot structure and function in the healthy first-degree relatives of subjects with intermittent claudication. *Journal of vascular surgery*, 48(6):1497-1503.

Black, P.H. 2003. The inflammatory response is an integral part of the stress response: implications for atherosclerosis, insulin resistance, type II diabetes and metabolic syndrome X. *Brain, behavior and immunity,* 17(5):350-364.

Blombäck, B. 1996. Fibrinogen and fibrin – proteins with complex roles in hemostasis and thrombosis. *Thrombosis research,* 83(1):1-75.

Blombäck, B. & Okada, M. 1982. Fibrin gel structure and clotting time. *Thrombosis research,* 25(1-2):51-70.

Blombäck, B., Carlsson, K., Hessel, B., Liljeborg, A., Procyk, R. & Åslund, N. 1989. Native fibrin gel networks observed by 3D microscopy, permeation and turbidity. *Biochimica biophysica acta,* 997(1-2):96-110.

Bouman, A.C., McPherson, H., Cheung, Y.W., Ten Wolde, M., Ten Cate, H., Ariëns, R.A.S. & Ten Cate-Hoek, A.J. 2016. Clot structure and fibrinolytic potential in patients with post thrombotic syndrome. *Thrombosis Research,* 137(Supplement C):85-91.

Bridge, K.I., Philippou, H. & Ariëns, R.A.S. 2014. Clot properties and cardiovascular disease. *Thrombosis and haemostasis,* 112(5):901-908.

Brzezinska-Kolarz, B., Kolarz, M., Walach, A. & Undas, A. 2014. Weight reduction is associated with increased plasma fibrin clot lysis. *Clinical and applied thrombosis/hemostasis,* 20(8):832-837.

Campbell, R.A., Overmyer, K.A., Selzman, C.H., Sheridan, B.C. & Wolberg, A.S. 2009. Contributions of extravascular and intravascular cells to fibrin network formation, structure, and stability. *Blood*, 114(23):4886-4896.

Carr, M.E. & Hermans, J. 1978. Size and density of fibrin fibers from turbidity. *Macromolecules,* 11(1):46-50.

Carr, M.E. & Alving, B.M. 1995. Effect of fibrin structure on plasmin-mediated dissolution of plasma clots. *Blood coagulation and fibrinolysis,* 6(6):567-573.

Carr, M.E., Shen, L.L. & Hermans, J. 1977. Mass-length ratio of fibrin fibers from gel permeation and light scattering. *Biopolymers,* 16(1):1-15.

Carter, A.M., Cymbalista, C.M., Spector, T.D. & Grant, P.J. 2007. Heritability of clot formation, morphology, and lysis: the EuroCLOT study. Arteriosclerosis, thrombosis and vascular biology, 27(12):2783-2789.

Casa, L.D.C., Deaton, D.H. & Ku, D.N. 2015. Role of high shear rate in thrombosis. *Journal of Vascular Surgery,* 61(4):1068-1080.

Cermak, J., Key, N.S., Bach, R.R., Balla, J., Jacob, H.S. & Vercellotti, G.M. 1993. C-reactive protein induces human peripheral blood monocytes to synthesize tissue factor. *Blood,* 82(2):513-520.

CFAMM (Central Facility for Advanced Microscopy and Microanalysis). 2016. Brief introduction to scanning electron microscopy (SEM). https://cfamm.ucr.edu/documents/sem-intro.pdf Date of access: 15 June 2017.

Chernysh, I.N. & Weisel, J.W. 2008. Dynamic imaging of fibrin network formation correlated with other measures of polymerization. *Blood,* 111(10):4854-4861.

Chung, D.W. & Davie, E.W. 1984. γ and γ' Chains of human fibrinogen are produced by alternative mRNA processing. *Biochemistry*, 23(18):4232-4236.

Clauss, A. 1957. Human fibrinogen heterogeneities 1. Gerinnungsphysiologische schnellmethode zur bestiminung des fibrinogens. *Acta Haematologica*, 17:237-246.

Collet, J.P., Woodhead, J.L., Soria, J., Soria, C., Mirshahi, M., Caen, J.P. & Weisel, J.W. 1996. Fibrinogen Dusart: electron microscopy of molecules, fibers and clots, and viscoelastic properties of clots. *Biophysical Journal,* 70(1):500-510.

Collet, J.P., Park, D., Lesty, C., Soria, J., Soria, C., Montalescot, G. & Weisel, J.W. 2000. Influence of fibrin network conformation and fibrin fiber diameter on fibrinolysis speed: dynamic and structural approaches by confocal microscopy. *Arteriosclerosis, thrombosis and vascular biology,* 20(5):1354-1361.

Collet, J.P., Allali, Y., Lesty, C., Tanguy, M.L., Silvain, J., Ankri, A., Blanchet, B., Dumaine, R., Gianetti, J., Payot, L., Weisel, J.W. & Montalescot, G. 2006. Altered fibrin architecture is associated with hypofibrinolysis and premature coronary atherothrombosis. *Arteriosclerosis, thrombosis and vascular biology,* 26(11):2567-2573.

Danesh, J., Lewington, S., Thompson, S.G., Lowe, G.D.O. & Collins, R. 2005. Plasma fibrinogen level and the risk of major cardiovascular diseases and nonvascular mortality: an individual participant meta-analysis. *Journal of American medical association,* 294(14):1799-1809.

Davie, E.W., Fujikawa, K. & Kisiel, W. 1991. The coagulation cascade: initiation, maintenance, and regulation. *Biochemistry,* 30(43):10363-10370.

De Moerloose, P., Boehlen, F. & Neerman-Arbez, M. 2010. Fibrinogen and the risk of thrombosis. *Seminars in thrombosis and hemostasis,* 36(1):7-17.

Devaraj, S., Xu, D.Y. & Jialal, I. 2003. C-reactive protein increases plasminogen activator inhibitor-1 expression and activity in human aortic endothelial cells: implications for the metabolic syndrome and atherothrombosis. *Circulation,* 107(3):398-404.

De Vries, P.S., Chasman, D.I.., Sabater-Lleal, M., Chen, M.H., Huffman, J.E., Steri, M., Tang, W., Teumer, A., Marioni, R.E., Grossmann, V., Hottenga, J.J., Trompet, S., Muller-Nurasyid, M., Zhao, J.H., Brody, J.A., Kleber, M.E., Guo, X., Wang, J.J., Auer, P.L., Attia, J.R., Yanek, L.R., Ahluwalia, T.S., Lahti, J., Venturini, C., Tanaka, T., Bielak, L.F., Joshi, P.K., Rocanin-Arjo, A., Kolcic, I., Navarro, P., Rose, L.M., Oldmeadow, C., Riess, H., Mazur, J., Basu, S., Goel, A., Yang, Q., Ghanbari, M., Willemsen, G., Rumley, A., Fiorillo, E., de Craen, A.J., Grotevendt, A. & Scott, R. & Taylor, K.D. & Delgado, G.E. & Yao, J. & Kifley, A., Kooperberg, C., Qayyum, R., Lopez, L.M., Berentzen, T.L., Raikkonen, K., Mangino, M., Bandinelli, S., Peyser, P.A., Wild, S., Tregouet, D.A., Wright, A.F., Marten, J., Zemunik, T., Morrison, A.C., Sennblad, B., Tofler, G., de Maat, M.P., de Geus, E.J., Lowe, G.D., Zoledziewska, M., Sattar, N., Binder, H., Volker, U., Waldenberger, M., Khaw, K.T., McKnight, B., Huang, J., Jenny, N.S., Holliday, E.G., Qi, L., McEvoy, M.G., Becker, D.M., Starr, J.M., Sarin, A.P., Hysi, P.G., Hernandez, D.G., Jhun, M.A., Campbell, H., Hamsten, A., Rivadeneira, F., McArdle, W.L., Slagboom, P.E., Zeller, T., Koenig, W., Psaty, B.M., Haritunians, T., Liu, J., Palotie, A., Uitterlinden, A.G., Stott, D.J., Hofman, A., Franco, O.H., Polasek, O., Rudan, I., Morange, P.E., Wilson, J.F., Kardia, S.L., Ferrucci, L., Spector, T.D., Eriksson, J.G., Hansen, T., Deary, I.J., Becker, L.C., Scott, R.J., Mitchell, P., Marz, W., Wareham, N.J., Peters, A., Greinacher,

A., Wild, P.S., Jukema, J.W., Boomsma, D.I., Hayward, C., Cucca, F., Tracy, R., Watkins, H., Reiner, A.P., Folsom, A.R., Ridker, P.M., O'Donnell, C.J., Smith, N.L., Strachan, D.P. & Dehghan, A. 2016. A meta-analysis of 120 246 individuals identifies 18 new loci for fibrinogen concentration. *Human Molecular Genetics,* 25(2):358-370.

Dunn, E.J. & Ariëns, R.A.S. 2004. Fibrinogen and Fibrin Clot Structure in Diabetes. *Herz,* 29(5):470-479.

Dunn, E.J., Ariens, R.A.S. & Grant, P.J. 2005. The influence of type 2 diabetes on fibrin structure and function. *Diabetologia,* 48(6):1198-1206.

Dunn, E.J., Ariëns, R.A.S., De Lange, M., Snieder, H., Turney, J.H., Spector, T.D. & Grant, P.J. 2004. Genetics of fibrin clot structure: a twin study. *Blood*, 103(5):1735-1740.

Evans, P.A., Hawkins, K., Williams, P.R. & Williams, R.L. 2008a. Rheometrical detection of incipient blood clot formation by Fourier transform mechanical spectroscopy. *Journal of non-newtonian fluid mechanics*, 148(1):122-126.

Evans, P.A., Hawkins, K., Lawrence, M., Williams, R.L., Barrow, M.S., Thirumalai, N. & Williams, P. R. 2008b. Rheometry and associated techniques for blood coagulation studies. *Medical engineering and Physics*, 30(6):671-679.

Faber, D.R., De Groot, P.G. & Visseren, F.L. 2009. Role of adipose tissue in haemostasis, coagulation and fibrinolysis. Obesity reviews, 10(5):554–563.

Fatah, K., Hamsten, A., Blombäck, B. & Blombäck, M. 1992. Fibrin gel network characteristics and coronary heart disease: relations to plasma fibrinogen concentration, acute phase protein, serum lipoproteins and coronary atherosclerosis. *Thrombosis and haemostasis,* 68(2):130-135.

Fatah, K., Silveira, A., Tornvall, P., Karpe, F., Blombäck, M. & Hamsten, A. 1996. Proneness to formation of tight and rigid fibrin gel structures in men with myocardial infarction at a young age. *Thrombosis and haemostasis,* 76(4):535-540.

Ferry, J.D. 1948. Protein gels. *Advances in protein chemistry,* 4:1-78.

Ferry, J.D. & Morrison, P.R. 1947. Preparation and properties of serum and plasma proteins; the conversion of human fibrinogen to fibrin under various conditions. *Journal of the American chemical society,* 69(2):388-400.

Fornace, A.J., Cummings, D.E., Comeau, C.M., Kant, J.A. & Crabtree, G.R. 1984. Structure of the human γ-fibrinogen gene. *Journal of biological chemistry*, 259(20):12826-12830.

Fransson, E.I., Batty, G.D., Tabák, A.G., Brunner, E.J., Kumari, M., Shipley, M.J., Singh- Manoux, A. & Kivimäki, M. 2010. Association between change in body composition and change in inflammatory markers: an 11-year follow-up in the Whitehall II study. J*ournal of clinical endocrinology and metabolism,* 95(12):5370-5374.

Friedlander, Y., Elkana, Y., Sinnreich, R. & Kark, J.D. 1995. Genetic and environmental sources of fibrinogen variability in Israeli families: the Kibbutzim family study. *American journal of human genetics,* 56(5):1194-1206.

Geisse N.A. 2009. AFM and combined optical techniques. *Materials today*, 12(7):40-45.

Gersh, K.C., Nagaswami, C. & Weisel, J.W. 2009. Fibrin network structure and clot mechanical properties are altered by incorporation of erythrocytes. *Thrombosis and haemostasis*, 102(6):1169-1175.

Guthold, M., Liu, W., Stephens, B., Lord, S.T., Hantgan, Y.R.R., Erie, Z.D.A., Taylor, R.M. & Superfine, R. 2004. Visualization and mechanical manipulations of individual fibrin fibres suggest that fibre cross section has fractal dimension 1.3. *Biophysical journal*, 87(6):4226-4236.

Hajer, G.R., van Haeften, T.W. & Visseren, F.L. 2008. Adipose tissue dysfunction in obesity, diabetes, and vascular diseases. *European heart journal,* 29(24):2959-2971.

Hategan, A., Gersh, K.C., Safer, D. & Weisel, J.W. 2013. Visualization of the dynamics of fibrin clot growth 1 molecule at a time by total internal reflection fluorescence microscopy. *Blood,* 121(8):1455-1458.

Heart and Stroke Foundation South Africa. 2017. Cholesterol. http://www.heartfoundation. co.za/cholesterol/ Date of access: 12 Sept. 2018.

Herbert, C.B., Nagaswami, C., Bittner, G.D., Hubbell, J.A. & Weisel, J.W. 1998. Effects of fibrin micromorphology on neurite growth from dorsal root ganglia cultured in three-dimensional fibrin gels. *Journal of biomedical materials research*, 40(4):551-559.

Hoffman, M. & Monroe, D.M. 2001. A cell-based model of hemostasis. *Thrombosis and haemostasis,* 85(6):958-965.

Houser, J.R., Hudson, N.E., Ping, L., O'Brien, E.T., Superfine, R., Lord, S.T. & Falvo, M.R. 2010. Evidence that αC region is origin of low modulus, high extensibility, and strain stiffening in fibrin fibers. *Biophysical journal,* 99(9):3038-3047.

James, S., Vorster, H.H., Venter, C.S., Kruger, H.S., Nell, T.A., Veldman, F.J. & Ubbink, J.B. 2000. Nutritional status influences plasma fibrinogen concentration: Evidence from the THUSA survey. *Thrombosis research,* 98(5):383-394.

Kamath, S. & Lip, G.Y.H. 2003. Fibrinogen: biochemistry, epidemiology and determinants. *International journal of medicine,* 96(10):711-729.

Kannel, W.B. 2005. Overview of hemostatic factors involved in atherosclerotic cardiovascular disease. *Lipids,* 40(12):1215-1220.

Kattula, S., Byrnes, J.R. & Wolberg, A.S. 2017. Fibrinogen and fibrin in hemostasis and thrombosis. *Arteriosclerosis, Thrombosis and Vascular Biology,* 37(3):e13-e21.

Kim, S. 2002. A study of non-newtonian viscosity and yield stress of blood in a scanning capillary-tube rheometer. Drexel: Drexel University. (Thesis – PhD).

Kotzé, R.C., Ariëns, R.A.S., De Lange, Z. & Pieters, M. 2014. CVD risk factors are related to plasma fibrin clot properties independent of total and or γ' fibrinogen concentration. *Thrombosis research,* 134(5):963-969.

Kritchevsky, S.B., Cesari, M. & Pahor, M. 2005. Inflammatory markers and cardiovascular health in older adults. *Cardiovascular research,* 66(2):265-275.

Kunz, F., Pechlaner, C., Erhart, R., Zwierzina, W.D. & Kemmler, G. 1992. Increased lipid binding to thrombi in coronary artery disease. Findings in patients without premedication in native (not anticoagulated) test systems. *Arteriosclerosis and thrombosis*, 12(12):1516-1521.

Lawler, D. 2005. Spectrophotometry: turbidimetry and nephelometry. (*In* Worsfold, P., Townshend, A. & Poole, C. 2005. Encyclopedia of analytical science. 2nd ed. Amsterdam: Elsevier. p. 343-351).

Lefevre, M., Kris-Etherton, P.M., Zhao, G. & Tracy, R.P. 2004. Dietary fatty acids, hemostasis, and cardiovascular disease risk 1. *Journal of the American dietetic association,* 104(3):410-419.

Li, R., Ren, M., Luo, M., Chen, N., Zhang, Z., Luo, B. & Wu, J. 2012. Monomeric C-reactive protein alters fibrin clot properties on endothelial cells. *Thrombosis research,* 129(5):e251-e256.

Libby, P., Ridker, P.M. & Hansson, G.K. 2009. Inflammation in atherosclerosis: from pathophysiology to practice. *Journal of the American college of cardiology,* 54(23):2129-2138.

Liebeskind, D.S., Sanossian, N., Yong, W.H., Starkman, S., Tsang, M.P., Moya, A.L., Zheng, D.D., Abolian, A.M., Kim, D., Ali, L.K., Shah, S.H., Towfighi, A., Ovbiagele, B., Kidwell, C.S., Tateshima, S., Jahan, R., Duckwiler, G.R., Vinuela, F., Salamon, N., Villablanca, J.P., Vinters, H.V., Marder, V.J. & Saver, J.L. 2011. CT and MRI early vessel signs reflect clot composition in acute stroke. *Stroke*, 42(5):1237–1243.

Lisman, T., de Groot, P.G., Meijers, J.C. & Rosendaal, F.R. 2005. Reduced plasma fibrinolytic potential is a risk factor for venous thrombosis. *Blood,* 105(3):1102-1105.

Litvinov, R.I. & Weisel, J.W. 2016a. Fibrin mechanical properties and their structural origins. *Matrix biology*, Epub ahead of print.

Litvinov, R.I. & Weisel, J.W. 2016b. What Is the Biological and Clinical Relevance of Fibrin? *Seminars in thrombosis and hemostasis,* 42(4):333-343.

Liu, W., Carlisle, C.R., Sparks, E.A. & Guthold, M. 2010. The mechanical properties of single fibrin fibers. *Journal of thrombosis and haemostasis,* 8(5):1030-1036.

Machlus, K.R., Cardenas, J.C., Church, F.C. & Wolberg, A.S. 2011. Causal relationship between hyperfibrinogenemia, thrombosis, and resistance to thrombolysis in mice. *Blood*, 117(18):4953-4963.

Mackie, I.J., Kitchen, S., Machin, S.J. & Lowe, G.D.Q. 2003. Guideline. *British journal of haemotology,* 121:396-404.

Mackman, N. 2008. Triggers, targets and treatments for thrombosis. *Nature,* 451(7181):914-918.

Malan, M.M. 1999. Fibrin network characteristics of obese African women. Potchefstroom: NWU. (Thesis - PhD).

Martinez, M.R., Cuker, A., Mills, A.M., Crichlow, A., Lightfoot, R.T., Chernysh, I.N., Nagaswami, C., Weisel, J.W. & Ischiropoulos, H. 2014. Enhanced lysis and accelerated establishment of viscoelastic properties of fibrin clots are associated with pulmonary embolism. American journal of physiology, lung cellular and molecular physiology, 306(5):L397-L404.

Mazur, P., Sobczynski, R., Zabczyk, M., Babiarczyk, P., Sadowski, J. & Undas, A. 2013. Architecture of fibrin network inside thrombotic material obtained from the right atrium and pulmonary arteries: flow and location matter. *Journal of thrombosis and thrombolysis,* 35(1):127-129.

Mills, J.D., Ariëns, R.A.S., Mansfield, M.W. & Grant, P.J. 2002. Altered fibrin clot structure in the healthy relatives of patients with premature coronary artery disease. *Circulation,* 106(15):1938-1942.

Morais, I.P.A., Tóth, I.V. & Rangel, A.O.S.S. 2006. Turbidimetric and nephelometric flow analysis: Concepts and applications. *Spectroscopy letters,* 39(6):547-579.

Mosesson, M.W. 1998. Fibrinogen structure and fibrin clot assembly, *Seminars in thrombosis and hemostasis,* 24(2):169-174.

Mosesson, M.W. 2005. Fibrinogen and fibrin structure and functions. *Journal of thrombosis and haemostasis,* 3(8):1894-1904.

Mosesson, M.W., Siebenlist, K.R. & Meh, D.A. 2001. The structure and biological features of fibrinogen and fibrin. *Annals of the New York academy of sciences,* 936:11-30.

Mosesson, M.W., DiOrio, J.P., Siebenlist, K.R., Wall, J.S. & Hainfeld, J.F. 1993. Evidence for a second type of fibril branch point in fibrin polymer networks, the trimolecular junction. *Blood,* 82(5):1517-1521.

Mosesson, M.W., Siebenlist, K.R., Hernandez, I., Wall, J.S. & Hainfeld, J.F. 2002. Fibrinogen Assembly and Crosslinking on a Fibrin Fragment E Template, *Thrombosis and haemostasis,* 87(4):651-658.

Nguyen, X.T., Lane, J., Smith, B.R. & Nguyen, N.T. 2009. Changes in inflammatory biomarkers across weight classes in a representative US population: a link between obesity and inflammation. *Journal of gastrointestinal surgery,* 13(7):1205-1212.

Okraska-Bylica, A., Wilkosz, T., Slowik, L., Bazanek, M., Konieczynska, M. & Undas, A. 2012. Altered fibrin clot properties in patients with premature peripheral artery disease. *Polskie archiwum medycyny wewnetrznej,* 122(12):608-615.

Palka, I., Nessler, J., Nessler, B., Piwowarska, W., Tracz, W. & Undas, A. 2010. Altered fibrin clot properties in patients with chronic heart failure and sinus rhythm: a novel prothrombotic mechanism. *Heart,* 96(14):1114-1118.

Pearson, T.A., Lacava, J. & Weil, H.F.C. 1997. Epidemiology of thrombotic-hemostatic factors and their associations with cardiovascular disease. *American journal of clinical nutrition,* 65(Supplement 5):1674-1682.

Pera, J., Undas, A., Topor-Madry, R., Jagiella, J., Klimkowicz-Mrowiec, A. & Slowik, A. 2012. Fibrin clot properties in acute stroke: what differs cerebral hemorrhage from cerebral ischemia? *Stroke,* 43(5):1412-1414.

Pieters, M. 2002. Fibrin network characteristics and red palm oil in hyperfibrinogenaemic hypercholesterolaemic subjects. Potchefstroom: NWU. (Thesis – PhD).

Pieters, M. & Vorster, H.H. 2008. Nutrition and hemostasis: a focus on urbanization in South Africa. *Molecular nutrition & food research,* 52(1):164-172.

Pieters, M., Undas, A., Marchi, R., De Maat, M.P., Weisel, J.W. & Ariëns, R.A.S. 2012. An international study on the standardization of fibrin clot permeability measurement: methodological considerations and implications for healthy control values. *Journal of thrombosis and haemostasis,* 10(10):2179-2181.

Pieters, M., Philippou, H., Undas, A., De Lange, Z., Rijken, D.C. & Mutch, N.J. 2018. An international study on the feasibility of a standardized combined plasma clot turbidity and lysis assay: communication from the SSC of the ISTH. *Journal of thrombosis and haemostasis,* 16(5):1007-1012.

Pieters, M., Covic, N., Van der Westhuizen, F.H., Nagaswami, C., Baras, Y., Loots, D.T., Jerling, J.C., Elgar, D., Edmondson, K.S., Van Zyl, D.G., Rheeder, P. & Weisel, J.W. 2008. Glycaemic control improves fibrin network characteristics in type 2 diabetes – a purified fibrinogen model. *Thrombosis and haemostasis,* 99(4):691-700.

Pretorius, E., Steyn, H., Engelbrecht, M., Swanepoel, A.C. & Oberholzer, H.M. 2011. Differences in fibrin fiber diameters in healthy individuals and thromboembolic ischemic stroke patients. *Blood coagulation and fibrinolysis,* 22(8):696-700.

Puccetti, L., Pasqui, A.L., Pastorelli, M., Bova, G., Cercignani, M., Palazzuoli, A., Auteri, A. & Bruni, F. 2001. Different mechanisms of fibrinolysis impairment among dyslipidemic subjects. *International journal of clinical pharmacology research*, 21(3-4):147-155.

Pulanić, D. & Rudan, I. 2005. The past decade: fibrinogen. *Collegium antropologicum,* 29(1):341-349.

Ratnoff, O.D. & Menzie, C. 1951. A new method for the determination of fibrinogen in small samples of plasma. *Journal of laboratory and clinical medicine*, 37(2):316-320.

Raymond, J.L. & Couch, S.C. 2012. Medical nutrition therapy for cardiovascular disease. (*In* Mahan, L.K., Escott-Stump, S. & Raymond, J.L. 2012. Krause's food, nutrition and diet therapy. 13th ed. Philadelphia, USA: Elsevier. p. 743).

Redman, C.M. & Xia, H. 2000. A review of the expression, assembly, secretion and intracellular degradation of fibrinogen. *Fibrinolysis & proteolysis,* 14(2-3):198-205.

Riedel, T., Suttnar, J., Brynda, E., Houska, M., Medved, L. & Dyr, J.E. 2011. Fibrinopeptides A and B release in the process of surface fibrin formation. *Blood,* 117(5):1700-1706.

Rooth, E., Wallen, N.H., Blomback, M. & He, S. 2011. Decreased fibrin network permeability and impaired fibrinolysis in the acute and convalescent phase of ischemic stroke. *Thrombosis research,* 127(1):51-60.

Rosing, J., Tans, G., Govers-Riemslag, J.W., Zwaal, R.F. & Hemker, H.C. 1980. The role of phospholipids and factor Va in the prothrombinase complex. *Journal of biological chemistry,* 255(1):274-283.

Ross, R. 1999. Atherosclerosis--an inflammatory disease. N*ew England journal of medicine,* 340(2):115-126.

Rudež, G., Meijer, P., Spronk, H.M.H., Leebeek, F.W.G., Ten Cate, H., Kluft, C. & De Maat, M.P.M. 2009. Biological variation in inflammatory and hemostatic markers. *Journal of thrombosis and haemostasis,* 7(8):1247-1255.

Ryan, E.A., Mockros, L.F., Weisel, J.W. & Lorand, L. 1999. Structural Origins of Fibrin Clot Rheology. *Biophysical journal,* 77(5):2813-2826.

Sakariassen, K.S., Orning, L. & Turitto, V.T. 2015. The impact of blood shear rate on arterial thrombus formation. *Future science OA,* 1(1): FSO30.

Salonen, E.M., Vartio, T., Hedman, K. & Vaheri, A. 1984. Binding of fibronectin by the acute phase reactant C-reactive protein. *Journal of biological chemistry,* 259(3):1496-1501.

Scrutton, M.C., Ross-murphy, S.B., Bennett, G.M., Stirling, Y. & Meade, T.W. 1994. Changes in clot deformability--a possible explanation for the epidemiological association between plasma fibrinogen concentration and myocardial infarction. *Blood coagulation and fibrinolysis,* 5(5):719-723.

Shah, G.A., Nair, C.H. & Dhall, D.P. 1985. Physiological studies on fibrin network structure. *Thrombosis research*, 40(2):181-188.

Siebenlist, K.R. & Mosesson, M.W. 1994. Progressive cross-linking of fibrin γ chains increases resistance to fibrinolysis. *Journal of biological chemistry,* 269(45):28414-28419.

Silvain, J., Collet, J.P., Nagaswami, C., Beygui, F., Edmondson, K.E., Bellemain-appaix, A., Cayla, G., Pena, A., Brugier, D., Barthelemy, O., Montalescot, G. & Weisel, J.W. 2011. Composition of coronary thrombus in acute myocardial infarction. *Journal of the American college of cardiology,* 57(12):1359-1367.

Simon, D.I., Fless, G.M., Scanu, A.M. & Loscalzo, J. 1991. Tissue-type plasminogen activator binds to and is inhibited by surface-bound lipoprotein (a) and low-density lipoprotein. *Biochemistry*, 30(27):6671-6677.

Siudut, J., Swiat, M. & Undas, A. 2015. Altered fibrin clot properties in patients with cerebral venous sinus thrombosis: association with the risk of recurrence. *Stroke,* 46(9):2665-2668.

Sjøland, J.A. 2007. Inflammation and fibrin structure in patients with end-stage renal disease. Denmark: University of Southern Denmark. (Thesis - PhD). http://www.dadlnet.dk/dmb/dmb_phd/doc/ Jonas_Angel_Sjoland-thesis.pdf Date of access: 1 March 2017.

Skrzydlewski, Z. 1976. Coupling of fibrin with low density lipoproteins. *Acta medica academiae scientiarum hungaricae*, 33(2):171-177.

Smith, S.A., Travers, R.J. & Morrissey, J.H. 2015. How it all starts: initiation of the clotting cascade. *Critical reviews in biochemistry and molecular biology,* 50(4):326-336.

Standeven, K.F., Ariëns, R.A.S. & Grant, P.J. 2005. The molecular physiology and pathology of fibrin structure/function. *Blood Reviews,* 19(5):275-288.

Stats SA (Statistics South Africa). 2015. Mortality and causes of death in South Africa, 2014: findings from death notification. http://www.statssa.gov.za/publications/ P03093/P030932015.pdf Date of access: 17 March 2017.

TA Instruments. 2017. Basic rheology course – ARES-G2. [PowerPoint presentation].

Taylor, K.E. & Van den Berg, C.W. 2007. Structural and functional comparison of native pentameric, denatured monomeric and biotinylated C-reactive protein. *Immunology,* 120(3):404-411.

Teo, K., Chow, C.K., Vaz, M., Rangarajan, S. & Yusuf, S. 2009. The Prospective Urban Rural Epidemiology (PURE) study: examining the impact of societal influences on chronic

noncommunicable diseases in low-, middle-, and high-income countries. *American heart journal*, 158(1):1-7.

Tracy, R.P. 2003. Thrombin, inflammation, and cardiovascular disease: an epidemiologic perspective. *Chest,* 124(Supplement 3):49-57.

Tsurupa, G., Hantgan, R.R., Burton, R.A., Pechik, I., Tjandra, N. & Medved, L. 2009. Structure, Stability, and Interaction of the Fibrin(ogen) αC-Domains. *Biochemistry,* 48(51):12191-12201.

Uitte de Willige, S., De Visser, M.C., Houwing-Duistermaat, J.J., Rosendaal, F.R., Vos, H.L. & Bertina, R.M. 2005. Genetic variation in the fibrinogen gamma gene increases the risk for deep venous thrombosis by reducing plasma fibrinogen gamma' levels. *Blood,* 106(13):4176-4183.

Undas, A. 2014. Fibrin clot properties and their modulation in thrombotic disorders. *Journal of thrombosis and haemostasis,* 112(1):32-42.

Undas, A. & Zeglin, M. 2006a. Fibrin clot properties and cardiovascular disease. *Vascular disease prevention*, 3(2):99-106.

Undas, A. & Ariëns, R.A. 2011a. Fibrin clot structure and function: a role in the pathophysiology of arterial and venous thromboembolic diseases. *Arteriosclerosis, Thrombosis and Vascular Biology,* 31(12):e88-e99.

Undas, A., Celinska-Lőwenhoff, M., Lőwenhoff, T. & Szczeklik, A. 2006b. Statins, fenofibrate, and quinapril increase clot permeability and enhance fibrinolysis in patients with coronary artery disease. *Journal of thrombosis and haemostasis,* 4(5):1029-1036.

Undas, A., Stepien, E., Tracz, W. & Szczeklik, A. 2006c. Lipoprotein(a) as a modifier of fibrin clot permeability and susceptibility to lysis. *Journal of thrombosis and haemostasis,* 4(5):973-975.

Undas, A., Stępień, E., Rudziński, P. & Sadowski, J. 2010a. Architecture of a pulmonary thrombus removed during embolectomy in a patient with acute pulmonary embolism. *Journal of thoracic and cardiovascular surgery,* 140(3):e40-e41.

Undas, A., Nowakowski, T., Cieśla-Dul, M. & SadowskI, J. 2011b. Abnormal plasma fibrin clot characteristics are associated with worse clinical outcome in patients with peripheral arterial disease and thromboangiitis obliterans. *Atherosclerosis,* 215(2):481-486.

Undas, A., Cieśla-Dul , M., Drążkiewicz, T. & Sadowski, J. 2012. Altered fibrin clot properties are associated with residual vein obstruction: Effects of lipoprotein(a) and apolipoprotein(a) isoform. *Thrombosis research*, 130(3):e184-e187.

Undas, A., Plicner, D., Stepien, E., Drwila, R. & Sadowski, J. 2007. Altered fibrin clot structure in patients with advanced coronary artery disease: a role of C-reactive protein, lipoprotein(a) and homocysteine. *Journal of thrombosis and haemostasis,* 5(9):1988-1990.

Undas A, Wiek I, Stêpien E, Zmudka K & Tracz W. 2008a. Hyperglycemia is associated with enhanced thrombin formation, platelet activation, and fibrin clot resistance to lysis in patients with acute coronary syndrome. *Diabetes care*, 31(8):1590–1595.

Undas, A., Slowik, A., Wolkow, P., Szczudlik, A. & Tracz, W. 2010b. Fibrin clot properties in acute ischemic stroke: relation to neurological deficit. *Thrombosis research,* 125(4):357-361.

Undas, A., Zawilska, K., Cieśla-Dul, M., Lehmann-Kopydlowska, A., Skubiszak, A., Ciepluch, K. & Tracz, W. 2009a. Altered fibrin clot structure/function in patients with idiopathic venous thromboembolism and in their relatives. *Blood,* 114(19):4272-4278.

Undas, A., Kaczmarek, P., Sladek, K., Stepien, E., Skucha, W., Rzeszutko, M., Gorkiewicz-Kot, I. & Tracz, W. 2009b. Fibrin clot properties are altered in patients with chronic obstructive pulmonary disease. Beneficial effects of simvastatin treatment. *Thrombosis and haemostasis,* 102(6):1176-1182.

Undas A., Szuldrzynski K., Stępień E., Zalewski J., Godlewski J., Tracz W., Pasowicz M. & Zmudka K. 2008b. Reduced clot permeability and susceptibility to lysis in patients with acute coronary syndrome: effects of inflammation and oxidative stress. *Atherosclerosis*, 196(2):551–558.

Undas, A., Zalewski, J., Krochin, M., Siudak, Z., Sadowski, M., Pregowski, J., Dudek, D., Janion, M., Witkowski, A. & Zmudka, K. 2010c. Altered plasma fibrin clot properties are associated with in-stent thrombosis. *Arteriosclerosis, Thrombosis and Vascular Biology,* 30(2):276-282.

Undas, A., Podolec, P., Zawilska, K., Pieculewicz, M., Jedlinski, I., Stepien, E., Konarska-kuszewska, E., Weglarz, P., Duszynska, M., Hanschke, E., Przewlocki, T. & Tracz, W. 2009c. Altered fibrin clot structure/function in patients with cryptogenic ischemic stroke. *Stroke,* 40(4):1499-1501.

Van Gelder, J. M., Nair, C. H. & Dhall, D. P. 1995. The permeability of fibrin network developed in human plasma. *Blood coagulation and fibrinolysis,* 6(4):293-301.

Vorster, H.H. 2002. The emergence of cardiovascular disease during urbanisation of Africans. *Public health nutrition*, 5(1a):239-243.

Weisel, J.W. 2004. The mechanical properties of fibrin for basic scientists and clinicians. *Biophysical chemistry,* 112(2-3):267-276.

Weisel, J.W. 2005. Fibrinogen and fibrin. (*In* Parry, D. & Squire, J. 2005. Advances in protein chemistry: Volume 70. California, USA: Elsevier Academic Press. p. 264-265.)

Weisel, J.W. 2007. Structure of fibrin: impact on clot stability. *Journal of thrombosis and haemostasis,* 5 (Supplement 1):116-124.

Weisel, J.W. & Nagaswami, C. 1992. Computer modeling of fibrin polymerization kinetics correlated with electron microscope and turbidity observations: clot structure and assembly are kinetically controlled. *Biophysical journal,* 63(1):111-128.

Weisel, J.W. & Medved, L. 2001. The structure and function of the alpha C domains of fibrinogen. *Annals of the New York academy of sciences,* 936:312-327.

Weisel, J.W. & Dempfle, C.H. 2013. Fibrinogen structure and function. (*In* Marder, V.J., Aird, W.C., Bennett, J.S., Schulman, S. & White, G.C. 2013. Hemostasis and thrombosis: basic principles and clinical practice. 6th ed. Philadelphia, USA: Lippincott Willams & Wilkins. p. 254-264).

Weisel, J.W. & Litvinov, R.I. 2013. Mechanisms of fibrin polymerization and clinical implications. *Blood,* 121(10):1712-1719.

Weisel, J.W., Stauffacher, C.V., Bullitt, E. & Cohen, C. 1985. A model for fibrinogen: domains and sequence. *Science,* 230(4732):1388-1391.

WHO (World Health Organisation). 2014. Global status report on noncommunicable diseases. http://www.who.int/nmh/publications/ncd-status-report-2014/en/ Date of access: 7 March 2017.

WHO (World Health Organisation). 2015. South Africa: WHO statistical profile. http://www.who.int/gho/countries/zaf.pdf?ua=1 Date of access: 5 June 2017.

WHO (World Health Organisation). 2016. Cardiovascular diseases (CVDs). http://www.who.int/mediacentre/factsheets/fs317/en/ Date of access: 9 March 2017.

Wolberg, A.S. 2010. Plasma and cellular contributions to fibrin network formation, structure and stability. *Haemophilia*, 16(Supplement 3):7–12.

Yang, Z., Mochalkin, I. & Doolittle, R.F. 2000. A model of fibrin formation based on crystal structures of fibrinogen and fibrin fragments complexed with synthetic peptides. *Proceedings of the national academy of sciences,* 97(26):14156-14161.

Zolcinski, M., Cieśla-dul, M. & Undas, A. 2012. Effects of atorvastatin on plasma fibrin clot properties in apparently healthy individuals and patients with previous venous thromboembolism. *Journal of thrombosis and haemostasis,* 107(6):1180-1200.

ADDENDA

NORTH-WEST UNIVERSITY
YUNIBESITI YA BOKONE-BOPHIRIMA
NOORDWES-UNIVERSITEIT

Private Bag X6001, Potchefstroom,
South Africa, 2520

Tel: (018) 299-4900
Fax: (018) 299-4910
Web: http://www.nwu.ac.za

Institutional Research Ethics Regulatory Committee

Tel: +27 18 299 4849

Email: Ethics@nwu.ac.za

ETHICS APPROVAL CERTIFICATE OF STUDY

Based on approval by **Health Research Ethics Committee (HREC)** on **04/07/2017** after being reviewed at the meeting held on **14/06/2017**, the North-West University Institutional Research Ethics Regulatory Committee (NWU-IRERC) hereby **approves** your study as indicated below. This implies that the NWU-IRERC grants its permission that provided the special conditions specified below are met and pending any other authorisation that may be necessary, the study may be initiated, using the ethics number below.

Sub-study title: Interpretation of maximum absorbance data obtained from turbidimetry in plasma samples with varying fibrinogen concentrations

Study Leader/Supervisor: Dr Z de Lange
Student: C Nunes-23554355

Ethics number:

N	W	U		0	0	0	3	4	-	1	7		A	1	-	0	1
Institution				Study Number						Year			Status			Sub-study	

Status: S = Submission; R = Re-Submission; P = Provisional Authorisation; A = Authorisation

Application Type: Sub-study
Commencement date: 2017-07-04 **Risk:** Minimal

Continuation of the study is dependent on receipt of the annual (or as otherwise stipulated) monitoring report and the concomitant issuing of a letter of continuation.

Special conditions of the approval (if applicable):

- Translation of the informed consent document to the languages applicable to the study participants should be submitted to the HREC (if applicable).
- Any research at governmental or private institutions, permission must still be obtained from relevant authorities and provided to the HREC. Ethics approval is required BEFORE approval can be obtained from these authorities.

General conditions:

While this ethics approval is subject to all declarations, undertakings and agreements incorporated and signed in the application form, please note the following:

- *The study leader (principle investigator) must report in the prescribed format to the NWU-IRERC via HREC:*
  - *annually (or as otherwise requested) on the monitoring of the study, and upon completion of the study*
  - *without any delay in case of any adverse event or incident (or any matter that interrupts sound ethical principles) during the course of the study.*
- *Annually a number of studies may be randomly selected for an external audit.*
- *The approval applies strictly to the proposal as stipulated in the application form. Would any changes to the proposal be deemed necessary during the course of the study, the study leader must apply for approval of these amendments at the HREC, prior to implementation. Would there be deviated from the study proposal without the necessary approval of such amendments, the ethics approval is immediately and automatically forfeited.*
- *The date of approval indicates the first date that the study may be started.*
- *In the interest of ethical responsibility the NWU-IRERC and HREC retains the right to:*
  - *request access to any information or data at any time during the course or after completion of the study;*
  - *to ask further questions, seek additional information, require further modification or monitor the conduct of your research or the informed consent process.*
  - *withdraw or postpone approval if:*
    - *any unethical principles or practices of the study are revealed or suspected,*
    - *it becomes apparent that any relevant information was withheld from the HREC or that information has been false or misrepresented,*
    - *the required amendments, annual (or otherwise stipulated) report and reporting of adverse events or incidents was not done in a timely manner and accurately,*
    - *new institutional rules, national legislation or international conventions deem it necessary.*
- *HREC can be contacted for further information or any report templates via Ethics-HRECApply@nwu.ac.za or 018 299 1206.*

The IRERC would like to remain at your service as scientist and researcher, and wishes you well with your study. Please do not hesitate to contact the IRERC or HREC for any further enquiries or requests for assistance.

Yours sincerely

Linda du Plessis

Digitally signed by Linda du Plessis
DN: cn=Linda du Plessis, o=NWU, ou=Vaal Triangle Campus, email=linda.duplessis@nwu.ac.za, c=ZA
Date: 2017.07.31 13:03:31 +02'00'

Prof Linda du Plessis *Chair NWU Institutional Research Ethics Regulatory Committee (IRERC)*

Addendum B: Plasma fibrinolytic potential protocol

Plasma fibrinolytic potential protocol (as performed on the PURE 2005 samples at the NWU, Potchefstroom)

(Modified set-up for Erasmus MC, Rotterdam – Method D.C. Rijken & J. Malfliet – Z. de Lange & M. Pieters)

1. Start the microplate reader (Multiskan Ascent) and set the temperature to 37°C.
2. Make an Assay Mixture at room temperature. Prepare 1400 µl for a full microtiter plate (we did not use columns 1 and 12, only measured 80 samples per plate).

   Stock solutions:

   Tissue factor (Innovin): make aliquots of 120 µl of a 2-fold diluted stock in assay buffer and store frozen (-20°C, use only once).

   $CaCl_2$: make a stock of 425 mM in MQ-H_2O and store at room temperature.

   tPA (Actilyse): make a stock of 0.01 mg/ml in buffer (in 50 mM HEPES, 0.1% (w/v) BSA pH 7.4), aliquot in 50 µl and store frozen.

   Phospholipids (phospholipids-TGT of Rossix): use the original stock solution of 0.5 mM, stored at 4 °C (use until done).

   Assay buffer: 25 mM HEPES; 137 mM NaCl; 3.5 mM KCl; 1% BSA; pH 7.4

Stock solution	Volume for 1400 µl Assay Mixture (µl)	Concentration in Assay Mixture	Final concentration in clot
Tissue Factor	149.3	18.75 x diluted	125 x diluted (use 2 x diluted stock)
$CaCl_2$	373.4	113 mM	17 mM
tPA	93.4	167 ng/ml	100 ng/ml
Phospholipids	186.6	67 µM	10 µM
Assay buffer	597.3		

3. **Dilution of plasma samples at room temperature:** to each well of a separate microtiter plate (untreated plates) add 71.4 µl of citrated plasma sample followed by 50.0 µl of assay buffer, using a multi-channel pipette, and shake on a plate shaker for 10 seconds at 1100 rpm. (Use 120 µl citrated plasma and 84 µl assay buffer for a measurement in duplicate).

4. Make Assay Mixture. Add 15 µl of the Assay Mixture per well of a microtiter plate (NUNC-Maxisorp).
5. Check if the plate reader is at the right temperature. (Note: The next steps have to be performed quickly because the reaction starts immediately when the plasma is pipetted into the assay mix).
6. Then, pipette using a multi-channel 85 µl of the diluted plasma samples over to the plate containing the Assay Mixture (because we also want to determine lag time, clotting time and max absorbance, a timer is set to determine the time from pipetting the plasma dilution to the assay mix to the start of the measurement).
7. Shake on a plate shaker 10 seconds at 1100 rpm.
8. Cover each well with 50 µl liquid paraffin oil (Merck, Darmstadt, Germany) (Note: The tips of the multi-channel have to be cut to facilitate pipetting the viscous liquid OR use wide-bore tips from Lasec).
9. Place the plate into the plate reader and start measuring the A405nm every 9 seconds for the first two minutes, every 15 seconds up to 30 minutes and every minute until the clots have broken down or up to 270 minutes (according to protocol by Lisman *et al* (2005)).
10. Determine the clot lysis time (CLT), which is defined as the time from the midpoint of clear to maximum turbidity transition (clotting time) to the midpoint of maximum turbidity to clear transition (lysis time). Clotting and lysis times are measured by sigmoidal curve fitting using the computer program Origin.

Comments

- Using a more diluted Assay Mixture and undiluted plasma might also be possible. The final plasma concentration should be 50%.
- A final tPA concentration of 100 ng/ml was selected to induce a clot lysis time of between 60 - 100 minutes using normal plasma. When samples with a low fibrinolytic potential are measured, one could consider using a higher tPA concentration.

References

Lisman, T., de Groot, P.G., Meijers, J.C. & Rosendaal, F.R. 2005. Reduced plasma fibrinolytic potential is a risk factor for venous thrombosis. *Blood*, 105(3):1102-1105.

.

Addendum C: Standardised permeability assay protocol

Standardised permeability (Ks) assay protocol (as performed on the PURE 2015 samples at the CEN, NWU, Potchefstroom)
(Standardised method by Pieters *et al.* (2012))

1. Stock solutions:

Tris buffer: make a stock of 0.05 M Tris (Merck, Dramstadt, Germany) and 0.10 M NaCl (Merck, Damstadt, Germany) in double distilled deionised H_2O, with a pH of 7.5, filtered through a 0.22-micron filter and store at 2-8 °C. (Note*:* Leave buffer at room temperature before initiating experiment to avoid air bubble generation).

Human α-thrombin: make aliquots of 50 µl of a diluted stock (50 U/ml) in Tris buffer and store frozen (-20°C, use only once).

$CaCl_2$: make a stock of 1 M in double distilled deionised H_2O and store at room temperature.

2. Preparation:

Humidity chamber: Make use of a container with glass bottles where the clot containers can be placed upright. Place a soaked folded piece of paper towel with distilled water at the bottom of the container. Keep container at room temperature.

Clot container: Use cut-off tips of 1 ml plastic, serological pipettes. Mechanically scratch the inside of the container, a total length that can be filled with 100 µl plasma sample, to improve sample adherence to the container. Cover the bottom edge of the container with parafilm M (Bemis NA, Neenah, USA).

Buffer container: Fill buffer container with Tris buffer to the required level, allowing the tubing connected to the clot container to be filled and clamped until permeation.
(Note: Ensure no air bubbles are present in buffer container or tubing. Keep covered with parafilm M until usage).

3. Thaw the frozen platelet poor plasma (PPP) samples at 37 °C in a water bath.
4. Prepare 100 µl activation mixture, consisting of human α-thrombin (Merck, Darmstadt, Germany), $CaCl_2$ (Merck, Darmstadt, Germany) and Tris buffer, at room temperature. Both the thrombin stock and activation mixture must be kept on ice for not longer than one hour to avoid thrombin deactivation.

Stock solution	Volume for 100 µl activation mixture (µl)	Concentration in Activation Mixture	Final concentration in clot
Human α-thrombin	22	11 U/ml	1 U/ml
$CaCl_2$	22	0.22 M	0.02 M
Tris buffer	56		

5. Add 12 µl of activation mix to 120 µl of plasma, thereafter quickly pipette 100 µl of the sample into a clot container. This step must be performed as accurately as possible to ensure no air bubbles are inserted into the clot. (Note: This assay is performed in triplicate for each sample).
6. Cover the clot container completely with parafilm M and place upright in the humid chamber. Leave the containers for two hours to polymerise and stabilise the fibrin gel structure through crosslinking.
7. During the two hour waiting period, weigh all collection tubes and record weights. Three collection tubes are required for each sample repeat.
8. After two hours, remove the top parafilm M seal from the container and fill with Tris buffer to the top of the container, ensuring no air bubbles are inserted.
9. Remove the clamp from the bottom end of the tubing and connect the clot container to the tubing, ensuring no air bubbles are present in the permeation system.
10. Clip the clot container in the designated clip on the permeation stand with the difference between the surface level of the bottom end of the clot container and the top of the buffer container being 4 cm water.
11. Remove the parafilm M seal from the bottom end of the clot container.
12. Collect first few drops of buffer in a waste container placed beneath the clot container.
13. Once the clot has been washed and plasma colour has cleared out, replace waste container with the pre-weighed collection tube.
14. Start the time when the first drop falls and stop timer when last drop falls, collecting similar volumes for each sample.
15. Weigh collection tube again, determining the weight of the permeate collected.
16. Calculate the permeability of clots using the following formula where the density of the 1.0 Tris-buffer and weight of permeate is used to determine the volume (Q) collected (Pieters et al., 2012):

$$Ks = \frac{\mathrm{Q \times L \times \eta}}{\mathrm{T \times A \times \Delta P}}$$

Where:

Q = volume of liquid (ml = cm^3)

L = clot length (cm)

η = viscosity (10^{-2} poise = 10^{-7} N s cm^{-2})

T = time (s)

A = cross-sectional area of clot container (cm^2)

ΔP = pressure drop (density x g x height = 1 x 980 x 4 = 3 920 dyne cm^{-2} = 0.0392 N cm^{-2}).

Comments

- The same clots used for this assay were used for the SEM analysis.

References

Pieters, M., Undas, A., Marchi, R., De Maat, M.P., Weisel, J.W. & Ariëns, R.A.S. 2012. An international study on the standardization of fibrin clot permeability measurement: methodological considerations and implications for healthy control values. *Journal of thrombosis and haemostasis,* 10(10):2179-2181.

Addendum D: Scanning electron microscopy protocol

Scanning electron microscopy (SEM) protocol (as performed on the PURE 2015 samples at the NWU, Potchefstroom)

Day 1

1. Use the same clots made for the permeability assay.
2. Stock solutions:

   Cacodylate buffer: make a stock of 50 mM cacodylate (Merck, Darmstadt, Germany) and 100 mM NaCl (Merck, Darmstadt, Germany) in double distilled deionised H_2O, brought to a pH of 7.4 with HCl.

   Ethanol solutions: make 5 dilutions of pure ethanol (Merck, Darmstadt, Germany) starting with 30%, 50%, 70%, 80%, 90% and 100%.

3. After completion of permeation, place clot in a glass container filled with cacodylate buffer and rinse twice for 10 minutes.
4. Fix clots with 2% glutaraldehyde (for 25% glutaraldehyde with a volume of 1 ml, 640 µl glutaraldehyde and 7 360 µl cacodylate buffer is used), cover with parafilm M and leave overnight in fridge at 4 °C.

Day 2

5. Remove clots from clot containers using slight pressure.
6. Rinse clots twice in cacodylate buffer for 10 minutes.
7. Dehydrate clots using ethanol in successive dose increases as follows:

Ethanol	Time
30%	10 minutes
50%	10 minutes
70%	10 minutes
80%	10 minutes
100%	15 minutes **x2**

8. Under fume hood: leave clots in a 50% HMDS (Merck, Darmstadt, Germany) solution (500 µl EtOH, 500 µl HMDS) for 10 minutes and then 100% HMDS (1 000 µl HMDS) for 10 minutes. Thereafter, replace HMDS with new 100% HMDS (1 000 µl HMDS) solution and leave overnight, uncovered in the fume hood.

Day 3

9. Mount clots on SEM stubs using carbon tape.
10. Sputter coat using an Eiko engineering ion coater IB-2 (Eiko Engineering, Ibaraki, Japan). Sputter coating takes place in two phases: carbon coating followed by gold / palladium coating.
11. Carbon coating:
    - Open the argon faucet and switch on the system by pressing the START button on the EMScope.
    - Allow the argon gas to break the vacuum by pressing the STOP button on the EMScope.
    - Place the SEM stubs on the holder.
    - Lift lid of the carbon coater and loosen the screws to replace the used carbon fibres and then tighten the screws.
    - Turn the plate over the carbon fibres and place hold with stubs on the stage of the coater.
    - Press the START button and allow vacuum to reach <0.06 Torr.
    - Thereafter press the OUTGAS button and allow the vacuum to restore to <0.06 Torr.
    - Turn the plate covering the stubs, to allow coating of samples, and press the COAT button.
    - Once coating is completed, press the STOP button to break the vacuum.
    - Lift the lid of the coater and remove holder with stubs.
    - Place holder on stage of the gold / palladium coater.
12. Gold / palladium coating:
    - Press the START button.
    - Restore vacuum to <0.06 Torr.
    - Set timer to 4 minutes and slowly open the argon inlet valve of the coater to control the volume of argon without the reading exceeding 5 mA.
    - Once coating is completed, close the argon valve and press the STOP button to break the vacuum.
    - Lift the lid of the coater and remove the SEM stubs.
    - Place the lid back and restore the vacuum by pressing the START button.
    - Close the argon faucet and switch off system once vacuum has been restored to <0.06 Torr.
13. SEM stubs are placed on the stage of the FEI Corporation Quanta 200SEM (Hillsboro, Oregon, USA) where the clots are imaged and photographed.

14. Select eight random areas per clot to be photographed at a magnitude of both 6 000X and 12 000X.
15. Use ImageJ (v 1.48, NIH, Bethesda, Maryland, USA) to measure the fibre diameter of individual clot fibres, by selecting the clearest five images per clot, systematically and in a standardized manner, measuring 100 areas (starting at the top left corner) in each image following the pattern as shown below.

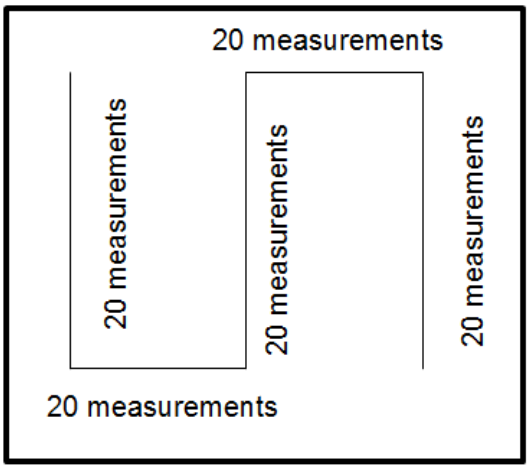

Addendum E: Rheometry protocol

Rheometry protocol (as performed on the PURE 2015 samples at the CEN, NWU, Potchefstroom)

1. Stock solutions:

Human α-thrombin: make aliquots of 20 µl of a diluted stock (50 U/ml) in Tris buffer and store frozen (-20°C, use only once).

$CaCl_2$: make a stock of 1 M in double distilled deionised H_2O and store at room temperature.

2. Method set-up in TRIOS (v4.3.1, New Castle, DE):

Geometry: Use a 40 mm 2.017º cone plate, stainless steel with a set geometry (truncation) gap of 0.045 mm and a loading gap of 15.0 mm.

Procedure: Oscillation time sweep, at a temperature of 37 °C, sampling interval of 3 points per second, 3 % strain, 5 radian per second frequency and sampling cycles of 10 half cycles for a duration of 40 minutes.

3. Thaw the frozen platelet poor plasma (PPP) samples at 37 °C in a water bath.
4. Pipette 499.2 µl of PPP and keep at room temperature. Thrombin stock must be kept on ice for not longer than one hour to avoid thrombin deactivation.

Stock solution	Volume (µl)	Concentration in stock solution	Final concentration in clot
Human α-thrombin	10.4	50 U/ml	1 U/ml
$CaCl_2$	10.4	1 M	0.02 M

5. Zero the gap of the geometry in order to apply the set temperature of 37 °C; thereafter the geometry can be raised up to the set loading gap (15.0 mm).
6. Add 10.4 µl $CaCl_2$ (Merck, Damstadt, Germany) and directly afterwards 10.4 µl human α-thrombin (Merck, Damstadt, Germany) to the plasma, mix using the pipette and place the activated plasma onto the base plate. This step must be performed as quickly as possible.
7. Lower the plate to the set geometric gap (0.045 mm).
8. Once the geometric gap has been reached, place immersion oil (100 – 120 mPa·s) around the plates with the use of a dropper.
9. Start the test to measure the elastic / storage modulus (G') and inelastic / loss modulus (G'') of the formed clot.

Addendum F: Fibrin content protocol

Fibrin content protocol (as performed on the PURE 2015 samples at the CEN, NWU, Potchefstroom) (Modified method by Pieters (2002) based on the method of Ratnoff and Menzie (1951))

1. Volume of plasma and reagents were reduced by a factor of 7 to compensate for limited, available plasma

	Original volumes	**Adjusted volumes**
Plasma	925 µl	132 µl
Thrombin mix: • 25 mM $CaCl_2$ • 1 U/ml human α-thrombin	75 µl: • 25 µl • 50 µl	10.7 µl: • 3.6 µl • 7.1 µl
2.5 M NaOH	1 ml	143 µl
Double distilled deionised H_2O	7 ml	1 ml
Na_2CO_3	3 ml	429 µl
Folin & Ciocalteu's reagent	650 µl	93 µl

2. The same method is followed for both sample analyses and formation of standard curve, with differences as shown in *italics* in the table below:

Standard curve	**Plasma**
132 µl human fibrinogen	*132 µl platelet poor plasma (PPP)*
10.7 µl Tris buffer	*10.7 µl thrombin mix*
Skip drying and washing step	*Dry and wash*
143 µl NaOH	143 µl NaOH
Leave overnight at 30℃	
857.3 µl double distilled deionised H_2O	*1 000 µl double distilled deionised H_2O*
429 µl Na_2CO_3	429 µl Na_2CO_3
93 µl Folin & Ciocalteu's reagent	93 µl Folin & Ciocalteu's reagent
Total volume: 1 665 µl	

3. Stock solutions:

Tris buffer: make a stock of 0.05 M Tris (Merck, Damstadt, Germany) and 0.10 M NaCl (Merck, Damstadt, Germany) in double distilled deionised H_2O, with a pH of 7.5 and store at room temperature.

9.1 pH buffer: make a stock of 0.02 M $NaHCO_3$ (Merck, Damstadt, Germany) and 0.13 M NaCl in double distilled deionised H_2O, with a pH of 9.1 (brought to pH with a mixed solution of 0.02 M Na_2CO_3 (Merck, Damstadt, Germany) and 0.13 M NaCl in double distilled deionised H_2O) and store at room temperature.

Human α-thrombin: make aliquots of 20 µl of a diluted stock (50 U/ml) in Tris buffer and store frozen (-20°C, use only once).

$CaCl_2$: make a stock of 1 M $CaCl_2$ (Merck, Damstadt, Germany) in double distilled deionised H_2O and store at room temperature.

NaOH: make a stock of 2.5 M NaOH (Merck, Damstadt, Germany) in double distilled deionised H_2O and store at room temperature.

Na_2CO_3: make a stock of 1.9 M Na_2CO_3 in double distilled deionised H_2O and store at room temperature.

Sample preparation

Day 1

4. Pipette 132 µl citrated PPP into 5 ml glass tubes.
5. Prepare thrombin dilution: add 10.5 µl Tris buffer to 7 µl human α-thrombin (Merck, Damstadt, Germany).
6. Add 7.1 µl diluted thrombin to 3.6 µl $CaCl_2$, to make a thrombin mix with a final concentration of 1 U/ml thrombin and 25 mM $CaCl_2$.
7. Add 10.7 µl of the thrombin mix to the plasma and leave overnight at room temperature for maximum polymerisation.

Stock solution	Volume for 10.7 µl thrombin mix (µl)	Concentration in thrombin Mixture	Final concentration in clot
Diluted thrombin	7.1	20 U/ml	1 U/ml
$CaCl_2$	3.6	1 M	0.025 M

Day 2

8. Centrifuge glass tubes with clots at 2 000 g for 15 mins at 15 ℃ and wash with Tris buffer alternately three times.
9. Remove excess fluid between washes using a dropper.
10. Add 143 µl NaOH to glass tubes, cover and leave tubes overnight in an incubator at 30 ℃.

Day 3

11. Add 1 ml double distilled deionised H_2O and 429 µl Na_2CO_3 to tubes and vortex the tubes.
12. Add 93 µl Folin & Ciocalteu's reagent (Merck, Damstadt, Germany) to tubes and mix.
13. Leave glass tubes for 20 minutes at room temperature.
14. Start the plate reader (Multiskan Ascent spectrophotometer - Labsystems, Virginia, USA).
15. Pipette 100 µl of each sample into a 96-well plate.
16. Place the plate into the reader and take a single, continuous measurement at an absorbance of 650 nm.

Standard curve

Day 1

17. **Fibrinogen stock solution:** dissolve 60% purified human fibrinogen (35.1 mg) (MP Biomedicals, Santa Ana, USA) in 2.1 ml 9.1 pH buffer, DON'T mix or vortex solution.
18. Make five fibrinogen dilutions, each with a total volume of 1 ml, as follows:

Dilution	Fibrinogen stock solution	9.1 pH buffer
D1: 8 g/L	800 µl	200 µl
D2: 6 g/L	600 µl	400 µl
D3: 4 g/L	400 µl	600 µl
D4: 2 g/L	200 µl	800 µl
D5: 0.5 gLl	50 µl	950 µl

19. Start the cuvette reader (UV-1601 spectrophotometer - Shimadzu, Kyoto, Japan) and set the absorbance to 280 nm.
20. Auto zero using two blanks (use cuvettes filled with Tris buffer).
21. Make 1% solution of the stock and thereafter each dilution in the cuvette, consisting of 10 µl dilution and 990 µl Tris buffer.
22. Place the cuvette into the reader and measure at an absorbance of 280 nm.
23. From the results, measure the actual fibrinogen concentration of each dilution calculated with 13.6 absorbance units (0.136 in a 1% solution) being the known absorbance of 10 g/l fibrinogen.

Day 2

24. Pipette 132 µl of each fibrinogen dilution into 5 ml glass tubes.
25. Add 10.5 µl Tris buffer to solution.
26. Add 143 µl NaOH to glass tubes, cover and leave tubes overnight in an incubator at 30 ℃

Day 3

27. Add 857.3 µl double distilled deionised H_2O and 429 µl Na_2CO_3 to tubes and vortex the tubes.
28. Add 93 µl Folin & Ciocalteu's reagent to tubes and mix.
29. Leave glass tubes for 20 minutes at room temperature.
30. Start the plate reader (Multiskan Ascent spectrophotometer).
31. Pipette 100 µl of each dilution into a 96-well plate.
32. Place the plate into the reader and take a single, continuous measurement at an absorbance of 650 nm.

Comments

- The preparation of samples and standard curve must be performed simultaneously.

References

Pieters, M. 2002. Fibrin network characteristics and red palm oil in hyeperfibrinogenaemic hypercholesterolaemic subjects. Potchefstroom: NWU. (Thesis – PhD).

Ratnoff, O.D. & Menzie, C. 1951. A new method for the determination of fibrinogen in small samples of plasma. *Journal of laboratory and clinical medicine*, 37:816-820.